CHALMERS
UNIVERSITY OF TECHNOLOGY

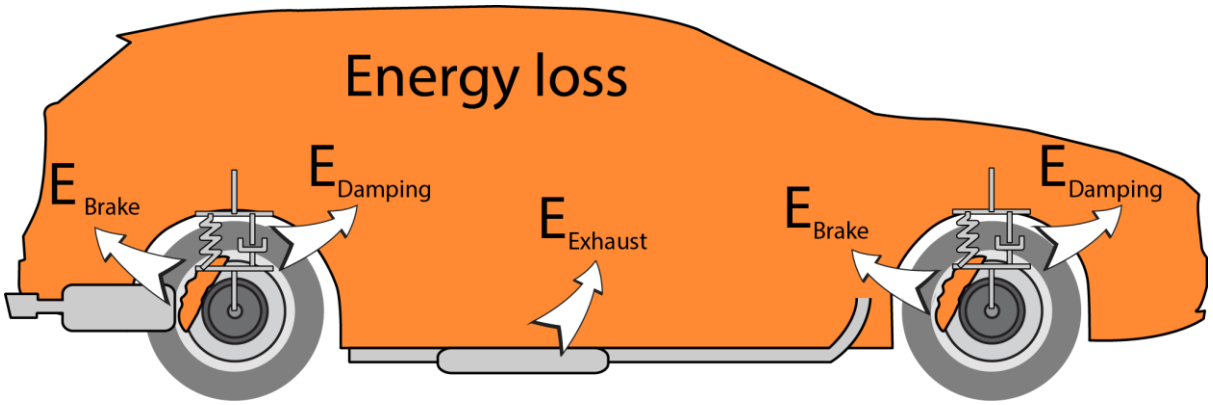

Energy recovery systems in cars and detail study of flywheel regenerative braking systems

JONATHAN FAHLBECK
JOHAN KINDAHL

Bachelor's thesis in Mechanical engineering 15 ECTS
Examensarbete Högskoleingenjör 15 hp

Department of Product and production development
CHALMERS UNIVERSITY OF TECHNOLOGY
Gothenburg, Sweden 2016

Energy recovery systems in cars and detail study of flywheel regenerative braking systems

Energiåtervinnande system i bilar och detaljstudie av regenerativa svänghjulsbaserade bromssystem

JONATHAN FAHLBECK
JOHAN KINDAHL

Supervisors at ÅF AB
Marcus Fasth, Section Manager Propulsion & Energy Management.
Jonas Wärnberg, PhD, Lead Integration Engineer, Propulsion & Energy Management.

Examiner
Kjell Melkersson, Lecturer Product Development

Department of Product and production development
CHALMERS UNIVERSITY OF TECHNOLOGY
Gothenburg, Sweden 2016

Bachelor's thesis/Examensarbete Högskoleingenjör 15 ECTS
Mechanical engineering/Maskinteknik 180 ECTS
Department of Product and Production Development
CHALMERS UNIVERSITY OF TECHNOLOGY
Gothenburg, Sweden 2016
SE-412 96 GOTHENBURG
SWEDEN
PHONE: +46 (0)31-772 10 00

Publisher:
Department of Product and Production Development
Gothenburg, Sweden 2016

ACKNOWLEDGEMENTS

This project was conducted as a bachelor thesis within the mechanical engineering program 180 ECTS at Chalmers University of Technology. The work encompassed 15 ECTS and was carried out in collaboration with ÅF AB during the spring of 2016.

We hereby want to thank the contributing supervisors at ÅF AB, Marcus Fasth and Jonas Wärnberg who both oversaw the whole process and gave good feedback throughout the project. We also want to award a big thank you to Ingrid Sjunnesson who provided help with the report in final stages of the thesis. Finally, we want to thank our examiner Kjell Melkersson who believed in our initial idea for a thesis project, supported us and provided constructive feedback along the way.

ABSTRACT

In today's society it is becoming increasingly more important to regenerate as much energy as possible to reduce the energy losses of any given system. This especially applies when it comes to systems within the automotive industry. Based on this fact, a market research has been conducted for the consulting company ÅF AB. This market research focused on different ways of regenerating energy losses in systems after the combustion process in cars. Included within its scope was systems installed in the chassis, exhaust and engine of the car. The results of the market research showed that an electric motor regenerative braking system was the superior solution. This with regards to the following criteria; cost, complexity and efficiency. The market research in turn lead to a detail study of a flywheel regenerative braking system. This since it was deemed a more interesting research subject by the stakeholders. In the detail study, different manufacturers and types of systems were examined. The most promising system was a purely mechanical flywheel system. Within the detail study, dimension calculations with regards to some volume and weight constraints for the flywheel itself were also conducted. The dimension calculations concluded that the flywheel should be designed as a light weight, fast rotating, annular disc with its mass at a large radius. The material used for this disc should be high strength and light weight, such as carbon fibre.

SAMMANFATTNING

I dagens samhälle blir det allt viktigare att återanvända så mycket energi som möjligt för att reducera förluster i varje givet system. Detta gäller speciellt när det kommer till system inom bilindustrin. Baserat på detta genomfördes en litteraturundersökning åt konsultföretaget ÅF AB, där olika sätt att återvinna förlustenergi i system efter förbränningsprocessen i personbilar betraktades. Områden som arbetet omfattade var system som var ämnade för installation i chassit, avgassystemet och i själva motorn. Resultaten från litteraturundersökningen visade att ett bromssystem baserat på regenerativ verkan i en bilens elmotor var det vinnande konceptet. Detta med avseende på följande, i förväg specificerade kriterier: kostnad, komplexitet och effektivitet. Litteraturundersökning ledde i sin tur till en detaljstudie av ett svänghjulsbaserat bromssystem. Detta eftersom det ansågs mer intressant ur intressenternas perspektiv. I detaljstudien undersöktes och utvärderades olika typer av system från olika tillverkare. Det mest lovande systemet var ett helt mekaniskt svänghjulssystem. Inom detaljstudien utfördes även dimensionsberäkningar för själva svänghjulet med avseende på volyms- och vikt-begränsningar. Beräkningarna visade att svänghjulet bör vara konstruerat som en lättviktig, snabbt roterande ihålig skiva, med massan koncentrerad till en stor radie. Materialet på denna skiva bör vara av hög styrka och låg vikt, förslagsvis någon typ av kolfibermaterial.

NOMENCLATURE

BSD	Ball Screw Damper
C.F	Carbon Fibre
CAD	Computer Aided Design
CATIA	CAD program
CFT	Clutch Flywheel Transmission
CVT	Continuously Variable Transmission
DC	Direct Current
EGR	Exhaust Gas Recirculation
EMRB	Electric Motor Regenerative Braking
EU	European Union
EV	Electric Vehicle
F1	Formula One
FEM	Finite Element Method
FRB	Flywheel Regenerative Braking
HED	Hydraulic Electromagnetic Damper
HEV	Hybrid Electric Vehicle
ICE	Internal Combustion Engine
KERS	Kinetic Energy Regeneration System
LMD	Linear Motion Damper
MF	Mechanical Flywheel
MGU-H	Motor Generator Unit – Heat
MGU-K	Motor Generator Unit – Kinetic
NEDC	New European Driving Cycle
ORC	Organic Rankine Cycle
PEG	Piezo Electric Generator
PHEV	Plug-in Hybrid Electric Vehicle
RPD	Rack-Pinion Damper
RPM	Revolutions Per Minute
SRB	Spring Regenerative Braking
SUV	Sport Utility Vehicle
TEG	Thermal Electric Generator
u	Radial displacement
v.M	von Mises (stress)

E [J]	Energy
b [m]	width
c	r/b ratio
I [kgm^2]	Mass moments of inertia
r [m]	radius
u [m]	Radial displacement
ν	Poisson's ratio
ρ [kg/m^3]	Density
σ [MPa]	Principle stress
ω [rad/s]	Angular velocity

TABLE OF CONTENTS

1. INTRODUCTION

In this chapter the core problem and aim of the project is described to substantiate the reason as to why the project is conducted.

1.1. Problem description

In the current society it is becoming increasingly important to optimize all available systems to use the energy as efficiently as possible. This is especially true when it comes to the transport industry since it is a large, contributing factor to today's global environment issues. When it comes to personal transportation such as automobiles, there are still a lot of models that utilize some sort of internal combustion engine. These engines have a relatively low efficiency, especially when looking at the energy per kg fuel used. It is therefore of great importance to try to reduce the energy loss from other systems in the car as much as possible.

1.2. Purpose

The project is founded in a need from ÅF AB to get a general picture of what is currently available and under development when it comes to systems that reuse and utilize energy that is otherwise regarded as loss energy in car systems. This in order to understand what type of systems could be applicable in their business.

The main aim of this project is to in a general way investigate systems that utilize loss energy from car systems after combustion, such as springs, brakes, thermal losses and vibrations etc. and use it in the propulsion of the car. This with respect to the following criteria: cost of system, how easy the system is to implement and the efficiency of the system.

1.3. Limitations

This project incorporates solutions which are intended for use in cars. Systems that are developed for heavier transportation such as busses and trucks could be investigated with regard to their applicability within the car industry, but the main focus is on systems intended for cars. The project is going to focus as much as possible on relatively new, existing solutions, but systems under development are also of great interest. Further limitations of the project are that it includes only systems revolving around the reuse of energy dissipated after combustion that is otherwise considered as energy loss. There will in other words be no consideration of systems intended for optimizing the efficiency of elements of the base engine. This excludes systems that act in the combustion process. Other limitations are that the detail study only incorporates selected parts of one system. Other parts may be mentioned in short, but not studied in detail.

1.4. Project questions

- What current systems are available that reuse and utilize energy losses when propelling the car?
- Which of these systems are most interesting to investigate with regards to future applications?
- How can the chosen system be enhanced and/or changed with regards to the following criteria: cost, efficiency and complexity?
- How well do the changes/enhancements comply with the theory when applied in a use case?

1.5. Disposition

This paper is divided into two different parts, part A and part B. Part A is a market research where different systems are evaluated with respect to the chosen criteria. Part B is a more detailed study of a selected subsystem from the market research. There is also a verification part of the results in the detail study briefly mentioned at the end of part B. This verification part is available in full in appendix 3.

The first two parts can be read separately, even though part B is a result of the conclusions drawn from part A. The verification part in appendix 3 is highly dependent on results from the part B and it is thus recommended to read part B first.

2. THEORETICAL BACKGROUND

In this chapter some basics about why energy regeneration systems are needed in automobiles are presented. The chapter also seeks to give some insight into which systems in the car that have the potential for energy recovery. Lastly the distinguishing characteristics between different hybrids are explained.

2.1. Hybrid systems

Even today in 2016 most cars are propelled by some form of Internal Combustion Engine (ICE). In some cases, there might be for example an electric motor providing extra power making the car a hybrid, but the majority of cars in use are still running on either diesel or petrol. Hybrid Electric Vehicles (HEV) and fully Electric Vehicles (EV) both utilize an electric motor to some degree. In the case of hybrid vehicles, the motor can be used for different purposes, depending on what type of hybrid that is regarded. There are three main types of hybrids: full hybrids, plug-in hybrids and mild hybrids (Cobb, 2014). Full hybrids can use their ICE to generate power to the electric generator, use the two systems in tandem or separately. Plug-in hybrids are very similar to full hybrids, but they generally have larger batteries to accommodate the option of plugging in the car to the electric grid when it is stationary. Mild hybrids have electric motors that always works in tandem with some sort of ICE-unit. They cannot operate on their own (Cobb, 2014).

2.2. Energy losses in car sub-systems

The problem with engine systems that are dependent on petroleum based liquids is in general that they can be considered quite ineffective with their relatively low efficiency. Added to that is the fact that energy dissipation is present in all sub-systems of the car. This in the form of losses in the brakes, dampers, parasitic[1] losses in the engine itself, heat losses in the exhaust system and so on (U.S Department of Energy, u.d.). Figure 1 illustrates some of the sub-systems in the car that experience energy losses. The losses illustrated are energy being converted in the brakes, damping and the exhaust system. Most of these losses are heat dissipating during mechanical processes, such as the friction. The brakes for example are installed to provide means of decelerating the vehicle, thus helping with speed alteration. This is usually done by applying a brake pad to a brake disc which in turn creates friction and slows down the wheel. In this instance the rotary kinetic motion of the wheel is turned into heat energy which heats the brake discs. In the case of the damping system it is designed to cushion the driver of the vehicle from the uneven road surface. When the damper moves up and down inside of the spring, potential kinetic energy is transformed. Again, most of this energy dissipates in the form of heat in the damper. Lastly the exhaust systems which has the function to redirect the exhaust gases from the combustion process in the engine compartment. This exhaust gas is very hot, making the exhaust pipe hot. This is yet another example of energy being converted to heat and having to be cooled down unwantedly.

[1]Systems that take energy without actually doing anything to propel the car, such as the car heater etc.

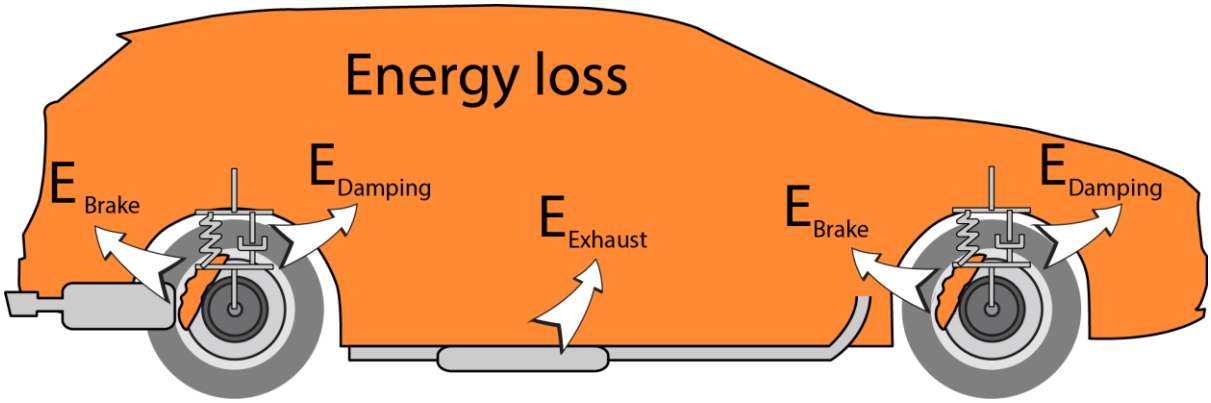

Figure 1: Illustrative figure of some energy loses from sub-systems in the car

2.3. Energy regeneration systems

As mentioned previously, all of these energy losses are unwanted. They are a by-product of the fact that energy can only be transformed and not destroyed, thus making it obviously preferable to have as low losses as possible. This is where energy regeneration systems come into play. The concept of energy regeneration is to, in some way convert the loss energy, store it and then use it in some useful way. The first and foremost way that the energy could be used is to actually propel the car. This can be done in a number of ways, some of which are going to be explained more thoroughly in part A. The short version is that the energy can be stored for example chemically in a battery or a supercapacitor or kinetically in some mechanical device then used and utilized to propel the vehicle for later use. Other ways of utilizing the recovered energy is of course possible such as a conventional. Although, in this report the focus lies on systems that in some way assist the cars movement.

3. METHOD

In this chapter the methods used in part A, B and C are described. These parts correspond to the gates/milestones set in the planning of the project work. Note that some of the methods are more thoroughly described in the chapter where they are used.

3.1. Energy regeneration systems

The energy regeneration chapter (part A) is in fact a market research chapter where different energy regenerative systems are presented and compared with respect to the following criteria: efficiency[2], complexity[3] and price[4]. The number of manufacturers and the stage/phase[5] of development that the concept was currently in were also of great interest.

First a brainstorming process was conducted. This was done to divide the upcoming system research into three different categories. The brainstorming resulted in a disposition of: engine related systems see section 4.1, chassis related systems see section 4.2 and braking systems see section 4.3. The research work itself was then conducted over a time period where every day had been assigned a specific research area, as can be seen in table 1. The research data was collected via an extensive database research, using different keywords.

WEEK	1	2	3	4	5
DAY 1	ENGINE: Heat	ENGINE: Buffer	CHASSIS: Damper	BRAKE: Spring	Summary, evaluation and choice of system
DAY 2	ENGINE: Kinetic	CHASSIS: Damper	BRAKE: Flywheel	Summary and evaluation	GATE 1
DAY 3	ENGINE: Vibration	CHASSIS: Damper	BRAKE: Regenerative	Summary and evaluation	

Table 1: Time schedule for the first phase of the project work.

When the research work was finished, an evaluation process using an evaluation/elimination matrix took place. The matrix used was a Kesselring matrix, where different concepts/systems were compared against each other numerically. This is more thoroughly described in section 4.4. Because the data connected to each system was difficult to compare against one another (since all tests conducted were based upon different scenarios using different evaluation methods) educated guesses had to be made as to what value to assign to each system. These educated guesses were based upon the data in the research material and consultation with the stakeholders. The reason why elimination matrices were used was partly to compare the different systems against one another and partly to support and justify the system chosen for a more detailed study. However, the system chosen for the detailed study was not exclusively supported by these matrices, but also by a discussion between the stakeholders involved. More details about this is available in section 4.5. Five Kesselring matrices were used. In the first step there was one for each category (engine, chassis and brakes). After this, the winners from each category was compiled into one matrix see section 4.4.4. Lastly the chosen system was put against the other winners-matrix see section 4.5.

[2] Estimation of how well the system could regenerate energy (regenerative ability)
[3] Estimation of how complex the system is and how hard it would be to install in a current car platform
[4] Estimated cost of the system
[5] At what stage/phase are the product in? Development-, fully implemented and available or in a research-phase?

3.2. Detail study of a flywheel system

Part B also began with a market research using keyword searches in databases. This research focused on two variants of a flywheel regenerative braking system namely mechanical and electro-mechanical. The aim was to find out the main components of a whole system, how they integrated with one another and what different manufacturers that was making this kind of system today.

Interesting components such as the flywheel gear box was observed and described, see section 5.2, in a general way. An interview with employees at Volvo Cars was held at the Volvo cars headquarters in Torslanda, Gothenburg. This since Volvo had co-developed a flywheel breaking system with a company called Torotrak. The interview was later on a large source of information when the dimension calculation took place. A number of questions were produced before the interview took place, these questions are attached in appendix 1. Most of the questions were answered during Volvos presentations of their system that was conducted during the interview.

All calculations were done using well documented formulas for the strength of material of an annular disk (flywheel) and mechanical energy formulas see section 5.4. The reason why the calculations were made was to justify and determine the best dimensions for the flywheel itself. This after applying a number of assumptions and limitations. The calculations were executed using the program MATLAB, see appendix 2 for the MATLAB code. The dimension calculations are to be found in section 5.4 where they are more thoroughly described.

3.3. Verification of stress/dimension calculations

To verify the accuracy of the analytically calculated dimensions and stresses, a Computer Aided Design (CAD) software called CATIA V5-6R2013 was used. In CATIA the flywheel itself and an arbitrary inner hub was modulated with respect to the calculated dimensions. This is described in appendix 3. When the two parts had been modulated the built in Finite Element Method (FEM) tool in CATIA was used.

The FEM tool was first applied to the flywheel itself to verify the stress calculations done in section 5.4. Constraints were attached to simulate a rotating disk. Later on the flywheel-hub assembly was simulated as a shrink-fitting connection to verify that the stress increased when this type of connection is applied.

4. PART A: ENERGY REGENERATION SYSTEMS IN CARS

This part is focused on a market research conducted with respect to the following criteria: cost of system, complexity of system and the efficiency of the system. It is laid out to survey the systems currently available and under development that utilize energy that is otherwise considered as loss energy in cars. This chapter is divided into three different subcategories: engine systems (section 4.1), chassis systems (section 4.2) and brake systems (section 4.3). The presented information is acquired through various databases.

4.1. Engine systems

This section is a compilation of different engine systems, specifically systems that are intended to be installed after the base engine[6] in the car. The section includes systems that reuse waste heat from exhaust gases, systems that harvest vibrational energy from the engine and a system which regenerates kinetic energy.

4.1.1. Turbo compound

There are two types of turbo compounds, mechanical and electronical (Latz, 2007). They are quite similar with respect to their functionality. Hot exhaust air flow through a turbine downstream the exhaust pipe which makes the turbine rotate. This is illustrated in figure 2. The power produced by the turbine can either be utilized by an electric generator or mechanically via gears connected to the crankshaft (Sherman, 2014). Turbo compounds are today used by Volvo trucks and Scania. A modified system called Motor Generator Unit Heat (MGU-H) was also used in 2014 F1 season (Ramsey, 2014).

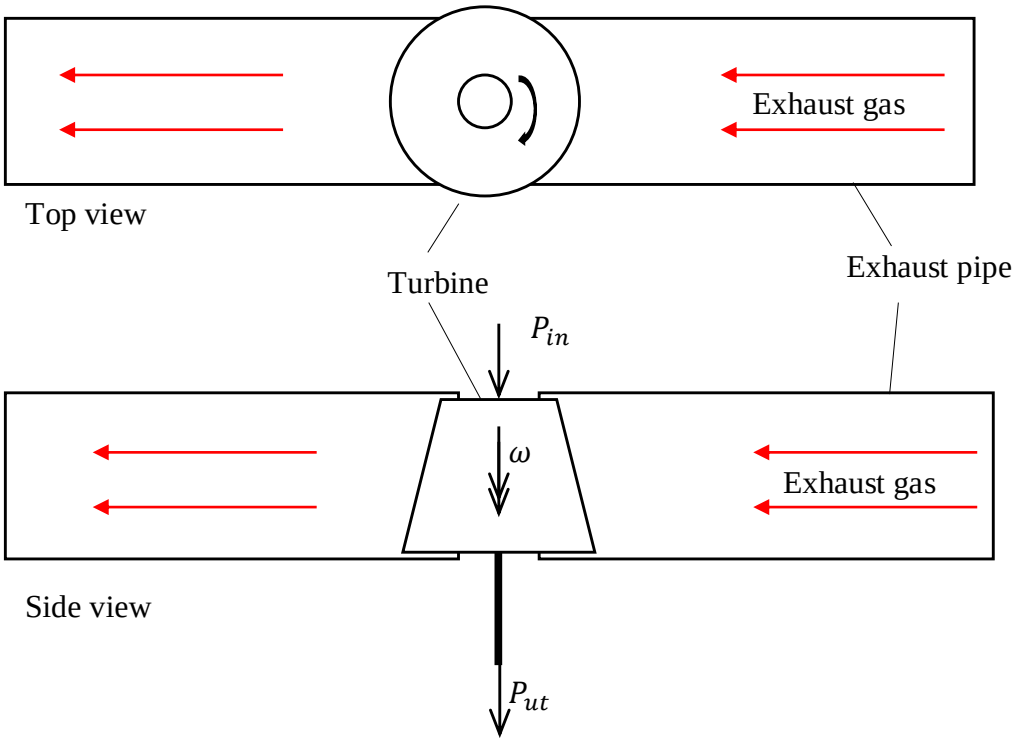

Figure 2: Illustration of hot exhaust air flowing through the exhaust pipe, making the turbine rotate.

[6] Base engine refers to the parts of the engine that are involved in the combustion process.

Ismail et. al (2015) state that a turbo compound system is easy to install and has a lower installation cost than for example the Rankine cycle system described in section 4.1.4. The turbo compound can either work as a standalone unit or, for more efficiency, it can be combined with a conventional turbo system. Simulations conducted by Legros, Guillaume, Diny, Zaidi, & Lemort (2014) show that a fuel consumption reduction of about 3%, without a conventional turbo configuration was achievable in the New European Driving Cycle (NEDC). The fuel reduction with a conventional turbo configuration and a turbo compound system was about 5% in the same cycle.

Summary and evaluation of Turbo compound

The turbo compound system has a medium to high complexity, depending on if the power is stored electrical or mechanically. If the turbine shaft is connected to an electrical generator there will be a lot fewer parts and therefore, a less complex construction. The car does on the other hand need to be a HEV if the regenerated power is intended to drive the car, when using a generator. The turbo compound system is estimated to have medium cost (Legros, Guillaume, Diny, Zaidi, & Lemort, 2014), but the electrical version is a bit cheaper than its mechanical counterpart.

4.1.2. Motor Generator Unit Heat (MGU-H)

The MGU-H system is mainly used in racing cars, such as Formula 1 cars. The system was introduced and developed for the 2014 F1-racers and has not been implemented or objectively tested for personal transportation vehicles yet (Nicolas, 2014). The system is attached to the turbo shaft (see figure 3) to generate electric power, which means that the MGU-H is driven by the exhaust gas (Mackenzie, 2014). MGU-H also functions as a regulator for the speed of the turbo, which indirectly affects the air flow to the engine when active (Petrány, 2014). This increases the power of the engine if done correctly.

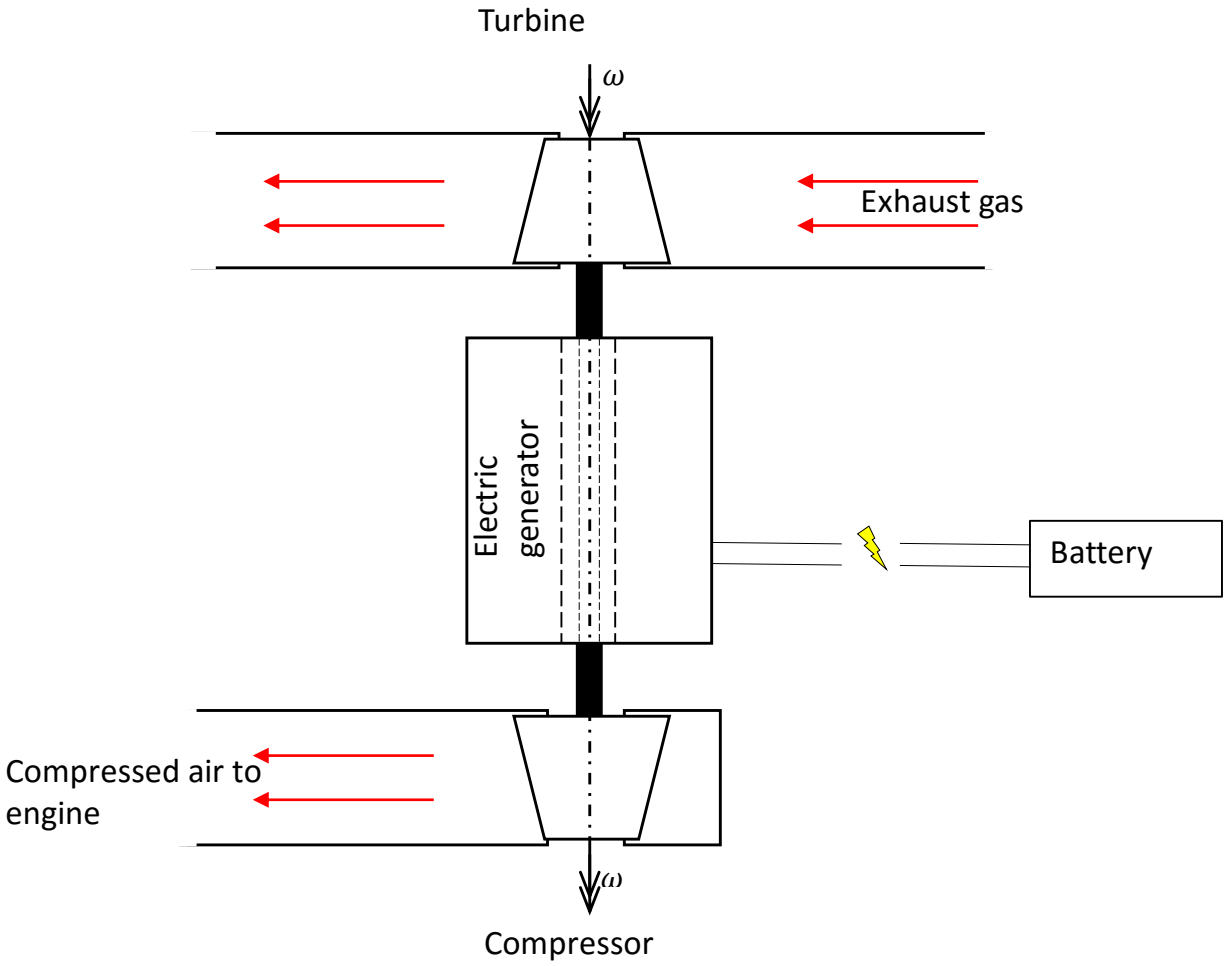

Figure 3: Illustration of a MGU-H harvesting energy from turbine shaft in a turbo.

Summary and evaluation of MGU-H

The MGU-H unit itself is a quite simple system with an electric generator and a rotating shaft. But in order to mount the MGU-H, the turbo system of the car must be re-engineered and some advanced optimization to the unit must be conducted in order to make it work both as a generator and a turbo booster. These changes and optimizations will most likely increase both cost and complexity. Because of this, further tests and research must be performed in order to draw conclusions as to if the system works in light duty vehicles[7].

4.1.3. Piezo Electric Generator (PEG)

The small amounts of energy that is produced when the engine compartment of an automobile vibrates while in motion is a possible source for energy harvesting. One way of doing this is through piezoelectric devices, see figure 4. One possible application for the energy this device is generating is to power low power sensors, without having to connect them to the on board power supply (Francesco, Igor, Helios, & Luca, 2013). The amount of energy that is produced depends on where the sensor is placed. Besides in the engine compartment, a specifically good spot to place the PEG in the trunk of the car where,

[7] Vehicles such as cars, lighter trucks etc.

according to (Zhu, Mingjie, & Yuanqin, 2012) a useful amount of energy is produced for sensors. The typical amount of energy produced by piezoelectric generators can be measured to be to up 150 µW, as shown in testing done by Glynne-Jones, Beeby, Tudor, & White (2004).

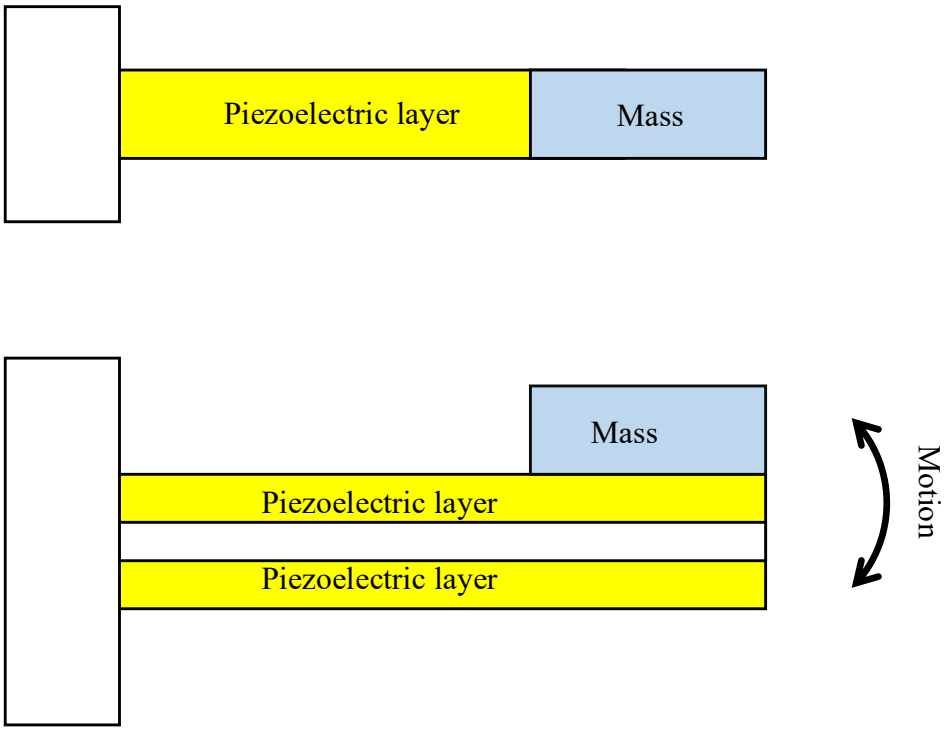

Figure 4: Illustration of a piezoelectric device

Summary and evaluation of vibration energy

Due to the low amount of output power produced by systems with piezoelectric generators, this particular solution is not of great interest when considering propelling the car or powering major subsystems of the car. The application of PEG is more relevant when it comes to remote sensors, such as temperature and pressure gages.

4.1.4. Organic Rankine Cycle (ORC)

An organic Rankine cycle is a process that is able to convert hot exhaust gas into electrical or mechanical energy by means of utilizing a simple closed system. The word organic refers to that the so called working fluid that receives heat being organic (Sprouse & Depcik, 2013).

The system consists, according to Latz (2013) of four parts in a loop. The working fluid is first pumped into a heat exchanger, see point 1 in figure 5, where it comes indirectly in contact with the hot exhaust gas. This transfers heat to the working fluid which turns it into a gas. The working medium then passes through a turbine where it expands and mechanical and/or electrical energy is extracted, see point 2 figure 5. The gas is then compressed back into a liquid in a condenser, see point 3 figure 5 and then goes back to the pump (Latz, 2007).

According to Latz (2013) no real implementation of an ORC systems have been done in passenger cars, though some tests have been conducted on heavy transportation, freight ships etc. These tests points to there being some merits to exhaust gas recirculation-systems but there is an inherent complexity to ORC-systems due to the volume they take up and them being heavier than some other alternative heat powered solutions (Latz, 2007). The fuel savings on research testing in passenger cars have been up to 10% with different systems implemented by Honda and BMW (Latz, 2007), however these figures are not definite.

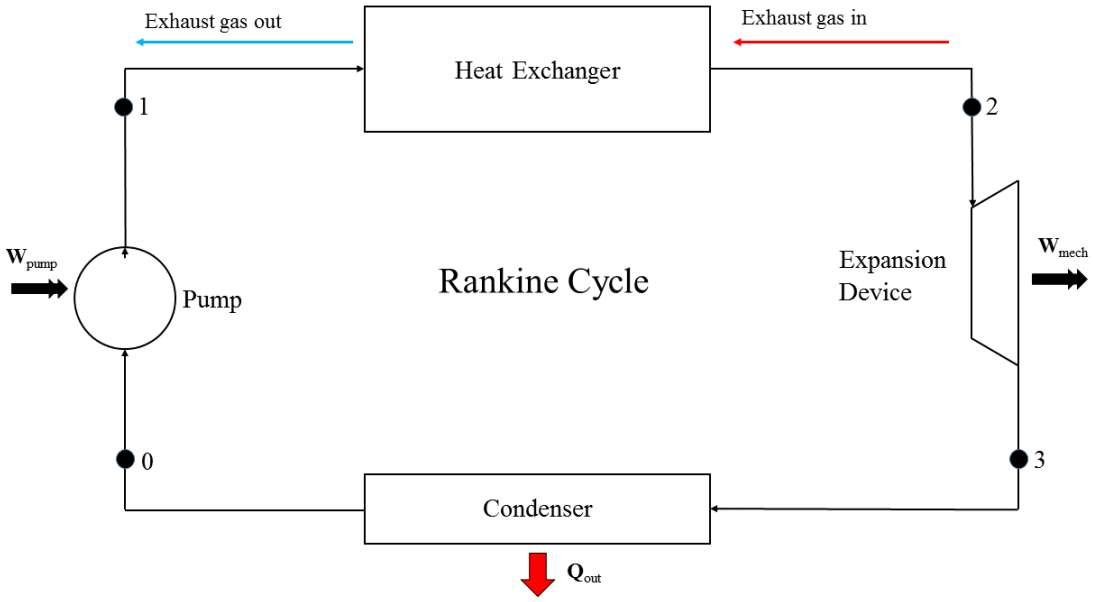

Figure 5: Schematic of Rankine cycle in a system

Summary and evaluation of ORC

When considering ORC-systems for light-duty vehicles there are problems with complexity due to the large volume of the system. This is something that could possibly tie into the cost of the system since more complex systems tend to be more expensive. The energy savings are up to now relatively unconfirmed, but shows promise when it comes to preserving waste heat energy. Further testing must be conducted thought to make any conclusions as to the applicability of the system in passenger cars.

4.1.5. Thermal Electric Generator (TEG)

Thermal Electric Generators (TEG's) work due to the so called Seebeck effect.
"It refers to the electrical potential generated when a temperature gradient is applied across the junctions of two dissimilar conductors" (Latz, 2007).

When the warm exhaust gas meets the hot side of the generator it gives potential energy to the electrons on that side, see figure 6. The temperature gradient that is now created between the cold side and the hot side makes the electrons move between the two types of semi-conductors that is placed between the two sides. This creates a current which can be used to charge a battery via an electric generator (Latz, 2007).

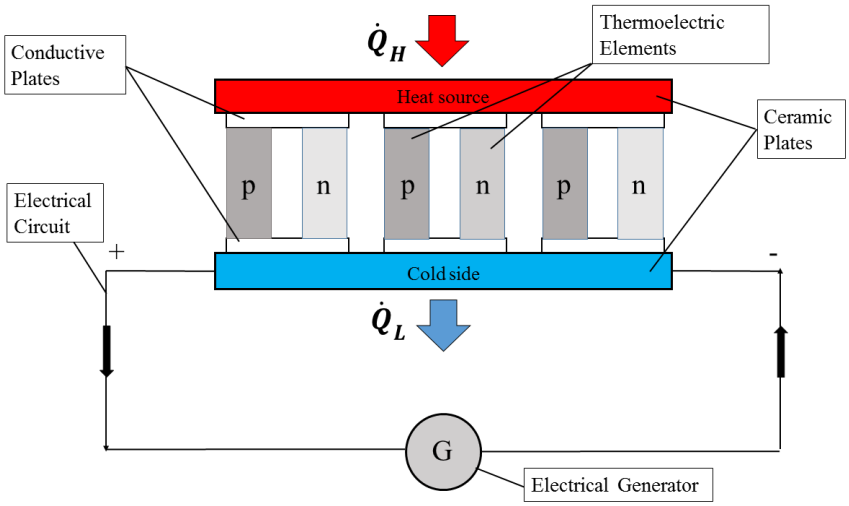

Figure 6: Schematic picture of TEG

The complexity of a system that is using TEG's depends on a number of different factors. One is that, according to Jeng & Tzeng (2013) there are some limitations as to (for example) during which rotational speed that the system can operate. In their experiment with at Toyota 2200 c.c. they concluded that a higher RPM than 2500 could result in the generators overheating and resulting in them being damaged. There is also an optimal air flow during which the TEG's produce optimum power (Jeng & Tzeng, 2013). Finally their testing show a resulting power output of 6 TEG's of 16 W.

Summary and evaluation of TEG

Thermal electrical generators could probably be implemented pretty easily in an existing exhaust pipe, as characterized in testing conducted by Prakash, Christopher, & Kumarrathinam (2015) where a TEG-unit was connected to an existing tailpipe silencer. The limitations of the system when it comes to complexity might be how many generators that are requried to get at sufficienct power output. There might possibly be a point where the system becomes useful in terms of energy output but where it is financially unviable. This information is however not avaible as of now.

The efficiency of TEG's seems to be relatively low. In a test where the TEG was connected to the tail pipe silencer Prakash, Christopher, & Kumarrathinam (2015) were able to regenerate a maximum power of 4 W. When comparing to testing conducted by Jeng & Tzeng (2013) were an amout of 16 W was produced by 6 generators it is obvious that the system is not very efficient yet.

4.2. Chassis systems

This section includes four different types of regenerative damping systems. There is also a general section aimed at explaining the theoretical power that a regenerative damping system could be able to achieve. It is important to note that the damper in a car is a part of the suspension system. It is placed inside the spring to dampen the oscillating movement of the car.

4.2.1. General about regenerative damping

Today there are no regenerative damping systems put in regular production cars. But reports say that some companies such as: Audi (Maric, 2015), Levant Power and Intertronic Gresser (Daryl, 2015) have experimented with the technology and its possible application in passenger cars. The regenerative suspension field shows great potential in the future, especially since HEV and EV are becoming more and more popular. Exactly how much energy a regenerative damping system can produce is relatively hard to estimate. Zuo & Zhang (2013) for example state that "What is the potential of harvestable power? The number in literature [4–11] varies in a very large range, from 46 W to 7500 W". This is obviously partly dependent on road conditions.

4.2.2. Rack-Pinion Damper (RPD)

The purpose of a rack-pinion damping system (RPD) is to turn the linear motion of the dampener into rotational motion (Zhang, Peng, Zhang, & Zhang, 2013). This can be done by attaching a rack gear to the inside of the outer casing of the dampener and connecting it to a pinion that is connected to the wall of the inner casing see figure 7. The power is then transferred via a planetary gear to a shaft which is connected to a generator (Zhongjie, George, Liangjun, & Yi-xian , 2013). The relative motion of the two casings can now be transformed into torsional force and thus generate for example electric power. The damping from this type of system is provided by the resistance of the electric generator (Xu & Guo, 2010).

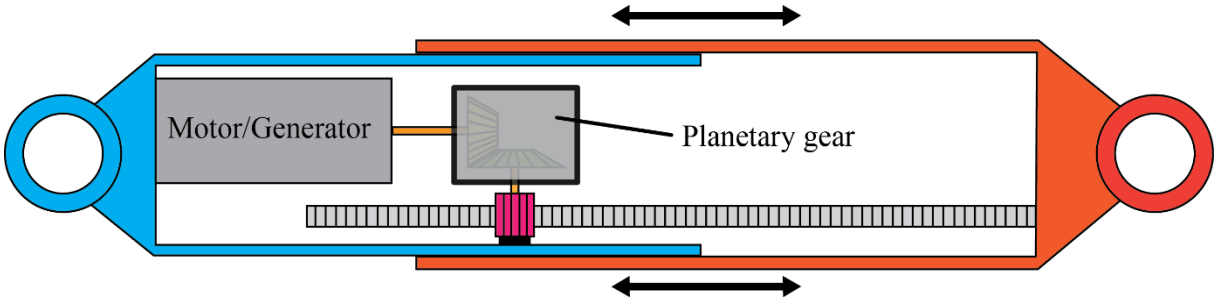

Figure 7: Rack-pinion dampening system

The rack-pinion system has some advantages when compared to other types of systems with linear to rotary motion conversion. The rack-pinion system is for example much more effective when working during higher frequencies than the ball-screw system mentioned in section 4.2.4 (Zhongjie, George, Liangjun, & Yi-xian , 2013). A system based on torsional motion can generally speaking produce a larger damping coefficient than linear systems considering the space required. When testing a rack-pinion system on a Chevrolet Surburban SUV 2002 model, Zhongjie et. al (2013) were able to extract 58 - 68 W/damper at peak power. The average power was however considerably lower at just 3,3 - 4,8 W per damper.

Implementations of this type of system requires a redesign of some parts of the vehicle due to the size of the components. This is however possible to work around by designing the system to be able to be retrofitted (Zhongjie, George, Liangjun, & Yi-xian , 2013). In the test conducted by Zhongjie et al (2013) it was for example the outer diameter of the bigger damper casing that needed resizing.

Summary and evaluation of RPD

The current form of rack-pinion damper is still premature, which means it is quite hard to estimate some aspects of the system if it were to be put into mass production. But when it comes to complexity it should be said that all systems using mechanical gears in this manner are inherently more complex and usually subject to greater losses in efficiency. The pure efficiency of the system described is relatively low, but as stated earlier in the general section 4.2.1, there is a large theoretical potential over all for spring mounted systems. Although RPD as a particular solution does not seem that promising.

The implementation of this system into existing vehicles should not be that difficult since it seems possible to alter the dimensions of the system in order to make it fit in the current wheelhouse of passenger cars. It is important to note though that changing the dimensions might affect power output. Lastly, the fact that this type of system can replace the current damping solutions present in the car could possibly lower the implementation cost of the system.

4.2.3. Hydraulic Electromagnetic Damper (HED)

The basic principle of a HED is to combine mechanical, hydraulic and electromagnetic elements into the shock-absorber. This in order to make use of the efficiency of an electromagnetic system while using the mechanical dampening properties of a hydraulic and mechanical system (Lin, Yang, Xuexun, & Jun, 2010).
The system can be constructed in a number of different ways, but as shown in the schematic figure 8, it usually contains: a hydraulic motor, a generator, a number of check valves (depending on the layout of the system) and an accumulator.

The system works in the following way see figure 8. During the extension stroke of the piston, check valve 1 is closed and check valve 2 is open. This forces the high pressure hydraulic fluid from the rod chamber into the pipe, through the hydraulic motor and thus provide power for the generator. While this is happening, low pressure hydraulic fluid is forced into the rod-less chamber and the accumulator compensates the cavity. During the compression stroke, check valve 1 is open and check valve 2 is closed. This forces the hydraulic fluid into the rod chamber, which increases its pressure (Zhang, o.a., 2014). The process is then repeated during each compression and extension.

Simulation models suggests that the efficiency of the HED system shown in figure 8 would be around 33 W per dampener. This when a constant frequency of compression and extension is applied (Zhang, o.a., 2014). However, a different simulation with a slightly different system layout supposed that an optimal power output of about 1.1 -1.7 kW could be extracted under similar conditions (Lin, Yang, Xuexun, & Jun, 2010). Though worth noting is that these designs may differ in for example cylinder diameter, fluid viscosity and so on. The

simulation models might furthermore not be comparable with respect to simulated road conditions.

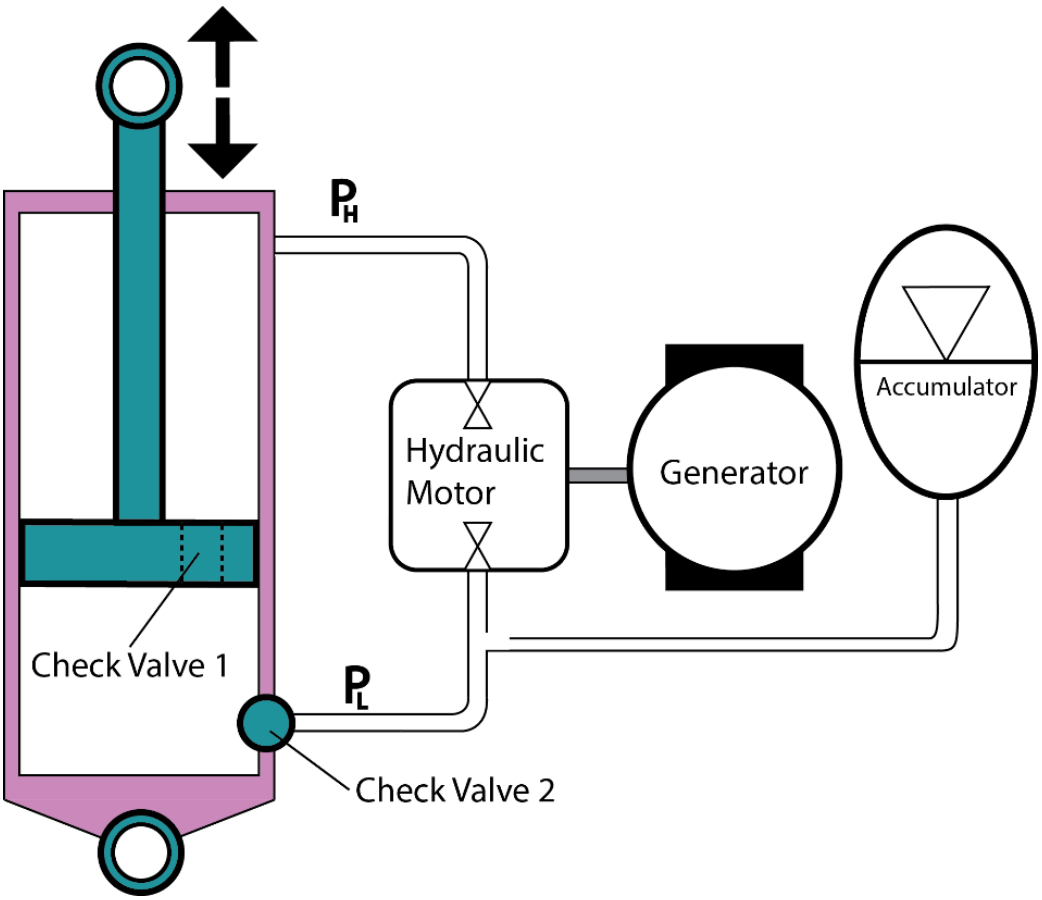

Figure 8: Schematic drawing of hydraulic electromagnetic damper

The proposed system is of similar dimensions as the current dampening system in cars. It also provides comparable dampening characteristics as a "normal" non-regenerative hydraulic dampener (Lin, Yang, Xuexun, & Jun, 2010). It does however require external parts to accommodate the hydraulic motor and other parts that are included in the hydraulic system.

Summary and evaluation of HED

As the number of implementations of this type of systems is limited in road vehicles, even within prototype test fleets, it is hard to judge several aspects of its viability in mass production. What can be said though is that it seems to provide a useful amount of output power, when considering above mentioned studies. It is important to note though that the last mentioned study produces a suspicious amount of output power when compared to other dampening systems and the numbers have to be evaluated further to verify the results.

The added cost and complexity of the generator in combination with parts included for the hydraulic part of the system might make the system less interesting from a mass production stand point. Intricate hydraulic systems tend to add a certain amount of complexity. To judge this system more conclusively there have to be more tests conducted on actual road vehicles.

4.2.4. Ball Screw Damper (BSD)

The BSD system is an alternative to a conventional damper, with the advantage of energy regeneration ability. This main components of this type of shock absorber system are a ball screw mechanism, which converts the translational movement into a rotational movement and a DC generator to change the mechanical energy into electrical (Kavianipour & Montazeri-Gh, 2014). These are illustrated in figure 9.

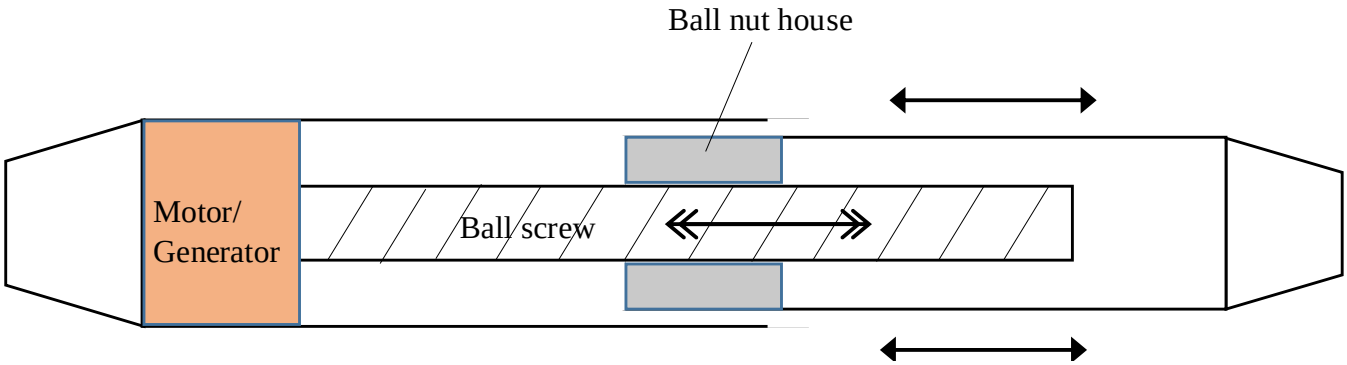

Figure 9: Illustration of a ball screw damper.

There have been a couple of tests and experiments with BSD conducted by Zhang, Huang, Yu, Gu, & Li (2007). They claim that they were able to regenerate 12 W on average from one damper during different road profiles in a vibrating test rig. Another experiment by Kawamoto, Suda, Inoue, & Kondo (2007) showed an average regeneration of 15 W per damper while simulated in a C-class[8] road at 80 km/h in a test rig as well.

Summary and evaluation of BSD

The ball screw system is still in a developmental stage and further testing and evaluation is needed before it can be put into large scale production. The system uses a quite simple method for harvesting energy with one rotating part and one oscillating part. The complexity therefore seems to be relatively low when compared to for example the rack pinion system, but it still has a higher complexity than for example a linear motion system described in section 4.2.5. When it comes to cost it is probably in the same range as the complexity, although it will require a great deal of research in order to make this type of system work as required which then would increase the price. The research which was presented earlier shows a fairly poor efficiency in this particular system. However, in the general text about regenerative dampers (section 2.4.1.) it was stated that this type of systems has pretty good theoretical efficiency, so with further testing and development the ball screw system might have applicability in the future.

4.2.5. Linear Motion Damper (LMD)

The linear motion damper essentially contains two independent parts to harvest energy. There is a stator coil and an array of permanent magnets creating a linear generator see figure 10. The whole concept a LMD device is that potential energy from the magnet shaft is converted into electric energy while moving up and down in the stator (Zuo, Scully, Shestani, & Zhou, 2010). When it comes to industry applications a company called Bose seems to be one of very few providers of linear motion shock absorbers and their product can regenerate 25 W on average per shock absorber (Xu & Guo, 2010). Hypothetically though, there is a potential

[8] A US standard for classifying road surface roughness

power output from for an LMD system of about 150 W in electrical energy per damper when driving at 90 km/h (Zuo & Zhang, 2013). However, this estimate is based on a simulation and real conditions will probably affect those numbers significantly.

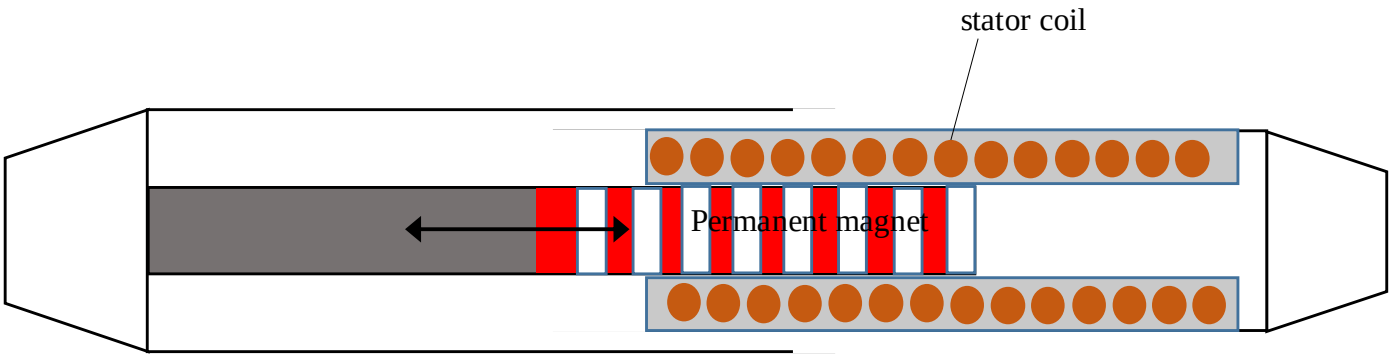

Figure 10: Illustration of a simplified linear motion shock absorber.

In a test where volume size was specified it was possible to retro fit this type of system into a BMW 530i (Gysen, van der Sande, Paulides, & Lomonova, 2011). This speaks somewhat about the low complexity of the system. In the conclusion from the BMW test it was stated that: ”The suspension system can generate power as a result of the various road vibrations”. However, their experiment was mostly about how to make an active suspension more efficient and not how to maximize the ability to recover energy. In another experiment where a quarter of a car was simulated, this type of system was able to recover around 40-43 W on average per shock absorber. In this test the system was implemented via reverse engineering and by modifying existing suspension parts (Khoshnoud, o.a., 2015).

Summary and evaluation of LMD

Exactly how efficient a LMD system can be with further development is hard to say. Earlier in this section an experiment suggest that it is possible to harvest around 160 W for a whole car with LMD. But a company that manufactures this type of system can only extract 100 W.

In both experiments mentioned earlier in this section, the LMD system was either fitted to an existing car without modifications or in an available suspension system that obviously had to be reengineered in able to fit it. A conclusion that can be drawn from that is that a linear motion shock absorber probably has a low complexity when it comes to installation into existing cars. At least compared to some of the other solutions such as HED.

Not much is mentioned about cost and price for systems which have the ability to regenerate energy in the data that has been collected. But in general electromagnetic suspension is only fitted to more expensive cars, which means that those type of systems tend to be expensive as well. Nevertheless, with more research and development, an increased efficiency to a lower price is to be expected.

4.3. Brake systems

Brake energy can be harvested in a number of different ways depending on system. This chapter covers three different ways of combining the normal, friction brakes with some sort of added brake system. This in order to divert as much energy as possible from the friction brakes and store it to be used for a useful purpose such as propulsion instead.

4.3.1. Electric Motor Regenerative Braking system (EMRB)

The concept of EMRB is to reverse the direction of the energy flow of the electric motor and thus converting it to a generator. When the driver pushes the brake pedal, the normal friction based braking system works in tandem with the EMRB system to slow down the vehicle. The generator offers a resistance which contributes to the car's stopping ability, while sending electric power via wires to a battery or superconductor (Lampton, 2009).

The EMRB system is present in all kinds of HEV's and EV's and can be implemented differently depending on the model. For more information about hybrids see section 2.1. In the Toyota Prius for example, the car is a full hybrid, utilizing the energy generated while braking in propelling the car (Lampton, 2009). Mazda and BMW both have energy regeneration systems which can charge up a battery and thus power electronics within the car, indirectly lowering fuel usage (BMW, u.d.) (Mazda, u.d.). Tesla on the other hand produce all electric cars and thus have the opportunity to utilize the electric motor directly since the throttle acts as a torque command, sending as much power as needed to the wheels. When the throttle command produce negative torque it regenerates power (Solberg, 2007). Figure 11 below is a schematic of a full hybrid with rear wheel drive, and the electric motor/generator placed in between the transmission and the ICE. Worth noting is that the layout might differ slightly in placing of the electric motor, whether the car is front or rear wheel drive etc. In the full hybrid Toyota Prius for example, the electric motor/generator is placed between the ICE unit and the transmission, just like in figure 11, but it could also be placed inside the transmission itself (Gable & Gable, 2014).

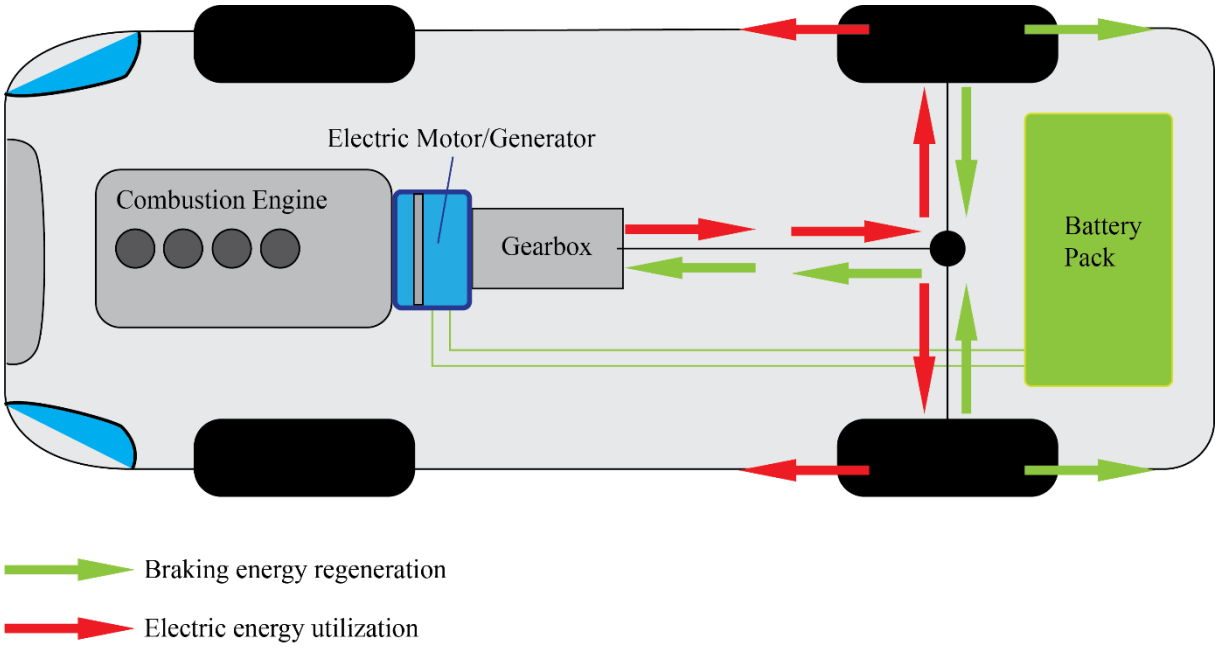

Figure 11: Rear wheel drive full hybrid with braking energy regeneration

When it comes to complexity it must be said that this type of system requires the car to have an electric motor, which means it can only really be implemented in HEV or EV cars. In for example full hybrid cars, the infrastructure already exists for controlling the current flowing to the electric motor. This means that when the driver takes the foot of the accelerator pedal, the motor stops receiving power and starts generating it, with the correct modifications to the system (Gable & Gable, 2014). In other words, when a car already is a hybrid it is a matter of programming the on board computer to be able to perform the regeneration process. One

problem in this area though might be to get the adequate amount of braking force, while producing the maximum amount of energy. Added to this is the problem of the regenerative power increasing the complexity of the driveline of the car and thus creating some safety and comfort-related issues that must be solved (Oleksowicz, 2013).

According to Yoong, et al. (2010) regenerative braking can increase the over all range of an EV with between 8-25%, this number is however just an estimate. According to Tesla, their regenerative braking system in the Tesla Roadster EV-car has a conversion efficiency from tires to battery and back to tires again of at most 64% (Solberg, 2007). Considering that the averge amount of energy dissapated (of the over all energy input in terms of fuel) while braking in a normal ICE-powered car is about 5-7% on avarage (U.S Department of Energy, u.d.), the theoretical maximal amount of energy that can be extracted probably would be about 3-4% (= 64% of 5-7%) in a Tesla.

Summary and evaluation of EMRB

This type of system requires, as previously stated, that the car has some sort of alternator or electric motor that can act as a generator. If the car is an EV or HEV already, the EMRB system could be implemented relatively easily. When it comes to EV it could be considered as a necessity to have some sort of motor regeneration. However, if you were to implement this type of system in a standard ICE car, it would be relatively complex and expensive since it would mean a rebuild of many systems in the car, as well as development of a control system for the hybrid system. It has been done however by BWM and Mazda, so they obviously thought the solution to be viable.

When it comes to efficiency there is a limited amount that can be extracted since there is a limited amount of energy that dissipates during braking with friction brakes. Although compared to other systems in this report, the EMBR system has a large potential for energy regeneration. A problem with EMBR is it being most efficient during certain points in the driving cycle. This means that the system will be more efficient in for example city traffic. Also the control system has to be calibrated for maximum energy extraction, while keeping the necessary braking function. The system does however have some merit which shows in the number of costumer cars currently available with EMRB.

4.3.2. Flywheel Regenerative Braking (FRB)

Flywheel as a concept has been around for many hundreds of years and the principle is fairly simple, a heavy rotating wheel/disk storing energy. This technology can be transferred to cars, using the flywheel as an energy storage device. The main idea is to store kinetic energy under braking using a flywheel, and then reuse the mechanically stored energy during acceleration via a transmission. In order to make sure that the flywheel system do not take any power from the engine, a clutch is needed between the driveline and the flywheel mechanism (Boretti, 2010). The system layout may vary a lot as can be seen in figure 12, but it has many similarities with an EMRB. This since the essential difference is that the energy is stored mechanically in a flywheel instead of chemically in a battery as is the case in an EMRB system (Dhand & Pullen, 2013). Cars that use flywheel regenerative braking systems may sometimes be referred to as “flybrids”.

One advantage with FRB based systems is that there are few energy transformations between the wheel and the storage. Therefore, does FRB systems have a theoretically higher potential of harvesting loss energy than for example EMRB systems. This is due to a lower number of

energy transformations. On the other hand the stored energy in FRB must be utilized pretty shortly after it is harvested due to friction losses and windage effects when the flywheel rotates (Boretti, 2010). The windage effects are however usually reduced by putting the flywheel in a near vacuum.

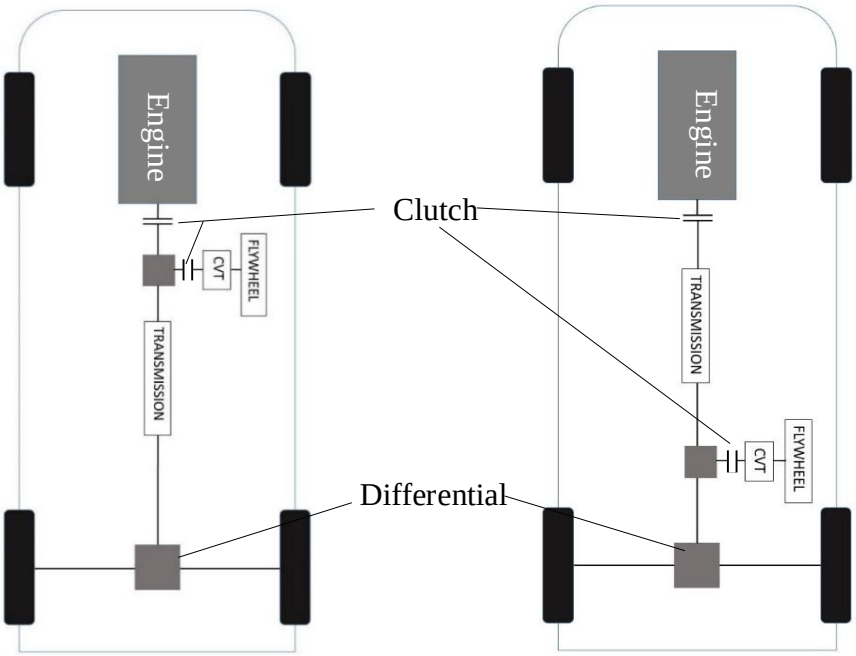

Figure 12: Schematic view of two different FBR systems. The one on the left has the system installed before transmission and the one on the right has it installed after the transmission. CVT = Continuously variable transmission

An exact number of how much fuel can be saved with this type of systems vary a lot depending on which source is reviewed. In some literature a theoretical amount of up to 30-35% better fuel consumption compared to a vehicle without the system is proposed depending on the driving scenarios (Cuspinera & Alejandro, 2013), (Ponce Cuspinera & Dunne, 2015).

Various manufacturers are working on or have been working recently on both purely mechanical solutions and electrical versions of the FRB system. In 2011 Jaguar presented a prototype vehicle containing a flywheel system and they claimed it could improve the fuel efficiency by 20%. Jaguar's development has on the other hand paused as of now since they are having problem with price and packaging. Volvo also have been working on a FRB and their prototype from 2013 may give 25% fuel reduction (Burns, 2014). Both of these percentages is in relation to the same system without the system installed. The Volvo cars prototype was purely mechanical and could add an additional 80 horse power. It was only connected to the rear wheels (Bingley, 2013).

Summary and evaluation of FRB

The FRB system shows great potential for future implementation, if the problem with cost and placing are solved. Today the system is in a prototype phase with several companies developing their own solution.

When it comes to complexity, the system requires quite a lot of space in order to fit all components. It also requires gearing optimizations and investigations of where the main

components is supposed to be mounted: directly on the differential, before or after transmission, a separate system or on the drive shaft?

Pricing for FRB could be considered as high. Jaguar cars even halted their research on a flywheel based regeneration system with the argument that it is too expensive and large, though this might have to do with the amount of cars that Jaguar is producing. It is now unclear as of now if the research is going to be continued.

When it comes to efficiency FRB shows great promise, with car manufacturers already claiming that their system prototypes have the ability to boost fuel economy with up to 25%. A theoretical maximum of around 30-35 % fuel reduction are to be found as reference in several cases. It is important to note that the energy is only recoverable while braking.

4.3.3. Spring Regenerative Brake (SRB)

A spring based system to regenerate power differs quite a bit from the two other described regenerative braking (FRB and EMRB) systems discussed earlier. In an SRB system, potential energy is stored in either a spiral or a helical spring. In figure 13, a helical spring solution is illustrated. The SRB system is connected to a non-drive shaft which begin to rotate when the vehicle starts to decelerate. This rotational motion is then transformed and stored as potential energy via gears to a spring (Nieman, 2014). When it is time to accelerate the car, potential energy is released and transformed to rotational motion and utilized to speed up the wheels via a Continuously Variable Transmission (CVT) (Myszka, Murray, Giaier, Jayaprakash, & Gillum, 2015). The system may also require some clutch mechanism in order to store and release energy.

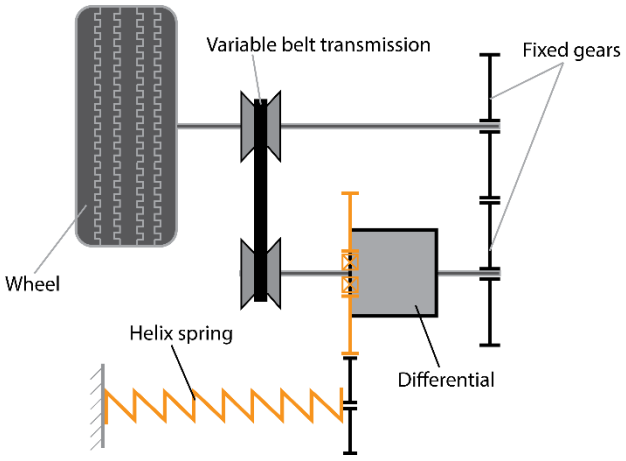

Figure 13: Principal view of a type of setup for a SRB

A test was conducted by Nieman (2014) with an SRB system in a test rig as well as in computer simulations. He propose that a fuel reduction of 8% might be possible when using an SRB system. Simulations have also been done by Myszka et al. (2015) and they show similar results, with 5.1% better fuel economy. These numbers were however based on simulations. No real life tests could be found in the literature.

Summary and evaluation of SRB

Due to all the extra components needed to implement this system in a car it has a semi-high degree of complexity. Also it will require quite a large space in the vehicle, since it is a largely separated system that is only connected to non-driven wheels. This system on the

other hand does not need a large battery pack which is a necessity when implementing for example an EMRB system. When it comes to efficiency it can be said that, from the two test results presented earlier that this system does not show great promise when compared to FRB or EMRB. Finally, the pricing is closely linked with complexity. In order to package the system into the car, certain areas must be reengineered, which increases the cost since reengineering is expensive.

4.4. Elimination

The method which has been chosen for the system elimination is the so called Kesselring matrix method. This due to it being used frequently in product development projects and other related fields. The premise of the Kesselring matrix is to grant every evaluation criterion a weighted value *w* from 1-5. The individual researched concepts are then given a value *a* of 1-5 describing how well they meet every criterion. Finally, the weighted values are multiplied with the given values for each concept $a \cdot w = t$ which are then finally summarized in the bottom of the matrix. The concept which obtain the highest score is then consider to be the best, based on the specified criteria.

In this elimination process five criteria have been chosen. These are as follows: efficiency, price, complexity, maturity and research-ability. The efficiency, complexity and price are all to determine how easily applicable the systems are in a current passenger car. The two last criteria are to determine how much information is currently available about the systems, a factor which is very important in the detail study, see part B in chapter 5.

The elimination process started with each group of systems being weighted in separate Kesselring matrices, see table 2-4. After this the winner of each category where compared in a final Kesselring matrix, see table 5. It is important to mention though, that the system that is the best according to the elimination process might not be the one chosen for further investigation. To determine which of the systems that were going to be part of the detail study the opinions of all stakeholders were taken into consideration as well.

4.4.1. Analysis Kesselring matrix of engine system

In the matrix in table 2, all of the engine systems are compared to each other with respect to the five above mentioned criteria. Turbo compound receives a relatively high weighted value for both research-ability and efficiency, this due to it being implemented in various other vehicles such as trucks and for having a comparatively big impact on the overall fuel reduction. The medium values on “low price, low complexity and maturity” are due to it: containing quite complex components, requiring some modification to the exhaust system of the car and not having been fitted to a road car as of yet.

TEG receives the lowest overall score in table 2. This is due to that TEG is deemed to have a low efficiency, high price and medium complexity compared to the other engine systems.

When it comes to MGU-H, it receives a high weighted value for efficiency due to the promising power output it has demonstrated within formula 1 racing. Otherwise it is scored quite low due to it being only really implemented in formula 1 and thus information about the system is scarce and the price and complexity is high.

Piezo electric generators (PEG) scores well on price and complexity as a result of them being small and based on quite accessible technology. They do not however produce anywhere near enough power for vehicle propulsion and was thus excluded from further investigation.

The organic Rankine cycle system (ORC) is over all not considered efficient, cheap and/or simple enough to receive a high end score. The heat exchanger cannot absorb enough heat to be a viable option for power production in the car. The system is also quite extensive and therefore both costly and complex.

Kesselring matrix - Engine													
Evaluation criteria		**Alternative**											
		Ideal		Turbo compound		TEG		MGU-H		PEG		ORC	
Term	**w**	a	t	a	t	a	t	a	t	a	t	a	t
High Efficiency	5	5	25	4	20	2	10	5	25	1	5	3	15
Low Price	5	5	25	3	15	2	10	1	5	5	25	2	10
Low Complexity	5	5	25	3	15	3	15	1	5	5	25	2	10
Maturity	3	5	15	3	9	3	15	2	6	2	6	3	9
Research-ability	4	5	20	5	20	2	10	1	5	3	12	3	12
Total		25	110	18	79	12	60	10	46	16	73	13	56
Rel. Total		100%	100%	72%	0.72	48%	0.55	40%	42%	64%	66%	52%	51%
Average		5	22	3.6	15.8	2.4	12	2	9.2	3.2	14.6	2.6	11.2
Ranking		**-**		**1**		**5**		**4**		**2**		**3**	

Table 2: Kesselring matrix for the engine systems.

After analyzing the end results of each system, and comparing them to each other and the ideal-value, the system that is chosen for the combined Kesselring matrix is the Turbo compound system. This is due to the system receiving the highest overall score of 72%

4.4.2. Analysis Kesselring matrix of chassis systems

In the Kesselring matrix in table 3, RPD and BSD receives quite low results in efficiency and pricing. This is connected to the low score on research-ability. This since the less amount that is written about a system, the more expensive it becomes on account of resources that has to be invested in development and optimization. RPD and LMD receives medium points in complexity and maturity. This due to the fact that they are about as hard to implement and test as most of the other solutions, with the difference that these two systems actually have been tested in cars. They therefore receive a medium score in maturity.

The HED together with LMD systems are given high efficiency numbers because of the earlier market research indicating that those two systems are the best to regenerate energy. However, the HED system is considered to be both more expensive and complex than the other systems in this category. Thus the low points are estimated on the basis that HED needs more space and surrounding devices, such as accumulator and generator. BSD and HED both receive a low score in maturity due to the fact that neither of these systems have been properly road tested. A medium score in research-ability are assigned to LMD and HED since both systems seems to have more accessible data then RPD and BSD.

Kesselring matrix - Chassis											
Evaluation criteria		**Alternative**									
		Ideal		**RPD**		**HED**		**BSD**		**LMD**	
Term	**w**	a	t	a	t	a	t	a	t	a	t
High Efficiency	5	5	25	2	10	4	20	2	10	4	20
Low Price	5	5	25	2	10	1	5	2	10	2	10
Low Complexity	5	5	25	3	15	1	5	3	15	3	15
Maturity	3	5	15	3	9	2	6	2	6	3	9
Research-ability	4	5	20	2	8	3	12	2	8	3	12
Total		25	110	12	52	11	48	11	49	15	66
Rel. Total		100%	100%	48%	47%	44%	44%	44%	44%	60%	60%
Average		5	22	2.4	10.4	2.2	9.6	2.2	9.8	3	13.2
Ranking		**-**		**2**		**4**		**3**		**1**	

Table 3: Kesselring matrix for the chassi systems

When the four chassis related systems are compiled and put against each other in the Kesselring matrix in table 3, LMD got the highest score and therefore becomes the best chassis system with respect to the evaluation criteria. LMD receives a 60% score of an ideal product and an average rating of 3.0 in each criterion.

4.4.3. Analysis Kesselring matrix of brake systems

The EMRB did very well overall, see table 4. It is considered to be both very mature, since it is currently available in a variety of different cars, and low priced with a high research-ability. This is due to it being easy to implement in all cars that are already HEV or EV and thus it also becomes cheap. The only two weighted values that are put at a lower level, is efficiency and complexity. EMRB is an efficient system when implemented in an electric car for example, but depending on the layout, it produces less power in an HEV. The lower score on low complexity is as a result of this system only being applicable on HEV's and EV's. Since it requires some sort of generator, retrofitting it into a normal ICE-car increases the complexity.

The FRB system is scored high on efficiency, since it has a relatively high fuel reduction effect of between 20-30%, and lower on price and complexity. This is as a result of the system being quite heavy, bulky and containing many parts. The system does however perform well when it comes to maturity and research-ability since it has been implemented at a research level by several big companies. As a consequence of this, there is relatively much information to be found about it. The flywheel solution is furthermore very old and well documented within other types of machinery, and there might thus be room for improvement within the novel, automotive application.

The SRB is scored relatively low on all accounts. It is not very efficient compared to the other systems, with a fuel reduction of only 5-10%. The system is also very complex and costly with differentials, many gears and moving parts. Finally, SRB is neither considered to be mature nor easy enough to research. There has been some testing done on research level in the past, but nothing substantial.

Kesselring matrix - Braking									
Evaluation criteria		**Alternative**							
		Ideal		**EMRB**		**FRB**		**SRB**	
Term	**w**	a	t	a	t	a	t	a	t
High Efficiency	5	5	25	3	15	5	25	2	10
Low Price	5	5	25	4	20	2	10	1	5
Low Complexity	5	5	25	3	15	1	5	1	5
Maturity	3	5	15	5	15	3	9	2	6
Research-ability	4	5	20	4	16	3	12	1	4
Total		25	110	19	81	14	61	7	30
Rel. Total		100%	100%	76%	73%	56%	55%	28%	27%
Average		5	22	3.8	16.2	2.8	12.2	1.4	6
Ranking		**-**		**1**		**2**		**3**	

Table 4: Kesselring matrix for the braking systems

With all the above mentioned scores, the system that receives the highest points in total is EMRB with 76% of the weighted value compared to the ideal, see table 4. Worth noting though is that the FRB system came in second place, and it does not necessarily require a hybrid system.

4.4.4. Analysis Kesselring matrix of the winners from each category

In this last evaluation, systems that gained the highest rating in previous eliminations see table 2-4, are now compared against each other, see table 5. This is in order to determine which system has the best overall rating when compared with solutions from other categories.

When considering “the winner’s Kesselring” in table 5 it can be concluded, quite unsurprisingly that the most implemented system in today’s cars also is the system which gain the best rating in this evaluation, namely EMRB. This system receives higher number in almost all criteria than its competitors. This is due to it being simpler to implement, having a better efficiency and costing almost nothing to implement in an HEV or EV.

The Turbo compound and LMD are rated very similarly in this matrix and it is hard to estimate which one of the systems truly are the best. The turbo compound system does however receive a higher rating than LMD, due to more stable medium numbers in efficiency, price and complexity.

Kesselring matrix - winners									
Evaluation criteria		**Alternative**							
		Ideal		**Turbo compound**		**LMD**		**EMRB**	
Term	**w**	a	t	a	t	a	t	a	t
High Efficiency	5	5	25	3	15	3	15	5	25
Low Price	5	5	25	3	15	1	5	5	25
Low Complexity	5	5	25	3	15	4	20	5	25
Maturity	3	5	15	2	6	4	12	5	15
Research-ability	4	5	20	4	16	3	12	3	12
Total		25	110	15	67	15	64	23	102
Rel. Total		100%	100%	60%	61%	60%	58%	92%	93%
Average		5	22	3	13.4	3	12.8	4.6	20.4
Ranking		**-**		**2**		**3**		**1**	

Table 5: Kesselring matrix for the highest rated system from each category

4.5. Chosen system for further investigation

According to the Kesselring matrices illustrated earlier, the EMRB system show most promise for current and future applications in light vehicles. This is due to its easy implementation, low cost and relatively high efficiency in HEV's and EV's. Also, considering the amount of large car manufacturers that have invested research time and funds into the EMRB technology the logical conclusion is quite simply that this system has a place in cars of today and tomorrow. Taking these facts into account it is time to determine which system is going to be the subject of the detail study.

After much consideration, in collaboration with all included project stakeholders, the system on which the detail study will be based on is the flywheel regenerative braking system (FRB). This decision is founded on several different factors. Firstly, the FRB system is not as mature as the EMRB system, but it has still been installed into test vehicles by large corporations such as Volvo Cars and Jaguar. This is considered an advantage since the stakeholders involved are interested in systems which are viable for cars, but which have not been implemented on a large scale. A substantial amount of research and information is available regarding the FRB system, but it is still novel enough to be interesting, even for a professional with technical knowledge of the automotive industry. Secondly the FRB system does not necessarily require an electric motor to provide power, it can operate purely mechanically. This means that it does not exclude the current ICE-only powered vehicles available on the market, and thus potentially could have a wider scale of implementation. Also, not needing a HEV or EV system to operate means not having to install a battery pack which contains substances harmful to both humans and the environment. Thirdly, the FRB system provides a large reduction in fuel usage, even compared to the EMRB system. Lastly, this system could be largely mechanical with its gears and a flywheel. This means that it can be analyzed from a mechanical engineering standpoint, which includes aspects of the system related to material choices and geometry.

In the following Kesselring matrix in table 6, winners from the earlier eliminations are compared to the selected FRB system. The matrix shows that EMRB still gets the highest score, but FRB claims a second place. One of the main reasons that FRB got on so well is due to an overall high efficiency and that it does not require an HEV/EV, which both LMS, EMRB and sometimes turbo compound does.

Kesselring matrix - WINNERS + FRB											
Evaluation criteria		**Alternative**									
		Ideal		Turbo compound		LMS		EMRB		FRB	
Term	**w**	a	t	a	t	a	t	a	t	a	t
High Efficency	5	5	25	2	10	2	10	4	20	5	25
Low Price	5	5	25	3	15	1	5	4	20	2	10
Low Complexity	5	5	25	2	10	3	15	4	20	1	5
Maturity	3	5	15	2	6	4	12	5	15	3	9
Research-ability	4	5	20	4	16	3	12	3	12	3	12
Total		25	110	13	57	13	54	20	87	14	61
Rel. Total		100%	100%	52%	52%	52%	49%	80%	79%	56%	55%
Average		5	22	2.6	11.4	2.6	10.8	4	17.4	2.8	12.2
Ranking		**-**		**3**		**4**		**1**		**2**	

Table 6: Kesselring matrix with the earlier winners and the chosen FRB system

The systems present in both table 6 and table 5 do not get the same values in both tables. This is due to that the "ideal system" changes from table 5 to 6 and thus the relative numbers changes. The reason for the ideal system changing is the addition of a FRB system.

5. PART B: DETAIL STUDY OF A FLYWHEEL REGENERATIVE BRAKING SYSTEM

The whole concept of using a flywheel system in a car is to use it as an energy storage unit when braking. When a car decelerates with friction brakes, a lot of energy is transformed into heat and is therefore wasted. With a flywheel regenerative braking (FRB) system a great deal of this wasted energy can instead be stored kinetically in a flywheel and then be used to accelerate the vehicle. Several studies suggest that fuel savings of up to around 30% is achievable in an urban environment (Cuspinera & Alejandro, 2013), (Ponce Cuspinera & Dunne, 2015).

Today there are several manufacturers working on FRB concepts, which will be described more toughly in next section. The solutions vary from purely mechanical to electrical systems with a flywheel as energy storage (Hedlund, Lundin, de Santiago, Abrahamsson, & Bernhoff, 2015).

There are three large factors which come into play when maximizing energy *E* in a flywheel, weight *m*, radius and rotational speed ω. This can be seen through the fundamental laws of mechanical rotational energy, illustrated in the following equations:

$$E = I\frac{\omega^2}{2}$$

$$I = \frac{1}{2}m(R^2 + r^2)$$

"I" in this equation is the mass moments of inertia and contains both mass m and radii r in square. This will be more thoroughly described in the dimension calculations, see section 5.4. However by just briefly examining the energy equation above it can be concluded that a higher angular velocity ω makes a more significant impact on energy storability than for example the mass of the flywheel.

In figure 14, a basic schematic picture of how a flywheel system could be configured is shown. A shaft connects the braking/accelerating wheel with a flywheel gearbox of some sort, which in turn is connected to the flywheel itself. As shown in the figure, the angular velocity is changed within the power conversion of the flywheel gearbox. It is thus very important to make the gearbox as efficient as possible to make sure that the system achieves the intended maximum output and input power. This makes it especially important to choose

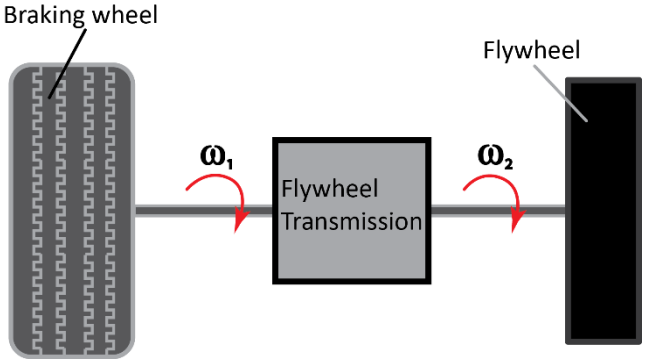

Figure 14: Principle view of flywheel connection.

the correct gearbox for the use case. A brief review of some options for flywheel gearboxes is presented in section 5.2.

5.1. Different systems

There are mainly two different kinds of FRB solutions implemented in the automotive industry, namely mechanical solutions and electro-mechanical solutions. These type of systems are described briefly in the following sections. After that, an evaluation and summary concerning which system is going to be analysed further is conducted.

5.1.1. Mechanical Flywheel (MF)

The mechanical flywheel system uses a purely mechanical device to store and then utilize regenerated brake energy. One example of a MF system is Volvo Cars concept S60 flybrid. It contained a Kinetic Energy Regeneration System (KERS) fitted to the rear wheels. The energy was stored into a flywheel via a CVT. Volvos test was the first full scale test conducted on a front wheel drive car with the KERS connected to the rear wheels (Crowe, 2014). In Volvos case the KERS was not connected to the engine in any way, this is not always the case however. There are several alternative solutions which are presented by (Dhand & Pullen, 2015) were the flywheel is directly connected to the drivetrain[9]. The typical components included in a MF system are a flywheel, a protective case, some sort of CVT and a clutch system to connect or disconnect the system to the drivetrain (Dhand & Pullen, 2015).

The volume and mass required for this type of system is highly dependent on how large the flywheel is and which kind of flywheel gearbox that is in use. Size and mass of the flywheel are then on the other hand important factors when considering the total amount of storable energy. For example the Volvos system weighed around 60 kg and had the ability to increase fuel efficiency with up to 20% and add an additional 80 horse power, under the right conditions (Burn, 2014). Volvos test system was based on the Torotrak Flybrid KERS with a 6 kg, 200 mm in diameter, carbon fibre flywheel, revolving at maximum 60 000 rpm. It also contained a toroidal[10] CVT (Volvo Cars, 2014). Jaguar has experimented with a Torotrak system but with one major difference to Volvos, it was connected to the existing drivetrain via a modified differential (Squatriglia, 2010), (Ireson, 2010). The Jaguar system did have a weight of 65 kg and can achieve fuel savings up to 20% (Hedlund, Lundin, de Santiago, Abrahamsson, & Bernhoff, 2015). Figure 15 illustrates the basic differences between Volvo Cars and Jaguars system.

Another mechanical flywheel system called mecHybrid is a result of a research collaboration between Punch Powertrain, Bosch, SKF, CCM and the Technical University of Eindhoven, around 2010. The mecHybrid system uses a quite heavy 20 kg solid steel flywheel with a diameter of 150 mm, which can rotate at speeds up to 35.000 rpm. A push-belt[11] CVT was used (Ashley, 2014), (Hedlund, Lundin, de Santiago, Abrahamsson, & Bernhoff, 2015). Punch Powertrain claim on their website that the mecHybrid system can improve fuel economy with up to 10%.

[9] The drivetrain are the components in cars, such as driveshaft, that transmits power from the power unit to the wheels. The term does however not include the power unit itself.
[10] See toroidal CVT in section 5.2.1.
[11] See V-belt CVT in section 5.2.1.

One major flaw with a mechanical solution is that it has to be connected directly to the drivetrain (as with Jaguar) or to the braking wheels via a drive shaft (as with the Volvo). This disadvantage limits where this type of system can be installed especially if the car is front wheel drive and the MF is installed to the front wheels. This since MF then either has to take up space in the engine compartment or be connected via long shafts from (for example) the trunk or elsewhere where the system can be fitted in a car. If the system is connected to the rear wheels instead it could take some space in the trunk or somewhere further back in the existing drivetrain.

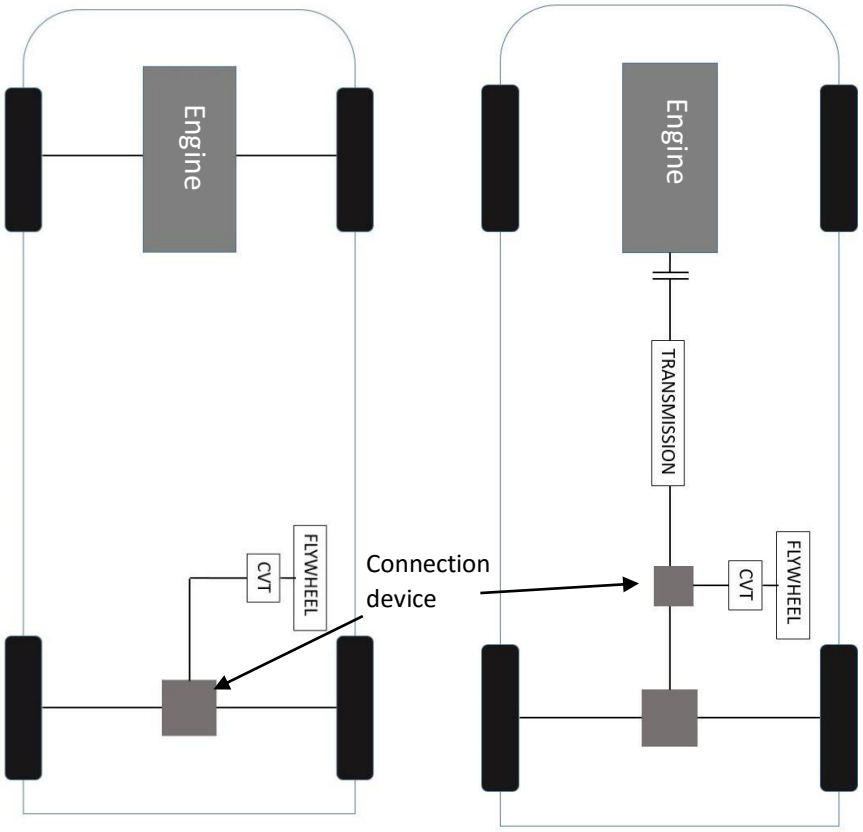

Figure 15: Principle view of connection options for a mechanical flywheel solution. The left illustrates the basics of the Volvo layout and the right basics for the Jaguar system.

5.1.2. Electro-mechanical flywheel

The main goal of an electro-mechanical flywheel system is to use a flywheel instead of a battery or supercapacitor in order to store energy. In a normal battery system, the electrical energy from, for example an electric generator is stored chemically, whereas in a flywheel system the energy is instead converted into kinetic energy (NASA, 2012). The electro-mechanical system has many uses, both within industries and automotive. This due to it being more environmentally friendly, experiencing less degradation with extended use and having lower maintenance requirements than conventional battery set-ups (NASA Glenn Research Center, 2015).

An electro-mechanical system installation requires there to be one or more electric motors/generators installed at a position where it/they can regenerate the power created upon braking. The power is then transferred via a high voltage cable to another motor/generator which in turn spins up/down the flywheel (Williams Hybrid Power, 2013). The last

mentioned motor/generator can either accelerate or decelerate the flywheel depending on which direction the power is flowing, thus either storing or providing extra power. The flywheel is suspended on bearings in a vacuum-sealed casing to reduce friction-losses and minimalize aerodynamic drag (Xiongxin , 2010).

One electro-mechanical flywheel configuration is made by a company called GKN Hybrid Power (former Williams Hybrid Power). A basic, schematic picture of this type of system can be seen in figure 16. In this system, the flywheel is placed inside a carbon fibre casing on an axel going straight through the casing. The stator that is providing the energy for movement is placed inside the flywheel itself. This makes the system more compact.

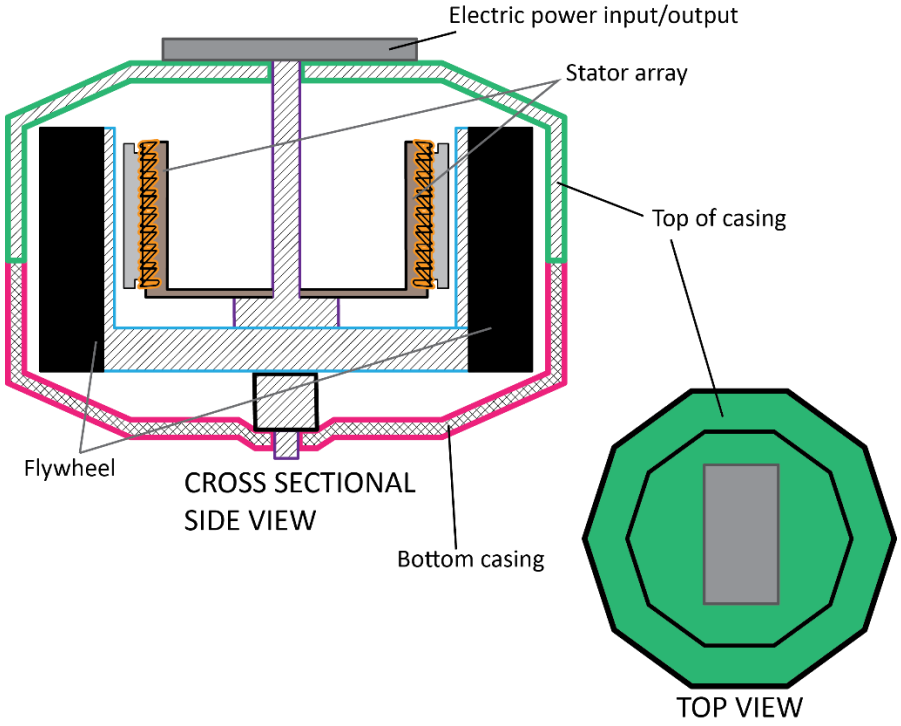

Figure 16: Schematic, cross-sectional and top view of a GKN electro-mechanical system

One version of the GKN system was first developed for use in the 2009 formula 1 racing championship and the system has been developed further since then for use in commercial vehicles (Williams F1, u.d.). One of the most notable uses of this system is within the public transport sector where it has been implemented in London on some of the city buses. Porsche and Audi have also used versions of the system in their race cars during endurance races such as Le Mans and the Nurnbergring 24. These implementations were quite successful, with both teams saving a lot of fuel in their individual races (Williams F1, u.d.).

When it comes to weight, the GKN system implemented in the Porsche GT3R ended up weighing about 57 kg all and all, with the flywheel part of the design contributing with about 47 kg. The last mentioned includes both the flywheel, axels, bearings and outer shell etc. of the flywheel part. The Audi system was much lighter weighing about 27 kg all and all, with the flywheel part weighing about 19 kg (Williams Hybrid Power, 2013). It did however have a lower maximum output power capability, and was also designed for the Audi e-tron R18 Le Mans car which means production cost and other such factors were probably not really considered to be as important as it usually is in a commercial car.

The power of the GKN system is around 180 kW at peak power for the Porsche version and 150 kW at peak power for the Audi version. This when rotating at 36,000-45,000 rpm, which is the maximum rotational speed for the flywheel (Williams Hybrid Power, 2013).

When it comes to volume, this type of system naturally takes up a fair bit of space since there has to be room large enough to accommodate all the mechanical components. Though it is hard to say how the GKN system would perform in a normal passenger car since it has really only been implemented in buses and race cars.

5.1.3. Summary and evaluation of the systems

After considering the two systems described previously in this section, it is not entirely easy to determine which system has the most potential for implementation in passenger cars. This since the distinction between the performance and weight of the systems are not easy to compare due to that the electro-mechanical system made by GKN only has been implemented in race cars and heavier transportation vehicles, such as busses. The mechanical flywheel on the other hand has been installed and tested by three companies in prototype passenger cars. Applications involving racing and busses differ quite significantly from normal passenger cars, both when considering the cost of the system and amount of energy that can be extracted from braking within a cycle. In for example race car applications, cost is not always the defining factor since the performance of the car always has have the highest priority, especially in races such as le Mans. Also race cars and busses are both subject to a higher amount of braking, which in turn makes regenerative energy extraction more efficient given the right circumstances. The braking forces that a race car is subject to can therefore be hard to compare with the ones being simulated in for example the new European driving cycle (NEDC).

With respect to the above mentioned criteria, the system chosen for a closer analysis in this detail study is the mechanical flywheel system. The reasons for doing so is that the MF system has actually been implemented and tested in standard driving cycles for passenger cars. Also, for logistical reasons, it is more convenient to make further research and ask questions to the people involved with the development of the Torotrak system. Lastly, in its final stages this project is largely focused on mechanical solutions, which makes a mechanical system a far more suitable candidate for the type of methods chosen for later detail study.

5.2. Flywheel gearbox

When having a mechanical flywheel configuration in a passenger car it is necessary to have some sort of transmission connecting the flywheel and the braking wheels. There are a number of alternative solutions for this gearbox implementation. In this section two different varieties are presented, which are CVT and Clutch based Flywheel Transmissions (CFT).

5.2.1. Continuously variable transmission (CVT)

The purpose of a CVT is straight forward what the full name says, a transmission which has an infinite number of ratios between input and output shaft. There are several different ways of producing this continuously variable speed ratio. However, they can roughly be divided in two types, either a belt CVT or rolling CVT. A V-belt CVT is described in this section as well as a roller toroidal CVT. The types mentioned briefly in the mechanical flywheel section 5.1.1 are thus described in this section. A main reason why CVT's are used is that they have the ability to always use the right ratio between input and output shafts.

V-Belt CVT

A V-belt CVT is often composed of two belt pulleys who are able to move axially, a V-belt and some sort of mechanism that can apply axial force to the movable pulley half so that the V-belt can move up and down the pulleys and thus changing the ratio. Figure 17 shows a principle view of how a V-belt CVT works. The axial force mechanism can be controlled via a spring load, hydraulics, centrifugal force, electric motors and so on. Figure 18 shows an automatic belt CVT using centrifugal force, a torque ramp and springs to control the gear ratio. When the belt moves up and down the belt pulleys, the speed ratio changes (Mägi & Melkersson, 2014). There are also V-belt CVT solutions where the distance between the pulleys are changed in order to control speed ratio.

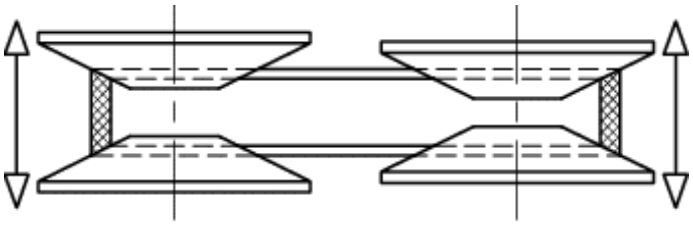

Figure 18: Principle view of V-belt CVT. Source with permission: Kjell Melkersson

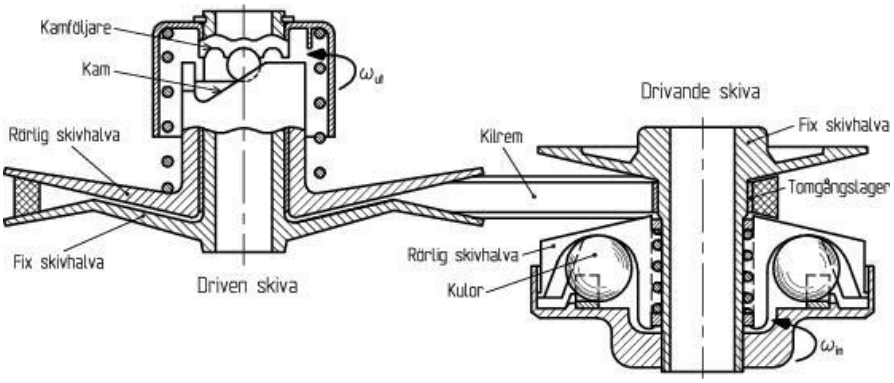

Figure 17: Automatic V-belt CVT. Source with permission: Kjell Melkersson

Toroidal CVT

A toroidal CVT is a special type of rolling CVT. The toroidal CVT contain an input shaft with two (or more) input discs connected to it. There is further an output disc, rollers between in- and output discs and some sort of control unit to vary the speed ratio. Figure 19 shows a typical layout of a toroidal CVT solution. The principle for this type of CVT is that the rollers can be tilted and via this tilting, an infinite number of ratios are made possible, from lowest to highest ratio. The control unit may, as in the case of Torotrak's toroidal CVT unit, contain hydraulic pistons which control the tilting of the rollers (Torotrak, 2010). If these rollers have a too high tilting angle the rollers will begin to slip. This makes the toroidal CVT physically limited to a max gear ratio (Hedlund, Lundin, de Santiago, Abrahamsson, & Bernhoff, 2015).

Figure 19 shows a toroidal CVT with its angle velocities. Both end discs have the same velocity in the same direction. As they are connected with an input shaft which goes through the whole system (not shown in figure). The rollers are connected via an axle to an outer casing which in turn is connected to a hydraulically operated arm. The tilting is thus occurring in the plane of the picture, while the arm is connected to the rollers in the direction perpendicular to the plane. With reference to figure 19 the nominal (slip neglected) speed ratio becomes $\frac{\omega_1}{\omega_2} = \frac{R_2}{R_1}$.

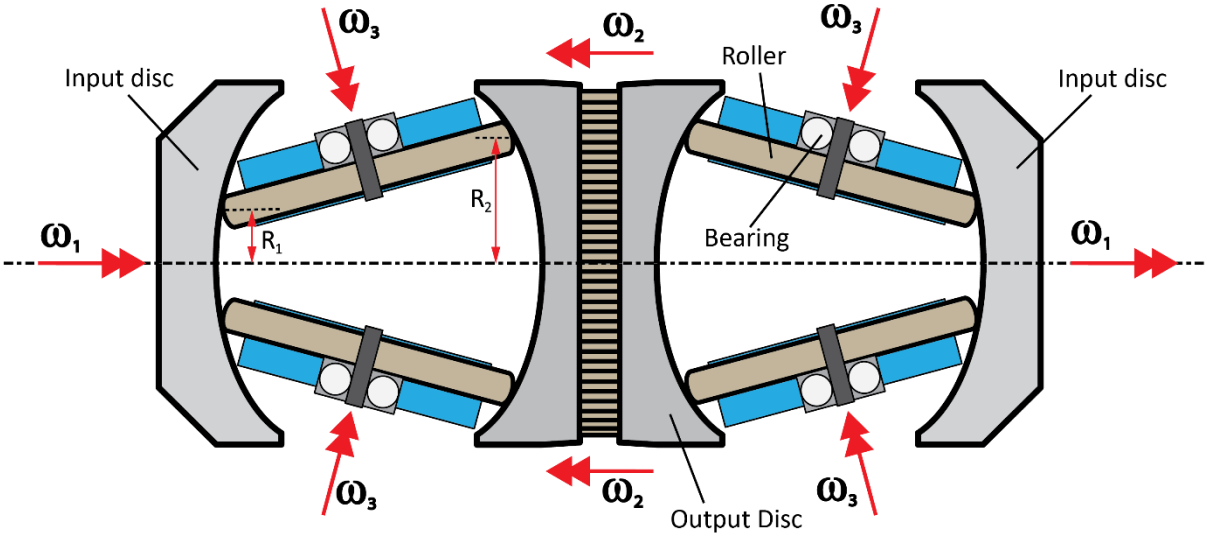

Figure 19: Schematic illustration of a toroidal CVT

In the interview with Volvo (Jörgensson & Andersson, Volvo meeting, 2016) it was stated that both v-belt CVTs and toroidal CVTs are more expensive than a clutch based CVT and have a more complex control unit and limited gear ratio. Volvo also described in the interview that toroidal CVT's are both complex to control, has a limited max gear ratio and are quite costly.

5.2.2. Clutch based flywheel transmission (CFT)

The clutch based transmission also mentioned later in section 5.3 which is developed and patented by the company Torotrak (formerly known as Flybrid automotive). It can be applied in different ways, one of which is via a connection to the main vehicle gearbox, thus enabling a much wider gear ratio between wheels and flywheel (Torotrak Development ltd , 2015). Another way of installing the CFT system is by having it connected to the flywheel, then through a sequence of gears to the rear drive shaft. This is the solution proposed by Volvo Cars in their research of a mechanical flywheel system (Jörgensson & Andersson, Volvo meeting, 2016).

The system works by having three output shafts which all have different fixed gear ratios, see figure 20. These shafts are connected to individual clutches which are able to slip, thus enabling flywheel and shaft to acquire the same speed. This slipping action of course means residual losses. The clutch that has the ratio closest to the one of the flywheel at any time engages, whilst the others disengages. The whole process is managed by hydraulics. Because the CVT's described previously have such low efficiency according to Volvo Cars the CFT becomes an alternative solution to the CVT, even though it has slip losses. Volvos research claim that the system has the potential to be both less expensive, less complex and have nearly equal efficiency as for example a toroidal CVT (Jörgensson & Andersson, Volvo meeting, 2016).

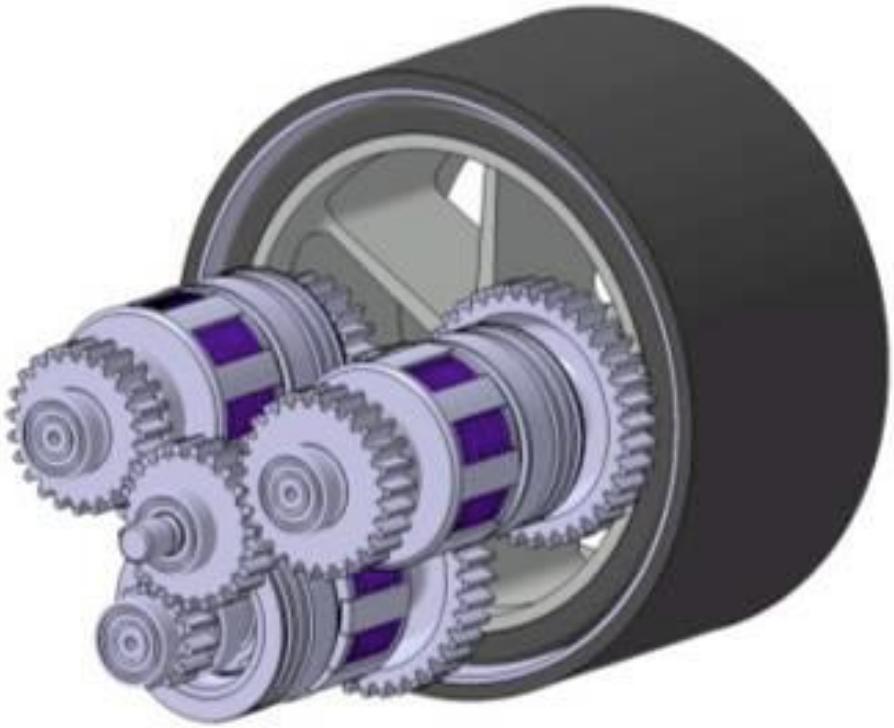

Figure 20: Illustration of a CFT. Source: Jörgensson, Sjögren, & Eriksson, Volvo Car Group Flywheel KERS project, 2013. With permission from Volvo Cars

5.3. Volvo meeting – compilation

A meeting was conducted on the 11th of March 2016 at Volvo Cars in Torslanda with Volvo Cars employees Lennart Andersson (senior manager Volvo Car Corporation, transmission engineering) and Mathias Jörgensson (Volvo Car Corporation, transmission engineering). The discussed subject was the research conducted in collaboration with SKF among other, using a grant issued by a Swedish government agency. The project resulted in a Volvo car prototype using the Torotrak flywheel regenerative braking system. Both Lennart Andersson and Mathias Jörgensson were a part of the development process of this prototype.

5.3.1. Volvo Flywheel solution – background

Since the requirements for emissions continue to stricter, with new EU regulation being discussed for 2025, Volvo needed to investigate alternatives to cars propelled solely by an ICE-unit. There is a limit as to how efficient an ICE can be made, and that was the reason why Volvo Cars started to look at alternative hydrid solutions, according to Mathias Jörgensson (Jörgensson & Andersson, Volvo meeting, 2016). At the time of the project the company had a plug in hybrid V60 with an electrically powered rear axle and a fleet of C30 fully electric test vehicles. The plug in hybrid and full electric test vehicles were however considered quite expensive, and there was thus a need for a cheaper solution as well, to lower the overall emissions of the vehicle fleet.

Since a lot of energy is dispersed into heat while braking with normal friction brakes (Jörgensson, Sjögren, & Eriksson, 2013), Volvo decided to look into the so called “mild” and “medium” hybrids with brake regeneration and acceleration boost. This led them to the possibility of installing some kind of mechanical kinetic energy recovery system (KERS) since it was up to four times cheaper than the equivalent plug in hybrid when considering power output, see figure 21. It also did not require changing the electrical architecture of the car since it was possible to work it into the 12 V layout of the current ICE-cars, which in turn made it less expensive to implement (Jörgensson & Andersson, Volvo meeting, 2016). Volvo Cars choose to use the Torotrak MF system. The reason for them choosing a MF solution was that they wanted to obtain some basic knowledge about flywheel KERS in general. When considering for example the electro-mechanical flywheel system implemented by Porsche amongst others, it was deemed too complex by Volvo for their purposes. The low weight and long life span of the mechanical system was also an advantage compared to equivalently powered battery packs.

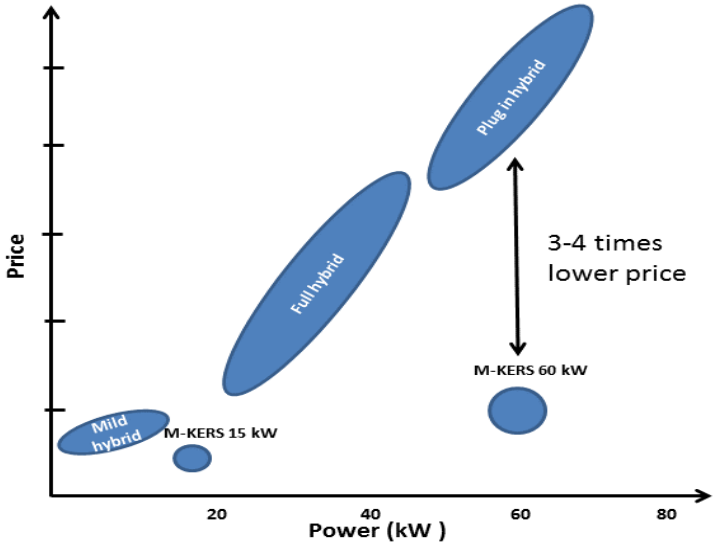

Figure 21: Graph showing the price as a function of maximum power output Source: Jörgensson, Sjögren, & Eriksson, Volvo Car Group Flywheel KERS project, 2013. With permission from Volvo Cars

5.3.2. Volvo system layout

The KERS that was implemented by Volvo Cars into a test car was the Torotrak flywheel system. The system contained a flywheel with casing, connected to a toroidal CVT via a so called planetary gear set, which in turn was connected to the rear drive shaft via a succession of gears, see figure 22. The last mentioned gears were designed by Volvo themselves. The reason for choosing a toroidal CVT was that Torotrak had worked on an implementation of a very similar system in formula one cars. Thus, the toroidal CVT as a system had already been tested and proven, according to Mathias (Jörgensson & Andersson, Volvo meeting, 2016). It should also be mentioned that the flywheel setup in the Volvo prototype had a two speed configuration, made possible by a range extender ratio. This was to make the system produce a high top speed whilst being able to maintain high torque. In the final prototype this solution made it possible to have both an "eco-mode" where the regenerated energy was used as quickly and as efficiently as possible and a "performance mode" where the system used the energy to boost acceleration performance as much as possible (Jörgensson, o.a., 2012). The maximum rotational speed of the flywheel was 60 000 rpm and the maximum output power capacity was 60 kW.

The system was connected to the control unit on the Volvo V60 hybrid of the time and placed in the back of the car due to the proximity to the rear wheel axle and the excess of space since the V60 is front wheel drive. This meant that much of the control strategy and software could be carried over directly from their model with a hybrid electric rear axle. The system was not however able to fit entirely into the available space in the car, and thus took up some of the luggage space from the rear luggage compartment (Jörgensson & Andersson, Volvo meeting, 2016).

Volvo has worked with flywheel solutions before, for example in the prototype Volvo 260 from the late 1970's. What made them interested to resume investigation of flywheels as a viable option for energy regeneration was new materials that has been more available and widely implemented since then (Jörgensson & Andersson, Volvo meeting, 2016). Such a

material is carbon fibre, with its low weight and high strength. This is why the Torotrak made the flywheel out of this material, though the hub of the flywheel is still made out of steel.

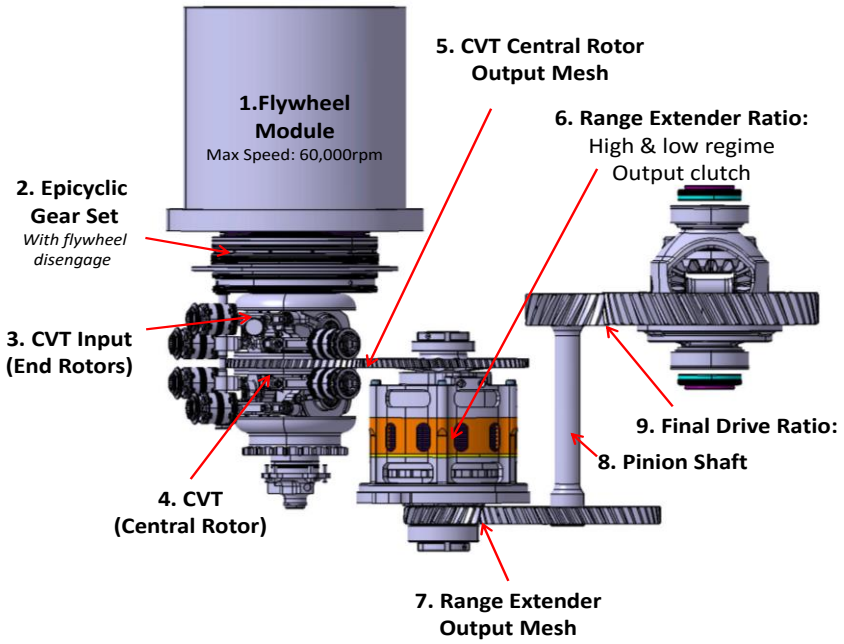

Figure 22: Illustration of the layout of the Volvo-Torotrak system. The planetary gear is here called a epicyclic gear set. Source: Jörgensson, Sjögren, & Eriksson, Volvo Car Group Flywheel KERS project, 2013. With permission from Volvo Cars

The system was running on the 12 V layout of a Volvo V60 hybrid car. If Volvo where to install a battery pack and a generator with the equivalent amount of maximum power output, the system would have to be upgraded to accommodate 48 V (Jörgensson & Andersson, Volvo meeting, 2016).

The system implemented into the Volvo V60 prototype was a high capacity system with a maximum power output of 60 kW. The research team also investigated the possibility of implementing a lower maximum power output system of 15 kW with a storing capacity of 0.21 MJ for the purposes of mass production. The last described system was never produced in physical form, but was simulated in driving cycles and implemented virtually into the new generation of Volvo Cars platform (Jörgensson, Sjögren, & Eriksson, 2013). It was connected to the existing sub frame of the new Volvo XC90.

A flywheel system such as the 15 kW prototype could in theory be a more viable alternative to other types of hybrids since it would possibly cover up to 80% of the desired driving scenarios whilst costing less (Jörgensson & Andersson, Volvo meeting, 2016). This since it is lighter and, because of it being physically smaller, less demanding and cheaper to manufacture. A 15 kW system would also be cheaper than the equivalent battery system, as can be seen in figure 20.

5.3.3. Performance results

As previously mentioned, the system implemented in the physical prototype had two different settings in its control strategies. One was the eco mode and the other was the performance mode. These are quite common to have within conventional hybrid systems with battery packs and electric motors. In the eco mode, Volvo wanted to make sure that the system used as much of the stored energy as possible. This usually means, in conventional hybrid-electric systems, to keep the stored energy for the so called plateaus in the driving cycles, which can be seen in figure 23-24. Note that the shaded parts in these figures are the areas that the system is able to use/store energy from/in the flywheel. In a car with a flywheel system it is however important to use the stored energy as quickly as possible to ensure that as majority of it is put to use. Volvo Cars estimates that the State Of Charge (SOC) of the flywheel system is diminished with up to 50% after just five minutes of driving, and that all the energy may be lost after 30 minutes. This is due to the losses within the flywheel configuration. In the performance mode Volvo wanted to make sure that the system always had a 50% charge to ensure its capacity for assisting the vehicle during acceleration. The reason for aiming towards always having a 50% charge was to ensure a certain stability in the behaviour and response of the system. This power surplus was made possible by dragging the flywheel and thus leaching energy from the internal combustion engine. The power mode does however reduce the systems fuel saving capability (Jörgensson & Andersson, Volvo meeting, 2016).

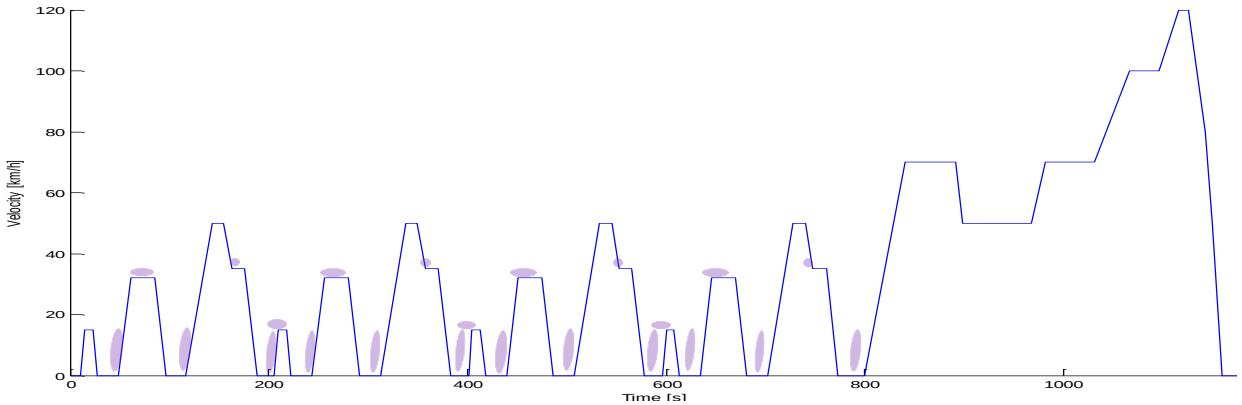

Figure 23: Using energy when accelerating (NED-C). Source: Jörgensson, Sjögren, & Eriksson, Volvo Car Group Flywheel KERS project, 2013. With permission from Volvo Cars

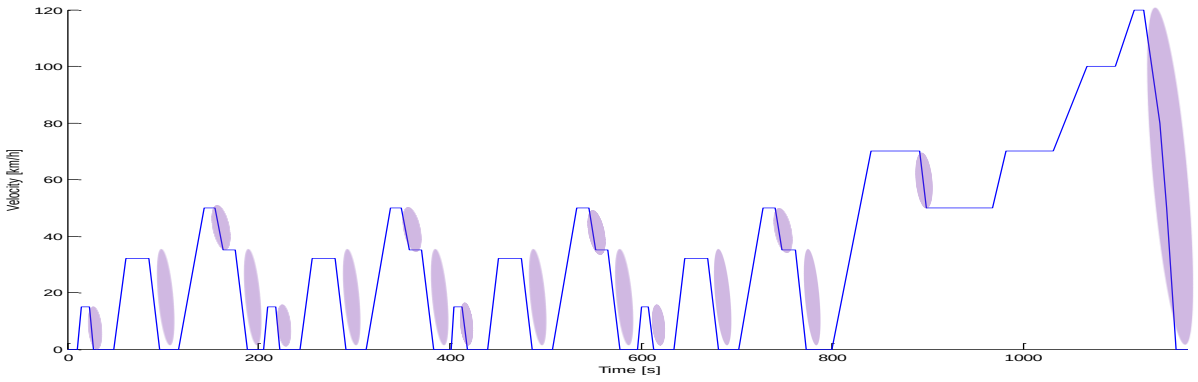

Figure 24: Charging flywheel at braking (NED-C). Source: Jörgensson, Sjögren, & Eriksson, Volvo Car Group Flywheel KERS project, 2013. With permission from Volvo Cars

The performance of the Volvo prototype was never calculated with a physical rig constellation or in the car, but instead calculated virtually by Simulink simulations. In Eco mode the reduction in CO_2 was measured to be between 10-20% depending on which cycle was used. The cycle with the highest reduction in CO_2 emissions is focused on city traffic with many stop and start scenarios incorporated. The performance gain by the performance mode was simulated to be an around 20% increase in acceleration capacity when starting from a standstill and an around 30% increase in acceleration capacity when accelerating from 80-120 km/h. The fuel reduction in the NEDC was around 10%, also calculated by computer simulations. The same type of system has been implemented into a physical testing rig by Land Rover and they have gotten a reduction CO_2 emissions of about 10% (Jörgensson & Andersson, Volvo meeting, 2016).

When it comes to safety, Torotrak has been conducting tests in test rigs where their flywheel design has been driven to its breaking point. What can be concluded from these tests is that the carbon fibre basted flywheel is more or less pulverized to a powder, which can be captured by the casing. This means that no dangerous shrapnel is created when the flywheel is failing. This is however not true with other materials such as a pure steel flywheel, which breaks into parts, and thus requires additional safety testing and design of the container before being a viable option for mass production (Jörgensson & Andersson, Volvo meeting, 2016). It should also be noted that the Torotrak flywheel is designed with a large safety factor. This means that it is able to sustain its function while spinning up to about twice the maximum operation rotational speed.

5.3.4. Drawbacks

The CVT used in the Volvo Cars prototype was a toroidal CVT. This may not be the best solution however, as there are some concerns that it might be too complex and hard to manufacture, making it possibly more expensive compared with other solutions. If Volvo Cars were to continue their research on flywheel systems, they would like to look into for example a CFT. This type of transmission is described in section 5.2.2. The reason for Volvo not testing a CFT system in its V60 prototype was that it was not as implemented and tested in combination with the particular flywheel technology as the toroid CVT at the time (Jörgensson & Andersson, Volvo meeting, 2016). Another problem with the toroidal CVT implemented in the prototype was its gear span, which according to Jörgensson was quite narrow compared to other solutions.

The KERS implemented in Volvos prototype did also contain some mechanical losses. These losses did not only come from the shaft of the flywheel with its bearings, but there were also transmission losses within the gears themselves. This was a contributing factor to the system not being able to remain charged for a longer period of time, as mentioned earlier. This is also something that would be important to review in a further investigation of the system.

Some of the components used in the Torotrak system contained straight cut gears, which meant that the system did produce some excess sound, similar to the sound made by a turbine. This was notable from inside of the car cabin during acceleration. Also, due to the nature of gears, there were some noise contributions from other parts of the system as well (Jörgensson & Andersson, Volvo meeting, 2016). This is something, in combination with the vibrations produced by the system that has to be solved if the flywheel is going to be put into mass production according to Andersson.

The system was lastly not entirely comparable to an equivalent battery system since the mileage increase with a flywheel system is substantially lower. The two systems are in essence designed for slightly different purposes. The Volvo-Torotrak flywheel system was made to give a short boost in acceleration, and thus reducing the fuel consumption. Whereas a battery pack and an electric motor is made to increase the overall range of the vehicle. Also, the energy has to be used quite soon after the regeneration process has occurred in a flywheel. This is not the case with battery packs which have a longer storage capacity and thus have the ability to work at more consistently throughout the driving cycle (Jörgensson & Andersson, Volvo meeting, 2016).

5.3.5. Summary Volvo meeting

As of right now (2016), Volvo Cars is not conducting any active research in flywheel technology. This is in part due to the trend in the motor industry towards battery based solutions and them being a lot more proven in real life scenarios. However, Andersson does still personally believe in the flywheel technology since it is cost effective and has a lot of potential when it comes to performance. It should also be said that there is still an active investigation ongoing at Volvo to determine their strategy for reaching the 2025 emissions goals (Jörgensson & Andersson, Volvo meeting, 2016).

It is furthermore possible to determine that the 15 kW system would be preferable for mass production purposes. It would take up considerable less space, be cheaper to manufacture whilst covering up to 80% of the driving scenarios within the test cycles compared to a more powerful solution. Also if Volvo Cars were to continue the research for mass market applications the use of the flywheel gearbox would have to be investigated further. Lastly more testing would have to be conducted to ensure the comfort of the passengers, with respect to noise and vibrations.

5.4. Dimension calculations of a flywheel

The following dimension calculations are conducted to optimize the dimensions for the flywheel itself. In the first section 5.4.1, a ratio between the inner radius r and the width b is calculated and evaluated for a flywheel, using numerical mathematics via Matlab. The code for the program is attached in appendix 2 and table 7 shows the list of symbols used in this chapter. Figure 25 is a principle view on which the calculations are based upon. The final computation will result in a comparison of how much energy two compared materials can store with respect to the strength of each material. The materials which are going to be evaluated are a high carbon steel and an epoxy/hs carbon fibre (C.F).

E [J]	Energy	σ_y [MPa]	Yield strength
I [kg m^2]	Mass moments of inertia	σ_r [MPa]	Radial stress
r_r [m]	Arbitrary radius in the disk	σ_t [MPa]	Tangential stress
r [m]	Inner radius	$\sigma_{v.M}$ [MPa]	von Mises stress
R [m]	Outer radius	ρ [kg/m3]	Density
b [m]	Width	ν	Poisson's ratio
ω [rad/s]	Angular velocity	c	r/b ratio
σ_a [MPa]	Allowed tension	C.F.	Carbon fibre
$\sigma_{a,steel}$ [MPa]	Allowed tension, steel		
$\sigma_{a,c.f}$ [MPa]	Allowed tension, carbon fibre		

Table 7: List of symbols used.

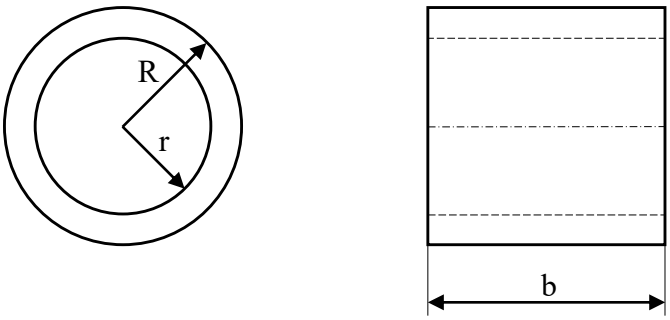

Figure 25: Principle view of evaluated flywheel

The calculations are based on the following assumptions and limitations:

- The total mass of the flywheel m = 5 kg.
- The outer radius R = 100 mm.
- The maximum width b = 200 mm.
- 500 < ω < 7000 [rad/s]
- No preload forces.
- Four times safety against yield strength, $\sigma_a < \frac{\sigma_y}{4}$
- Materials evaluated as isotropic material

The main reason why these limitations and assumptions are set is due to that a lightweight high speed flywheel is evaluated. In addition, limitations in the automotive industry are often volume and weight constraints. One aim is also to match "Volvos 15 kW" flywheel since it is comparatively cheap and would cover up to 80% of all driving scenarios. Because of this, there is a fixed weight value 5 kg and fixed value of outer radius of 100 mm. Other

dimensions and assumptions are estimated. Worth mentioning is that Volvos system only had 77 mm in outer radius, but a larger radius equals more storable energy.

In order to conduct the numerical analysis of r/b ratio and the energy storability, the following equations are used. First is the energy equation (Grahn & Jansson, 2013):

$$E = \frac{1}{2} I\omega^2 \ . \ . \ . (1)$$

Then, mass moments of inertia I, for an annular disc is calculated via the following formula:

$$I = \frac{1}{2} m(R^2 + r^2) \ . \ . \ . (2)$$

When considering the energy equation, it can be concluded that, in order to gain as much energy as possible it is much more efficient to increase angular velocity and radius instead of the mass. This due to the fact that both ω and radius have an exponent of two, see equation 1 and 2. In other words, in order to gain as much energy as possible, a flywheel should be designed with most of its mass on a large radius rotating at a high speed. An annular disk will therefore contain a lot more energy than a solid disk, with the same mass. The computations will later on endorse this hypothesis.

The two materials examined in this evaluation process are high carbon steel and an epoxy carbon fibre. The material data was gathered from CES EduPack™ and is presented in table 8. Several similar materials were also compared in an early stage but these two are good representations of each material family. This since they have desirable material data with a reasonable price.

	High carbon steel	Epoxy/HS Carbon fibre
Density, ρ	7800 [kg/m^3]	1650 [kg/m^3]
Yield strength, σ_y	800 [MPa]	2000 [MPa]
Poisson's ratio, ν	0,29	0,33
cost*	3,5 [SEK/kg]	260 [SEK/kg]

*Table 8: Material data table. *Price are raw material cost, not manufacturing price.*

5.4.1. Ratio r/b calculation.

In this first stage the most energy dense relation between inner radius r and the width b are computed with respect to the strength of each material. These calculations are done via letting the width b of the flywheel shrink from 200 mm to 96.5 mm. Meanwhile angular velocity ω are allowed to vary between 500-7000 rad/s. Because the mass is fixed at m = 5 kg and the outer radius is fixed at R = 100 mm, the inner radius r changes with the width b due to laws of volume and mass relations for solids, see equation 3. The smallest width b_{min} is calculated to be 96.5 mm. If it were to be less than that, the carbon fibre with its low density would not be able to reach a 5 kg weight. The steel however could have a b_{min} = 20.5 mm. Although this case is not evaluated in this first section.

$$r = \sqrt{R^2 - \frac{m}{\pi\, b\, \rho}} \ . \ . \ . (3)$$

In order to ensure that the materials can withstand the stress, when rotating at high angular velocity, a four-time safety factor is applied to the yield strength of each material. Equations 4.b and 5.b are used to calculate radial and tangential stress respectively (Ugural & Fenster, 2012). Equation 6 for von Misses stress is also used (Dahlberg, 2001). The stress equations are based upon there being no internal or external forces (except centrifugal forces) applied to the disk.

$$\sigma_r = \frac{3+\nu}{8}\left(R^2 + r^2 - r_r^2 - \frac{R^2 r^2}{r_r^2}\right)\rho\omega^2 \ldots (4.a)$$

$$\sigma_{r,max} = \frac{3+\nu}{8}(R-r)^2\rho\omega^2 \ldots (4.b)$$

$$\sigma_t = \frac{3+\nu}{8}\left(R^2 + r^2 - \frac{1+3\,\nu}{3+\nu}r_r^2 + \frac{R^2 r^2}{r_r^2}\right)\rho\omega^2 \ldots (5.a)$$

$$\sigma_{t,max} = \frac{3+\nu}{8}\left(2R^2 + r^2 - \frac{1+3\,\nu}{3+\nu}r^2\right)\rho\omega^2 \ldots (5.b)$$

$$\sigma_{v.M} = \sqrt{\frac{1}{2}\{(\sigma_1-\sigma_2)^2 + (\sigma_2-\sigma_3)^2 + (\sigma_3-\sigma_1)^2\}}, \qquad [In\ our\ case] \implies$$

$$\sigma_{v.M} = \sqrt{\frac{1}{2}\{(\sigma_t-\sigma_r)^2 + \sigma_t^2 + \sigma_r^2\}} \ldots (6)$$

In this section, one material is evaluated at the time and the program works as follows. An angular velocity ω that varies from 500 to 7000 rad/s is applied. For each ω the inner radius r (see eq 3) is calculated to a b sized vector. b decreases from b_{max} to b_{min}. The different stresses (eq 4.b, 5.b and 6), mass of inertia (eq 2) and energy (eq 1) are then computed with respect to *r*, *b* and ω. If the maximum stress overrides $\frac{\sigma_{y,steel/C.F}}{4}$ the program brakes and plots stress $(\sigma_r, \sigma_t, \sigma_{v.M})$ vs r in one plot and r/b vs E in another. The most energy dense ratio between r and b is then illustrated via red dots. The program also prints out the value of r/d ratio, the energy and the ω at which the program stopped.

Steel r/d ratio and maximum angular velocity

The steel design manages an angular velocity of up to 1615 rad/s before the stress levels gets too high and the program brakes. As shown in figure 26 (left) the max stress then reaches 200 MPa which is the maximum allowed stress for a steel disk in this test, since $\sigma_{a,steel} = \frac{800}{4} =$ 200 MPa. The most energy dense ratio for a steel flywheel with earlier mentioned assumptions and limitations is furthermore, as shown with a red dot in figure 26 (right) *r/b* = 0.474. The maximum amount of energy expected from this solution is roughly 0.062 MJ.

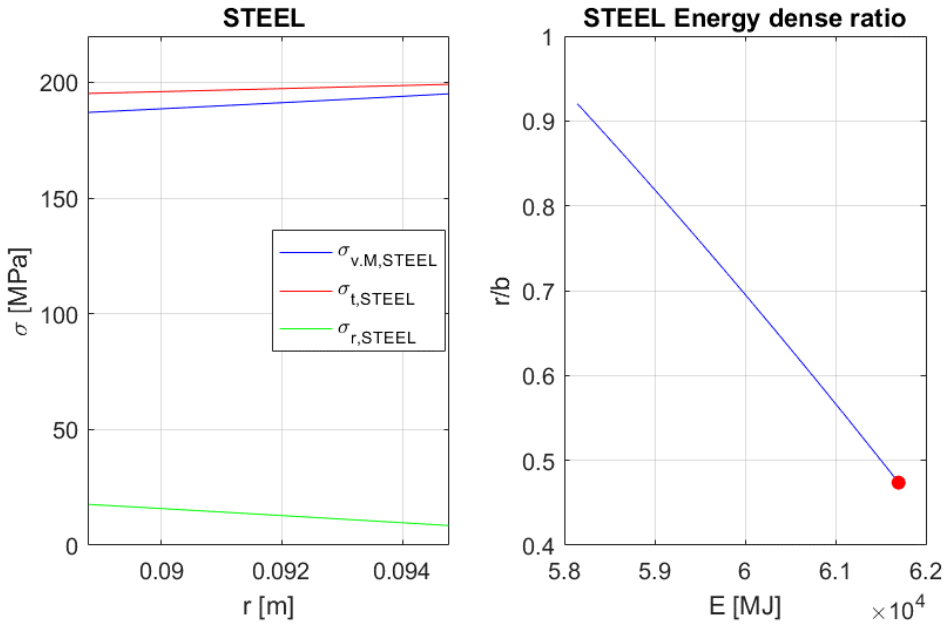

Figure 26: The left figure illustrates how tension change with different values on inner radius r for a steel flywheel. The right figure how the energy changes with r/b – ratio for a steel flywheel.

Carbon fibre r/b ratio and maximum angular velocity

For the C.F solution it is shown in figure 27 (left) that it manages $\sigma_{a,c.f} = \frac{2000}{4} = 500\ MPa$, this occurred when the angular velocity was 5740 rad/s. In figure 27 (right) the optimal energy ratio is illustrated with a red dot and the value of *r/b* for the carbon fibre is 0.360. The carbon fibre solution also manages to store a maximum energy amount of around 0.625 MJ.

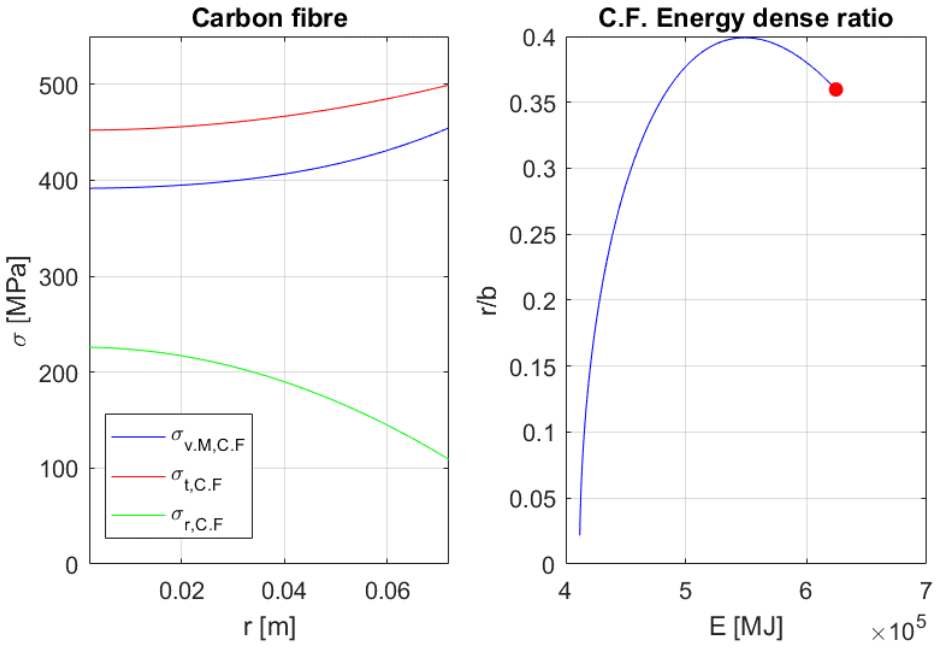

Figure 27: The left figure illustrates how tension change with different values on inner radius r for a C.F flywheel. The right figure how the energy changes with r/b – ratio for a C.F flywheel.

5.4.2. Dimension optimization

In this section the real dimensions for inner radius r and width b are calculated based upon the $c = r/b$ ratios, $c = 0.474$ for steel and $c = 0.360$ for an epoxy carbon fibre. The stress levels across the whole disk are computed as well. After that the energy per SEK are evaluated.

In order to find the dimensions, r is expressed as a function of the width b, see eq 7. Then an function f(b) is created based upon rearrangement of equation 3 together with eq 7. f(b) ends up in eq 8. The principle in this regard is to use Newton–Raphson method on f(b) = 0 and find the zeros in one dimensional problems, se eq 9 for Newton–Raphson method. When f(b) = 0 is found, there will be two solutions to the problem, either a large r and a wide flywheel or a small r and a thinner flywheel.

$$r = c\,b \quad \ldots(7)$$

$$f(b) = \rho b \pi (R^2 - (c\,b)^2) - m \quad \ldots(8)$$

$$b_{i+1} = b_i - \frac{f(b)}{df(b)} \quad \ldots(9)\text{, where}$$

$$df(b) = \frac{df}{db} = \rho\pi(R^2 - 2c^2b^2)$$

The Matlab program then calculates solutions for the width b and the corresponding inner radius r. In figure 28 it is shown with red dots that b for the steel flywheel is [20.6 mm; 200 mm], the associated r steel is calculated via equation 7 to [9.76 mm; 94.8 mm]. For carbon fibre red dots in figure 29 visualize b to be as shown in the following matrix [118 mm; 200 mm]. r is then expressed as follows [42.3 mm; 71.9 mm] via equation 7.

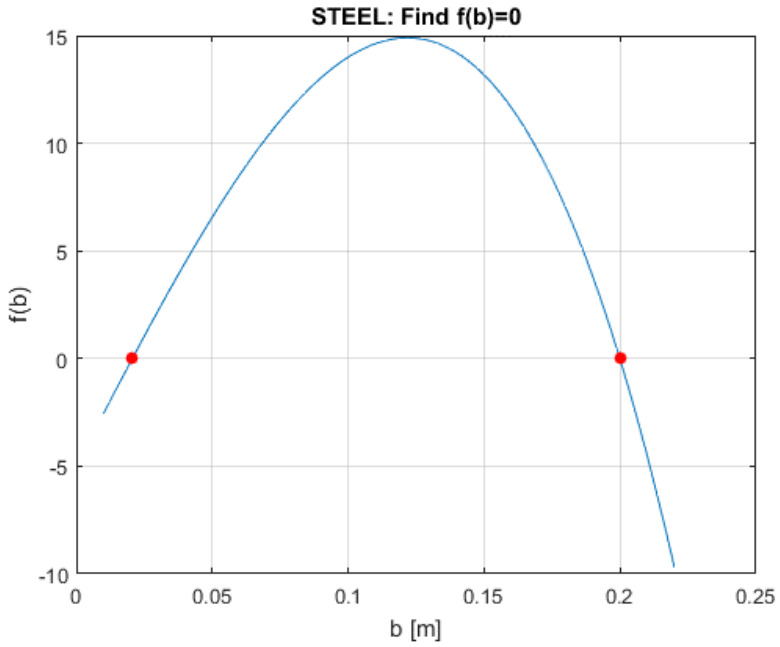

Figure 28: Solution for f(b)=0 to a steel flywheel. b_1=0.021 m and b_2=0.200 m

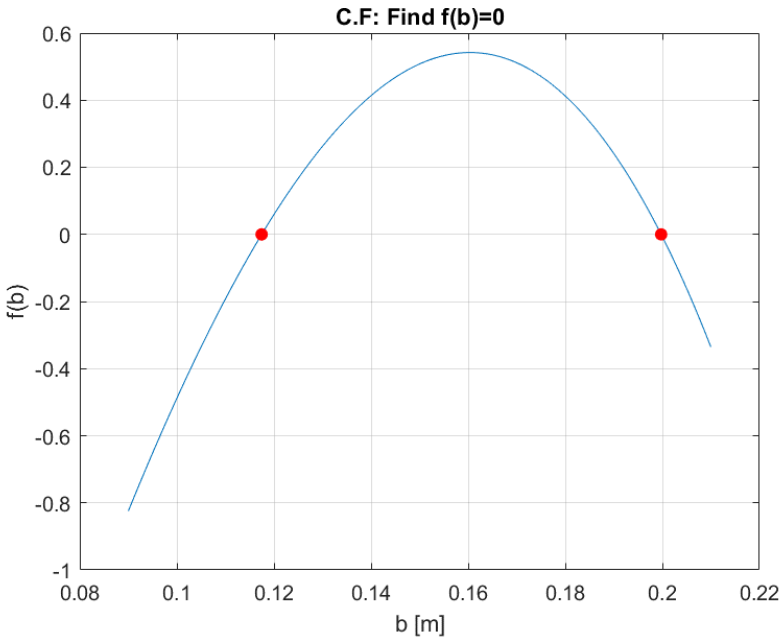

Figure 29: Solution for f(b)=0 to a carbon fibre flywheel. b_1=0.118 m and b_2=0.200 m

The next step is to compute and illustrate tangential-, radial and von Misses stress over the alternative solutions for both materials. Equations 4.a, 5.a and 6 are used to calculate the stress throughout the flywheel discs. Keep in mind that the steel flywheel is evaluated at 1615 rad/s and the carbon fibre solution at 5740 rad/s. This is due to the results in section 5.4.1.

Steel flywheel calculations

Figure 30 illustrates how the stress changes throughout the steel flywheel and table 9 shows the corresponding data calculated. For r = 9.8 mm the maximum stress reaches almost 168 MPa and when r = 94.8 mm stress level maximally 200 MPa. At 1615 rad/s the steel flywheel can only store 33 kJ respectively 62 kJ, which if compared to Volvo's 15 kW solution is substantially less than their 0.21 MJ. The steel flywheel designed as an annular disk seems unpromising on all levels except cost and energy per price unit.

$\sigma_{a,steel} = 200$ [MPa] $\omega = 1615$ [rad/s] Price* = 17.5 SEK	r = 9.8 mm	r = 94.8 mm
b	20.6 mm	200 mm
$\sigma_{v.M,max}$	168 MPa	200 MPa
$\sigma_{t,max}$	168 MPa	200 MPa
$\sigma_{r,max}$	68 MPa	0.2 MPa
E	33 kJ	62 kJ
E/Price	1.88 kJ/SEK	3.54 kJ/SEK

*Table 9: Data calculated for the steel flywheel solution. *Raw material price, not manufacturing cost.*

The r = 9.8 mm solution does not reach 200 MPa, which means that technically there is a little bit more energy to be extracted from that solution. However, it still does not surpass the energy level of the r = 94.8 mm solution.

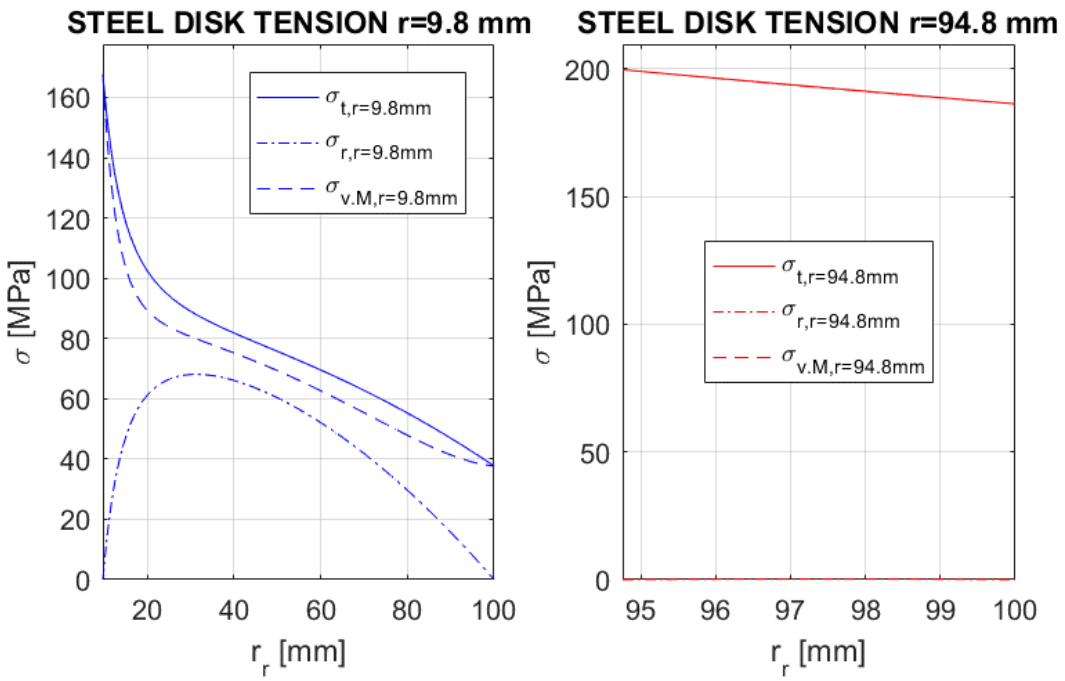

Figure 30: Stress thru the steel disks, left for r=9.8 mm and right r=94.8 mm. Note in the right figure that σ_r is almost zero and that $\sigma_{v.M}$ coincides with σ_t

Carbon fibre calculations

The calculated data for the carbon fibre flywheel solutions are presented in table 10. Figure 31 shows how the stress is distributed across the carbon fibre annular disk. The stress reaches quite high levels but they are still within the allowed region. The maximum stress recorded in the r = 71.9 mm cases is 500 MPa and the max allowed stress is 500 MPa. When it comes to energy, the solution with the larger inner radius (r = 71.9 mm) also has the ability to store the most energy, up to 0.63 MJ, which is quite a bit more than the proposed 15 kW Volvo system which could hold up to 0.21 MJ. The r = 42.3 mm test also shows great energy storing ability with up to 0.49 MJ. The energy per price unit [kJ/SEK] is 0.37 kJ/SEK for the smaller radius and 0.48 kJ/SEK for the r = 71.9 mm solution.

$\sigma_{a,C.F} = 500$ [MPa] $\omega = 5740$ [rad/s] Price* = 1300 SEK	r = 42.3 mm	r = 71.9 mm
b	118 mm	200 mm
$\sigma_{v.M,max}$	469 MPa	500 MPa
$\sigma_{t,max}$	469 MPa	500 MPa
$\sigma_{r,max}$	75 MPa	18 MPa
E	0.49 MJ	0.63 MJ
E/Price	0.37 kJ/SEK	0.48 kJ/SEK

*Table 10: Data calculated for the carbon fibre flywheel solution. *Raw material price, not manufacturing cost.*

The r = 42.3 mm solution does not reach 500 MPa, which means that technically there is a little bit more energy to be extracted from that solution. However, it still does not surpass the energy level of the r = 71.9 mm solution.

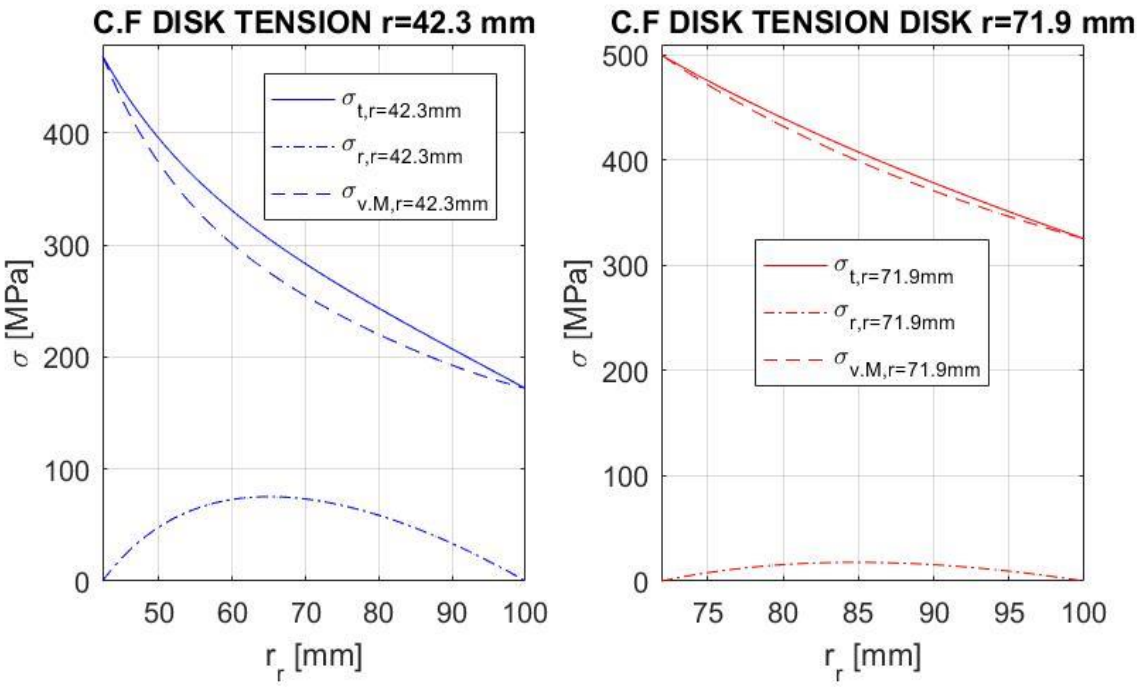

Figure 31: Tension thru the carbon fibre disks, left for r=42.3 mm and right r=71.9 mm.

5.4.3. Summary and evaluation of dimension calculations

The hypothesis stated earlier namely that it is more efficient to increase the angular velocity and radius than the mass can now be answered. It can be concluded that all computations show for both steel and C.F flywheels that more energy is found in the disks where most of the mass is concentrated at a wider radius. In other words, to gain as much energy as possible in a flywheel, it should be designed for a high angular velocity with a large width and a large radius with respect to how much stress the material allows.

Based on this evaluation process it is clear that a carbon fibre is the superior choice of the two materials in almost every category. The only area where the steel disk had a better result than C.F was concerning the price. Steel had both a much lower raw material cost and scored well in energy per price unit. But despite this, a steel flywheel cannot in any way be recommended when evaluated with the assumptions and limitations set in this test. In the later part, when the best ratio already was set (dimension optimization, section 5.4.2) the steel solution could not simply manage the demanded requirements of at least one fourth of the yield stress while also storing a substantial amount of energy.

So this dimension calculation section ends up with a recommendation of an epoxy carbon fibre flywheel as the optimal solution. This is partly due to the materials great energy storability and much higher safety factor against yield strength than the steel alternative, when tested at the same speed. The recommended dimensions are straight from the most energy dense solution, outer radius R = 100 mm, inner radius r = 72 mm, width b = 200 mm, angular velocity ω = 5740 rad/s (55 000 rpm). These recommendations obviously only apply under circumstances similar to this tests limitations and assumptions. Especially note that the carbon fibre is assumed to be isotropic, this is not the case for all composites. The isotropic assumption may also be the largest reliability issue in the results. Finally, the flywheel should

be designed so it can withstand high speeds and have most of the mass on a large radius, this in order to store as much energy as possible.

The radial displacement u at ω = 5740 rad/s, for the recommended flywheel design is computed via equation 10 to be 250 µm at the inner radius r. This is also the maximum radial displacement. The module of elasticity E_{CF} for the epoxy carbon fibre is 142 GPa.

$$u = \frac{(3+\nu)(1-\nu)}{8\,E_{CF}}\left(R^2 + r^2 - \frac{1+\nu}{3+\nu}r^2 + \frac{1+\nu}{1-\nu}R^2\right)\rho\omega^2 r \quad . \; . \; . (10)$$

5.4.4. FEM verification of stress calculations

To verify the results from the previously presented dimension and stress calculations section 5.4, the Finite Element Method (FEM) software built into the Computer Aided Design (CAD) programme CATIA were used. The specific load case and limitations used previously were applied to a model of a solid annular disc. Another scenario was also tested where a generic hub was placed with a pressure fitting connection inside of the annular disc. This was to prove that the addition of a hub would significantly increase the stress levels. For much more detailed information about the modelling of flywheel and hub, see appendix 3.

The results from the FEM analysis show that the highest stress levels occur, as calculated in section 5.4.2, at the inner radius of the flywheel. The levels then decrease as the radius increase. It can also be observed that the most critical stress is occurring in the tangential direction with levels around 530 MPa. The stress in the radial direction are low enough (about 30 MPa) to be neglected for the purposes of this report. Worth mentioning is that all of these results are when the flywheel is rotating at maximum rotational speed of 55 000 rpm. For a more detailed analysis and description see, appendix 3.

When considering the flywheel and hub assembly there are an increase in the maximum stress levels. The stress at the inner radius of the flywheel reaches around 800 to 860 MPa in the tangential direction. In this instance only the stress levels in the annular disc with respect to forces applied by the inner hub are regarded. This means that the stress occurring on for example the spokes of the flywheel are not of great interest. Whilst the stress in the tangential direction increased by a factor of about 1.5-2, the stress in the radial direction increased with almost a factor of 10. This means that the v.M stress, which takes all stresses in principal direction into account, reaches levels of about 980 to 990 MPa. With all of these values taken into consideration it can be concluded that the stress levels do increase with the addition of a hub on the inside of the flywheel. For a more detailed analysis and description of this, see appendix 3.

In summation the results from the analysis with only a flywheel did coincide very well with the values calculated previously in Matlab. Also the hypothesis that the addition of a flywheel hub will increase the stress levels in the flywheel can also be confirmed with the data attained from the FEM analysis.

5.5. Recommendations

When considering the research, interviews and calculations presented earlier in this chapter, some conclusions can be made that can be seen as recommendations for further investigation. The calculations will also be subject to further investigation since, in part C, FEM computer simulations are going to be made to examine the validity of the results. The recommendations are divided into subcategories. It is important to note that this is not a conclusive view of for example all forms of CVT's, all types of flywheel solutions or all types of available variations of flywheel material. It is only a narrow detail study of solutions found to be applied or applicable into consumer cars. This has to be taken into consideration when assimilating these recommendations.

5.5.1. Type of flywheel system

It is concluded from the research that a MF system is more suitable for mass production purposes. This is in part due to the relatively low cost, since it does not require high voltage circuits, and is thus able to use the wiring currently available in most cars. Furthermore, it has a lower complexity when compared to for example an electro-mechanical system. This is partly because of the previously mentioned electric infrastructure in the car, and also in part due to mechanical system having a higher power per weight unit. Lastly, as of now, the system is closer to being implemented in passenger cars.

5.5.2. Output power of system

When it comes to the maximum amount of output power that the system can produce, it governs the weight of the system as well as volume and cost. From what can be gathered by the researched information, it is preferable to have a lower maximum output power system. This is mostly because during calculations done by Volvo Cars, a 15 kW system covers up to 80% of all driving scenarios. If compared to a 60 kW system, which covers nearly a 100% of driving scenarios. Considering the much lower cost of the 15 kW system it makes sense to lower the maximum output power, since it will not affect performance significantly.

5.5.3. Material and dimension

As the dimension calculation section showed, an epoxy carbon fiber solution is the preferable choice for the flywheel itself. This is due to it having a much higher energy storability in relation to the stress it is able to withstand, when compared to a steel flywheel.

The dimensions of the flywheel are in this case an outer radius of 100 mm, an inner radius of 72 mm and a width of 200 mm. This when the flywheel is designed with respect to the previously stated assumptions and limitations in section 5.4. A flywheel with these dimensions would be able to withstand the stresses and strain caused by a rotation of 55 000 rpm (5740 rad/s). However, it would be preferable with a lower rpm, since this would mean a higher safety margin.

5.5.4. Flywheel gearbox

A choice of flywheel gearbox cannot be determined as a result of this detail study. It would require a more comprehensive investigation with more specific data and knowledge about the workings of a CVT and similar solutions. However, the people interviewed at Volvo Cars suggested having a closer look at the CFT system, described earlier in section 5.2, since it might have the potential to be cheaper and less complex than some of the alternatives.

5.5.5. Placement of flywheel

The optimal placement of the system varies from car to car. This depending upon variables such as space, weight distribution and how the system is connected to the wheels. If a recommendation were to be made of the most common car on the road, namely front wheel drive cars, the system would optimally be placed in the back of the car. This is partly due to the space available and the proximity to the rear axle. Also placing a mechanical system, which weigh about 60 kg in the back would improve a front wheel drive cars overall weigh distribution. This since the engine is in the front in a front wheel drive car and it is thus contributing to a lot of weight there.

6. CONCLUSIONS AND DISCUSSION

In this chapter conclusions, discussions and what is most interesting to be investigated further is presented.

6.1. Conclusions

The initial market research resulted in a description of different systems that was divided into three categories. The evaluation process that then followed revealed that when considering engine systems, a turbo compound system was regarded as the best solution with respect to the chosen criteria. When it came to chassis systems LMD achieved the highest score and was thus concluded to be the preferable alternative. Lastly the braking system matrix showed that an EMBR is prior to the other braking systems. The final matrix showed that the EMBR was superior to the best systems from all categories. However, it was concluded that a FRB system was a more interesting research subject to investigate further.

The detail study of the FRB system revealed that there are two types of major systems currently under development, namely mechanical FRB and electro-mechanical FRB. The systems chosen for further evaluation was the mechanical FRB solution. This was partly due to it being more tested in passenger cars. Furthermore, a MF is less expensive compared to an equivalently powered battery solution. In addition, an MF solution can be installed with the current electrical infrastructure present in most passenger cars. Some negative aspects of a MF system are that it has lower capacity to sustain its SOC, it does produce quite a bit of sound. Lastly it is difficult to compare it to battery powered solutions due to the differences in the design and function of the different systems.

Further conclusions that was made regarding the flywheel itself was that a light weight, fast rotating flywheel is preferable to a heavy, slow rotating flywheel. The flywheel should also be designed so that the mass is concentrated at large radius, for maximum energy storability. Therefore, a lightweight high strength material is to be recommended such as an epoxy carbon fibre material. When it comes to the stress levels in a flywheel it was concluded that the highest stress levels where attained on the inner surface, this in a tangential direction. The radial stress was furthermore concluded to be relatively low, however it did increase a lot when adding an inner hub of some description.

6.2. Suggestions for further investigation

Regarding what can be done in further investigations of the MF solution it should be said that a more precise use case has to be determined in order to draw more specific conclusions. This especially concerning the type of flywheel transmission that is going to be used and where the entire system is to be placed. The last mentioned constraint is very important since it dictates which volume and weight the system is allowed to have. Also the maximum amount of output power required by the system is important to specify. This since the use cases and function of the system is very dependent on what power can be produced.

Also of great interest when conducting further research on this type of system is a more precise material analysis, a more conclusive inner hub design and a safe design and material of the outer casing of the flywheel. The last mentioned aspect is important as the system must be used without endangering passengers and the surrounding environment.

6.3. Discussion

The concept of a flywheel regenerative braking system is a promising prospect. It has a great potential when it comes to energy regeneration and cost. However, to fully utilize the many upsides of the systems more companies and other stakeholders have to engage in the development and research. As of right now there are only a few committed to make the technology more plausible for use in every day cars. It would probably also be preferable if there were to be a car designed specifically from the ground up with a MF system in mind. This would enable the car to be more optimized when it comes to the placement and size of the system. It is believed by the authors of this project that a small car designed for city driving would benefit immensely from a MF system, since there are many starts and stops while queuing and such in big cities. This solution is however not realistic since there are many other components in an ICE powered car taking up space.

Lastly it can be concluded that battery systems are more widely used and implemented than MF type of systems. This could in part be due to the momentum that battery power has as of right now, and the number of companies that invest in the technology. It could also be due to the flywheel being of higher safety concern since it has a high rotating speed and the potential of harming passengers and others. Also the problem with a fast discharge of the energy available in the flywheel could be of concern to those interested in flywheel technology. It is therefore believed by the authors that MF could be a future technology or at least a step in between the technology of today and the solutions of tomorrow.

7. REFERENCES

Ashley, S. (den 08 July 2014). *SAE INTERNATIONAL*. Hämtat från Punch Powertrain pushes its flywheel-CVT hybrid technology: http://articles.sae.org/13226/

Bingley, L. (Regissör). (2013). *Volvo V60 KERS prototype* [Film]. GreenMotor.co.uk. Hämtat från https://www.youtube.com/watch?v=VP13yhEnxes

BMW. (u.d.). Hämtat från Power from your brake pedal: http://www.bmw.com/com/en/insights/technology/efficient_dynamics/phase_2/technologies/brake_energy_regeneration.html den 16 Februari 2016

Boretti, A. (2010). Comparison of fuel economies of high efficiency diesel and hydrogen engines powering a compact car with a flywheel based kinetic energy recovery systems. *International Journal of Hydrogen Energy*, 8417-8424.

Burn, J. (den 25 Mars 2014). *Auto EXPRESS*. Hämtat från Volvo flywheel KERS tech revealed: http://www.autoexpress.co.uk/volvo/s60/86320/volvo-flywheel-kers-tech-revealed

Burns, C. (den 27 1 2014). *theguardian*. Hämtat från Can flywheel technology drive out the battery from car hybrids?: https://www.theguardian.com/science/blog/2014/jan/27/flywheel-hybrid-flybrid

Cobb, J. (den 8 May 2014). *Hybrid Cars*. Hämtat från The Three Main Types Of Hybrids Explained - HybridCars.com: http://www.hybridcars.com/the-three-main-types-of-hybrids-explained/ den 16 Februari 2016

Crowe, P. (den 27 3 2014). *hybridCARS*. Hämtat från Volvo Testing KERS Technology For Your Next Car: http://www.hybridcars.com/volvo-testing-kers-technology-for-your-next-car/

Cuspinera, P., & Alejandro, L. (2013). *Optimal control of a flywheel-based automotive kinetic energy recovery system*. Sussex: ProQuest Dissertations Publishing.

Dahlberg, T. (2001). *Teknisk hållfasthetslära*. Lund: Studentlitteratur AB.

Daryl, E. (den 7 5 2015). *Clean Technica*. Hämtat från New EV Technology Aims To Increase Range: Regenerative Suspension System: http://cleantechnica.com/2015/05/07/new-ev-technology-promises-double-range-regenerative-suspension-system/

Dhand, A., & Pullen, K. (2013). Review of flywheel based internal combustion engine hybrid vehicles. *International Journal of Automotive Technology*, 797-804.

Dhand, A., & Pullen, K. (2015). Review of battery electric vehicle propulsion systems incorporating flywheel energy storage. *INTERNATIONAL JOURNAL OF AUTOMOTIVE TECHNOLOGY*, 487 - 500. doi:10.1007/s12239-015-0051-0

Francesco, O., Igor, N., Helios, V., & Luca, G. (2013). Nonlinear vibration energy harvesting at work: an application for the automotive sector. *Circuits and Systems (ISCAS), 2013 IEEE International Symposium on*, 2735-2738.

Gable, C., & Gable, S. (den 15 December 2014). *alternativefuels.about.com.* Hämtat från What is Regenerative Braking in a Hybrid Car?: http://alternativefuels.about.com/od/hybridvehicles/a/regenbraking.htm

Glynne-Jones, P., Beeby, S., Tudor, M., & White, N. (2004). An electromagnetic, vibration-powered generator for intelligent sensor systems. *Sensors and Actuators A: Physical*, 344-349.

Grahn, R., & Jansson, P.-Å. (2013). *Mekanik* (3 uppl.). -: Studentlitteratur.

Gysen, B. L., van der Sande, T. P., Paulides, J. J., & Lomonova, E. A. (May 2011). Efficiency of a Regenerative Direct-Drive Electromagnetic Active Suspension. *IEEE Transactions on Vehicular Technology*, ss. 1384-1393.

Hedlund, M., Lundin, J., de Santiago, J., Abrahamsson, J., & Bernhoff, H. (10 2015). Flywheel Energy Storage for Automotive Applications. *ENERGIES*, 10636 - 10663. doi:10.3390/en81010636

Ireson, N. (den 17 September 2010). *Motor Authority*. Hämtat från Jaguar Testing KERS-Like Flywheel Hybrid For XF: http://www.motorauthority.com/news/1049456_jaguar-testing-kers-like-flywheel-hybrid-for-xf#image=100322638

Ismail, Y., Chesse, P., Chalet, D., & Menegazzi, P. (2015). A methodology for evaluating the turbocompound potential for an automotive engine. *Journal of Automobile Engineering*, *229*, 1878-1893.

Jeng, T.-M., & Tzeng, S.-C. (Januari 2013). Development of Thermoelectric Conversion System for Waste Heat Recovery of Automobile Exhaust Gas. *Applied Mechanics and Materials*, 713-717.

Jörgensson, M., & Andersson, L. (den 22 Mars 2016). Volvo meeting. (J. Kindahl, & J. Fahlbeck, Intervjuare)

Jörgensson, M., Eriksson, S., Sjögren, R., Dzafic, A., Arvidsson, R., Verbakel, M., . . . Holweg, E. (2012). *F-KERS – Kinetic Energy Recovery System with mechanical flywheel sub 80g CO2 2020.* Fordonsstrategisk forskning och innovation.

Jörgensson, M., Sjögren, R., & Eriksson, S. (2013). *Volvo Car Group Flywheel KERS project.* Torslanda: Volvo Cars.

Kavianipour, O., & Montazeri-Gh, M. (2014). Road profile effects on the performance and energy regeneration of the electromagnetic suspension system. *Journal of Multi-body Dynamics*, 266-281.

Kawamoto, Y., Suda, Y., Inoue, H., & Kondo, T. (2007). Modeling of Electromagnetic Damper for Automobile Suspension. *Journal of System Design and Dynamics*, 524-535.

Khoshnoud, F., Zhang, Y., Shimura, R., Shahba, A., Jin, G., Pissanidis, G., . . . De Silva, C. W. (10 2015). Energy Regeneration From Suspension Dynamic Modes and Self-Powered Actuation. *IEEE ASME Transactions on Mechatronics*, ss. 2513-2524.

Lampton, C. (den 23 Januari 2009). *How Stuff Works.* Hämtat från How Regenerative Braking Works: http://auto.howstuffworks.com/auto-parts/brakes/brake-types/regenerative-braking.htm

Latz, G. (2007). *Waste Heat Recovery from Combustion Engines based on the Rankine Cycle.* Gothenburg: Department of Applied Mechanics CHALMERS UNIVERSITY OF TECHNOLOGY.

Legros, A., Guillaume, L., Diny, M., Zaidi, H., & Lemort, V. (2014). Comparison and Impact of Waste Heat Recovery Technologies on Passenger Car Fuel Consumption in a Normalized Driving. *Energies*, 5273-5290.

Lin, X., Yang, B., Xuexun, G., & Jun, Y. (2010). Simulation and Performance Evaluation of Hydraulic Transmission Electromagnetic Energy-regenerative Active Suspension. *2010 Second WRI Global Congress on Intelligent Systems*, (ss. 58 - 61).

Mackenzie, A. (den 24 Januari 2014). *Turbocharging and advanced hybrid tech coming to Formula 1 for 2014*. Hämtat från Gizmag: http://www.gizmag.com/formula-one-new-hybrid-tech/30560/

Mägi, M., & Melkersson, K. (2014). *LÄROBOK I MASKINELEMENT.* Göteborg: EcoDev International AB.

Maric, P. (den 11 11 2015). *Car Advice*. Hämtat från Audi working on world-first regenerative suspension system: http://www.caradvice.com.au/395598/audi-working-on-world-first-regenerative-suspension-system/

Mazda. (u.d.). Hämtat från Brake Energy Regeneration System: http://www.mazda.com/en/innovation/technology/env/i-eloop/ den 16 Februari 2016

Myszka, D. H., Murray, A., Giaier, K., Jayaprakash, V. K., & Gillum, C. (2015). A Mechanical Regenerative Brake and Launch Assist using an Open Differential and Elastic Energy Storage. *SAE International Journal of Alternative Powertrains*, 199-208.

NASA (Regissör). (2012). *NASA 360: Flywheel Energy Storage* [Film]. Hämtat från http://www.nasa.gov/mp4/642828main_nasa360-flywheel.mp4

NASA Glenn Research Center. (2015). Flywheel program. Hämtat från http://www.grc.nasa.gov/WWW/portal/pdf/flywheel.pdf

Nicolas, R. (den 10 1 2014). *The Honda 2015 F1 Power Unit explained*. Hämtat från car-engineer: http://www.car-engineer.com/honda-2015-f1-power-unit-explained/

Nieman, J. E. (2014). *A NOVEL, ELASTICALLY-BASED, REGENERATIVE BRAKE AND.* Dayton, Ohio: UNIVERSITY OF DAYTON.

Oleksowicz, S. (2013). Legal, Safety and Practical Regenerative Braking Control Challenges. *Measurement and control (London)*, 283-288.

Petrány, M. (den 22 Januari 2014). *How Formula One's Amazing New Hybrid Turbo Engine Works*. Hämtat från Jalopnik: http://jalopnik.com/how-formula-ones-amazing-new-hybrid-turbo-engine-works-1506450399

Ponce Cuspinera, L. A., & Dunne, J. F. (2015). Optimal Gear Ratio Planning for Flywheel-Based Kinetic Energy Recovery Systems in Motor Vehicles. *Journal of Dynamic Systems, Measurement, and Control*, 071012-071012-13.

Prakash, R., Christopher, D., & Kumarrathinam, K. (2015). Analysis of Surface Waste Heat Recovery in IC Engine by Using TEG. *Applied Mechanics and Materials*, 782-786.

Ramsey, J. (den 18 11 2014). *Autoblog*. Hämtat från Why turbo compounding may be the next big thing in powertrains: http://www.autoblog.com/2014/11/18/turbo-compounding-next-big-thing-powertrains/

Sherman, D. (den 12 11 2014). *Car and Driver*. Hämtat från Turbo Compounding Is the Next Big Thing in Energy Recovery: http://blog.caranddriver.com/turbo-compounding-is-the-next-big-thing-in-energy-recovery/

Solberg, G. (den 29 June 2007). *Tesla Motors*. Hämtat från The Magic of Tesla Roadster Regenerative Braking: https://www.teslamotors.com/blog/magic-tesla-roadster-regenerative-braking

Sprouse, C., & Depcik, C. (March 2013). eview of organic Rankine cycles for internal combustion engine exhaust waste heat recovery. *Applied Thermal Engineering, 51*, 711-722.

Squatriglia, C. (den 28 10 2010). *Wired*. Hämtat från KERS Comes to Cars as Jaguar Tests Flywheel Hybrid: http://www.wired.com/2010/10/flywheel-hybrid-system-for-premium-vehicles/

Torotrak (Regissör). (2010). *3D Animation: Torotrak Variator Promotional Animation 1* [Film]. Hämtat från https://www.youtube.com/watch?v=RqmJxnmx_Ew

Torotrak Development ltd . (2015). *CFT Transmission*. Hämtat från Flybrid® CFT KERS: http://cftkers.com/CFTtransmission.html

U.S Department of Energy. (u.d.). Hämtat från Where the Energy Goes: Gasoline Vehicles: http://www.fueleconomy.gov/feg/atv.shtml

Ugural, A. C., & Fenster, S. K. (2012). *Advanced Mechanics of Materials and Applied Elasticity 5th Edition* (5 uppl.). Westford, Massachusetts: Prentice Hall.

Volvo Cars. (den 26 Mars 2014). *Volvo Cars.* Hämtat från VOLVO CAR GROUP AND FLYBRID CONDUCT UK TESTING OF FLYWHEEL KERS TECHNOLOGY: https://www.media.volvocars.com/uk/en-gb/media/pressreleases/141626/volvo-car-group-and-flybrid-conduct-uk-testing-of-flywheel-kers-technology

Williams F1. (u.d.). *Case studies*. Hämtat från Successfully Incubating Technology - Flywheel Energy Storage: http://www.williamsf1.com/advanced-engineering/case-studies/incubating-technology

Williams Hybrid Power. (2013). Flywheel Energy Storage. Grove, Oxfordshire, UK. Hämtat från http://www.ukintpress-conferences.com/uploads/SPKPMW13R/d1_s1_p2_ian_foley.pdf

Xiongxin , F. (2010). A Novel Design for Flywheel Battery of Electric Vehicles. *International Conference on Intelligent System Design and Engineering Application*, (ss. 107 - 111). Shenzhen, China.

Xu, L., & Guo, X. (2010). Hydraulic Transmission Electromagnetic Energy-Regenerative Active Suspension and Its Working Principle. *2010 2nd International Workshop on Intelligent Systems and Applications* (ss. 1-5). Wuhan: Automobile Engineering School, Wuhan University of Technology. doi:10.1109/IWISA.2010.5473786

Yoong, M., Gan, Y., Gan, G., Leong, C., Phuan, Z., Cheah, B., & Chew, K. (2010). Studies of regenerative braking in electric vehicle. *2010 IEEE Conference on Sustainable Utilization and Development in Engineering and Technology* (ss. 40-45). Kuala Lumpur: IEEE.

Zhang, J.-q., Peng, Z.-z., Zhang, L., & Zhang, Y. (Juli 2013). A Review on Energy-Regenerative Suspension Systems for Vehicles. *Lecture Notes in Engineering and Computer Science*, ss. 1889 - 1892.

Zhang, Y., Huang, K., Yu, F., Gu, Y., & Li, D. (2007). Experimental verification of energy-regenerative feasibility for an automotive electrical suspension system. *IEEE International Conference on Vehicular Electronics and Safety* (ss. 1-5). IEE.

Zhang, Y., Zhang, X., Zhan, M., Guo, K., Zhao, F., & Liu, Z. (2014). Study on a novel hydraulic pumping regenerative suspension for vehicles. *Journal of the Franklin Institute*, 485-499.

Zhongjie, L., George, L., Liangjun, L., & Yi-xian , Q. (2013). Electromagnetic Energy-Harvesting Shock Absorbers: Design, Modeling, and Road Tests. *Advances in Mechanical Engineering, 62*(3), 1065 - 1074.

Zhu, Q., Mingjie, G., & Yuanqin, H. (2012). *Vibration Energy Harvesting in Automobiles to Power Wireless Sensors.* Xiamen, Fujian Province, China: Department of Mechanical and Electrical Engineering, Xiamen University.

Zuo, L., & Zhang, P.-S. (2013). Energy harvesting, ride comfort, and road handling of regenerative vehicle suspensions. *Journal of Vibration and Acoustics, 135*(1). doi:10.1115/1.4007562

Zuo, L., Scully, B., Shestani, J., & Zhou, Y. (04 2010). Design and characterization of an electromagnetic energy harvester for vehicle suspensions. *Smart Materials and Structures, 19*(4). doi:10.1088/0964-1726/19/4/045003

APPENDIX 1: QUESTIONS FOR THE VOLVO CARS VISIT

Basfrågor

- Hur kommer det sig att ni valde just en flywheel-lösning?
    - Har ni kikat på någon annan typ av regenerativ inbromsning?
- Varför valde ni en mekanisk lösning istället för exempelvis en elektrisk?
    - Till skillnad från Porsche och andra tillverkare.
    - Vad tror ni om svänghjulets potential i en elektrisk applikation, det vill säga när det används som en typ av batteri?
- Hur ser ni på svänghjuls-konceptets framtid?
    - Är det möjligt att göra det tillräckligt billigt att tillverka för att det skall gå att implementera i Volvos kommande modeller?
- Säkerhetsaspekten, är det något ni har utvärderat eller konstruerat mot i nuläget?
    - Hur fungerar själva höljet? Ev. material och tjocklek
    - Hur påverkar detta vikten av systemet?

Tekniska frågor

- **EXAKTA DIMENSIONER PÅ SVÄNGJUL!!!!!**
- **Volym för hela lösningen – hela systemet**
    - **Hur mycket plats finns i baggagelucka?**
- Vad är det för komponenter som ingår i kopplingen mellan hjul och flywheel?
    - Vad är det som styr när själva systemet skall användas till acceleration och retardation?
- Vad väger svänghjulet?
    - Vilket material är svänghjulet tillverkat av?
    - Varför har ni valt det materialet?
    - Varför inte ex. en solid stål-skiva
- Påverkas inbromsningsförmågan något av systemet, negativt eller positivt?
    - Finns det några svårigheter vare det gäller inbromsningsförmåga som man måste lösa innan konceptet är redo att användas kommersiellt?
    - Hur hanterar systemet olika bromsfall? Ex. inbromsningar i högre vs. Lägre hastigheter.
- Vilken typ av variator är det ni använder?
    - Hur kom ni fram till att ni skulle ha just en variator-lösning och inte exempelvis slirkopplingslösning eller remvariator?
- Vad har ni för lagring på svänghjulet?
    - Hur kom ni fram till att ni skulle använda den typen av lagring?
    - Ev. följdfrågor: ”Har ni kollat något på magnetisk lagring?”, ”varför inte använda konventionell lagring?”
- Vad är det för körcykel som användes när ni kom fram till siffran upp till 25 %?

APPENDIX 2: MATLAB CODE FOR THE CALCULATIONS

```
%%  OBJEKTIVE: RELATIONSHIP BETWEEN R/B FOR MAX ENERGY WITH RESPEKT TO
% STRENGTH OF MATERIALS
% Test different size on width and inner radius for a given mass m.
% Control the tension related to the size of inner radius.
clc
clear all
clf
n=4000;
m=5; b=linspace(0.2,0.0965,n); v=[0.29;0.33]; k=1;
rho=[7800;1650]; %w=[500; 1000; 1500; 2000; 4000; 6000;7000];
w=linspace(500, 7000, n);
R=0.1; sigma_till=[800/4; 2000/4]; % Four times safety against yield
for j=1:length(rho) % Loop for both materials
    r=@(b)sqrt(R^2-m./(pi.*b*rho(j)));
    rb=r(b);
    m=(R^2-rb.^2)*pi.*b*rho(j); % Only control
    rbb=rb./b;
    I(j,:)=1/2.*m.*(R^2+rb.^2); % Inertia


    for i=1:length(w) % Loop for different angular velocity
        E(:,i)=1/2*I(j,:).*w(i)^2; % Energy value with different radius
        sigma_r(:,i)=(3+v(j))/8*(R^2-rb.^2)*rho(j)*w(i)^2; % Radial stress
[Pa]
        sigma_r_mpa(:,i)=sigma_r(:,i)*10^-6; % Radial stress [MPa]
        sigma_t(:,i)=(3+v(j))/8*(2*R^2+rb.^2-
(1+3*v(j))/(3+v(j)).*rb.^2)*rho(j)*w(i)^2; % Tangential stress [Pa]
        sigma_t_mpa(:,i)=sigma_t(:,i)*10^-6; % Tangential stress [MPa]
        sigma_VM(:,i)=sqrt(1/2.*((sigma_t_mpa(:,i)-
sigma_r_mpa(:,i)).^2+sigma_t_mpa(:,i).^2+sigma_r_mpa(:,i).^2)); % v.M
stress [MPa]

        if sigma_t_mpa(:,i)<sigma_till(j) % Control if the material manage
the load.

        else
            break
        end
    end

    if j==1 % Plot graph's for steel
        text1='STEEL: w is %4.0f rad/s and r/d is %4.3f with Emax %4.3f MJ
\n' ;
        fprintf(text1,w(i-1), rbb(1), max(E(:,i-1))*1e-6)

        figure(1)
        subplot(1,2,1)
        plot(rb,sigma_VM(:,i-1), 'b'), hold on, grid on, %Visar hur
V.M_spanningen okar vid olika varden på r
        plot(rb,sigma_t_mpa(:,i-1), 'r'), hold on %Visar hur t_spanningen
okar vid olika varden på r
        plot(rb,sigma_r_mpa(:,i-1), 'g'), hold on, axis([min(rb) max(rb) 0
220]),  %Visar hur r_spanning okar vid olika startvarden på r
        title(['STEEL '])
        xlabel('r [m]'), ylabel('\sigma [MPa]')
        legend('\sigma_v_._M_,_S_T_E_E_L', '\sigma_t_,_S_T_E_E_L',
'\sigma_r_,_S_T_E_E_L', 'location', 'best')
        subplot(1,2,2)
        plot(E(:,i-1),rb./b,'b'), hold on, grid on
```

```
        scatter(max(E(:,i-1)),rbb(1), 'filled', 'r')
        title('STEEL Energy dense ratio')
        xlabel('E [MJ]'), ylabel('r/b')
        k=k+1;

    elseif j==2 % Plot graph's for carbon fibre
        text1='CARBON FIBER: w is %4.0f rad/s and r/d is %4.3f with Emax
%4.3f MJ \n' ;
        fprintf(text1,w(i-1), rbb(1), E(1,i-1)*1e-6)

        figure(k)
        subplot(1,2,1)
        plot(rb,sigma_VM(:,i-1), 'b'), hold on, grid on, %Visar hur
V.M_spanningen okar vid olika varden på r
        plot(rb,sigma_t_mpa(:,i-1), 'r'), hold on %Visar hur t_spanningen
okar vid olika varden på r
        plot(rb,sigma_r_mpa(:,i-1), 'g'), hold on, axis([min(rb) max(rb) 0
550]),  %Visar hur r_spanning okar vid olika startvarden på r
        title(['Carbon fibre'])
        xlabel('r [m]'), ylabel('\sigma [MPa]')
        legend('\sigma_v_._M_,_C_._F', '\sigma_t_,_C_._F',
'\sigma_r_,_C_._F', 'location', 'best')
        subplot(1,2,2)
        plot(E(:,i-1),rb./b,'b'), hold on, grid on
        scatter(max(E(:,i-1)),rbb(1), 'filled', 'r')
        title('C.F. Energy dense ratio')
        xlabel('E [MJ]'), ylabel('r/b')
    end

end
```

```
%% OBJEKTIVE: CALCULATION OF r AND b, TENSIONS THROUGH THE DISK AND
% STORABLE ENERGY FOR THE STEEL SOLUTION.
clear all
clc
clf
m=5; rho=7800; R=0.1; c=0.474; w=1615; v=0.29;
f=@(b)rho*pi.*(R^2-(c.*b).^2).*b-m; % volume - mass expressed in f(b)
df=@(b)rho*pi*(R^2-3*c^2*b^2); % df(b)/db
b=linspace(0.01,0.22);
figure(1)
plot(b,f(b)), hold on, grid on % Displays f(b) and approx zeros is found
title('STEEL: Find f(b)=0'), xlabel('b [m]'), ylabel('f(b)')
x0=[0;0.15]; % Approximant zeros for width
kmax=20; tol=0.5e-8;
for i=1:length(x0) % Newton's method f(b)=0
    x=x0(i);
    for j=1:kmax
        d=-f(x)/df(x);
        x=x+d;
        if abs(x)<tol, break, end
    end
    scatter(x,f(x), 'filled','r')
    k(i)=x; % Exact zeros for the f(b) equation
end

for i=1:length(k)
    r=k(i)*c; % Radius corresponding to the width
```

```
    m=rho*pi*(R^2-r^2)*r/c; % Control m=5 kg
    rr=linspace(r,R); % Radius thru the annular disk
    I=1/2*(R^2+r^2)*m;
    E=1/2*I*w^2*10^-6; % Energy in MJ
    price=m*3.5;
    sigma_r(:,i)=(3+v)/8*(R^2+r^2-rr.^2-R^2*r^2./rr.^2)*rho*w^2; % Radial
stress
    sigma_r_mpa(:,i)=sigma_r(:,i)*10^(-6);
    sigma_t(:,i)=(3+v)/8*(R^2+r^2-
(1+3*v)/(3+v).*rr.^2+R^2*r^2./rr.^2).*rho*w^2; % Tangential stress
    sigma_t_mpa(:,i)=sigma_t(:,i)*10^(-6);
    sigma_VM(:,i)=sqrt(1/2.*((sigma_t_mpa(:,i)-
sigma_r_mpa(:,i)).^2+sigma_t_mpa(:,i).^2+sigma_r_mpa(:,i).^2)); % v.M
stress
    text_4=('Sigma_v.M = %4.1f [MPa], Sigma_t,max = %4.1f [MPa],
Sigma_r,max = %4.1f [MPa], r = %4.2f [mm]\nd = %4.1f [mm], E = %4.3f [MJ],
m = %4.1f [kg], price = %4.2f [SEK], Energy/price = %4.2f [KJ/SEK] \n \n');
    ec=E*10^3/price;
    fprintf(text_4, max(sigma_VM(:,i)), max(sigma_t_mpa(:,i)),
max(sigma_r_mpa(:,i)),r*1000,k(i)*1000, E, m, price, ec)
    rmm=1000.*rr; % rr in mm

    if i==1 % Plot's first r and b solution
        figure(2)
        subplot(1,2,1)
        plot(rmm,sigma_t_mpa(:,i), 'b'), hold on
        plot(rmm,sigma_r_mpa(:,i), '-.b'), hold on
        plot(rmm,sigma_VM(:,i),'--b'), hold on, grid on
        title('STEEL DISK TENSION r=9.8 mm'), xlabel('r_r [mm]'),
ylabel('\sigma [MPa]')
        legend('\sigma_t_,_r_=_9_._8_m_m',
'\sigma_r_,_r_=_9_._8_m_m','\sigma_v_._M_,_r_=_9_._8_m_m', 'Location',
'NE')
        axis([r*1000 R*1000 0 max(sigma_VM(:,i))+10])
    elseif i==2 % Plot's second r and b solution
        subplot(1,2,2)
        plot(rmm,sigma_t_mpa(:,i), 'r'), hold on
        plot(rmm,sigma_r_mpa(:,i), '-.r'), hold on
        plot(rmm,sigma_VM(:,i),'--r'), hold on, grid on
        title('STEEL DISK TENSION r=94.8 mm'), xlabel('r_r [mm]'),
ylabel('\sigma [MPa]')
        legend('\sigma_t_,_r_=_9_4_._8_m_m',
'\sigma_r_,_r_=_9_4_._8_m_m','\sigma_v_._M_,_r_=_9_4_._8_m_m', 'Location',
'best')
        axis([r*1000 R*1000 0 max(sigma_VM(:,i))+10])
    end
end

%% OBJEKTIVE: CALCULATION OF r AND b, TENSIONS THROUGH THE DISK AND
% STORABLE ENERGY FOR THE CARBON FIBRE SOLUTION.
clear all
clc
clf
m=5; rho=1650; R=0.1; c=0.360; w=5740; v=0.33;
f=@(b)rho*pi.*(R^2-(c.*b).^2).*b-m; % volume - mass expressed in f(b)
df=@(b)rho*pi*(R^2-3*c^2*b^2); % df(b)/db
b=linspace(0.090,0.21);
figure(1)
plot(b,f(b)), hold on, grid on % Displays f(b) and approx zeros is found
title('C.F: Find f(b)=0'), xlabel('b [m]'), ylabel('f(b)')
x0=[0.1;0.18]; % Approximant zeros for width
```

```
kmax=20; tol=0.5e-8;
for i=1:length(x0) % Newton's method f(b)=0
    x=x0(i);
    for j=1:kmax
        d=-f(x)/df(x);
        x=x+d;
        if abs(x)<tol, break, end
    end
    scatter(x,f(x), 'filled','r')
    k(i)=x; % Exact zeros for the f(b) equation
end
for i=1:length(k)
    r=c*k(i); % Radius corresponding to the width
    m=rho*pi*(R^2-r^2)*r/c; % Control m=5 kg
    rr=linspace(r,R); % Radius thru the annular disk
    I=1/2*(R^2+r^2)*m;
    E=1/2*I*w^2*10^-6; % Energy in MJ
    price=m*260;
    sigma_r(:,i)=(3+v)/8*(R^2+r^2-rr.^2-R^2*r^2./rr.^2)*rho*w^2; % Radial
stress
    sigma_r_mpa(:,i)=sigma_r(:,i)*10^(-6);
    sigma_t(:,i)=(3+v)/8*(R^2+r^2-
(1+3*v)/(3+v).*rr.^2+R^2*r^2./rr.^2).*rho*w^2; % Tangential stress
    sigma_t_mpa(:,i)=sigma_t(:,i)*10^(-6);
    sigma_VM(:,i)=sqrt(1/2.*((sigma_t_mpa(:,i)-
sigma_r_mpa(:,i)).^2+sigma_t_mpa(:,i).^2+sigma_r_mpa(:,i).^2)); % v.M
stress
    text_4=('Sigma_v.M = %3.1f [MPa], Sigma_t,max = %3.1f [MPa],
Sigma_r,max = %3.1f [MPa], r = %3.1f [mm]\nd = %3.1f [mm], E = %4.3f [MJ],
m = %4.1f [kg], price = %4.2f [SEK], Energy/price = %4.2f [KJ/SEK] \n \n');
    ec=E*10^3/price;
    fprintf(text_4, max(sigma_VM(:,i)), max(sigma_t_mpa(:,i)),
max(sigma_r_mpa(:,i)),r*1000,k(i)*1000, E, m, price, ec)
    rmm=1000.*rr; % rr in mm

    if i==1 % Plot's first r and b solution
        figure(2)
        subplot(1,2,1)
        plot(rmm,sigma_t_mpa(:,i), 'b'), hold on
        plot(rmm,sigma_r_mpa(:,i), '-.b'), hold on
        plot(rmm,sigma_VM(:,i),'--b'), hold on, grid on
        title('C.F DISK TENSION r=42.3 mm'), xlabel('r_r [mm]'),
ylabel('\sigma [MPa]')
        legend('\sigma_t_,_r_=_3_8_._8_m_m',
'\sigma_r_,_r_=_3_8_._8_m_m','\sigma_v_._M_,_r_=_3_8_._8_m_m', 'Location',
'NE')
        axis([r*1000 R*1000 0 max(sigma_VM(:,i))+10])
    elseif i==2 % Plot's second r and b solution
        subplot(1,2,2)
        plot(rmm,sigma_t_mpa(:,i), 'r'), hold on
        plot(rmm,sigma_r_mpa(:,i), '-.r'), hold on
        plot(rmm,sigma_VM(:,i),'--r'), hold on, grid on
        title('C.F DISK TENSION DISK r=71.9 mm'), xlabel('r_r [mm]'),
ylabel('\sigma [MPa]')

legend('\sigma_t_,_r_=_7_4_._8_m_m','\sigma_r_,_r_=_7_4_._8_m_m','\sigma_v_
._M_,_r_=_7_4_._8_m_m', 'Location', 'best')
        axis([r*1000 R*1000 0 max(sigma_VM(:,i))+10])
    end
end
```

APPENDIX 3: VARIFICATION OF STRESS CALCULATIONS

In this chapter the results from the earlier conducted dimension calculation is verified. The verifications are conducted using the Finite Element Method (FEM) software built into the Computer Aided Design (CAD) programme CATIA V5, for a carbon fibre flywheel. Also an exemplified design of a complete flywheel with an inner hub is demonstrated.

All computations are based upon the dimensions showed in figure 32. They are straight from the recommendations presented in the detailed study. The flywheel is evaluated at an angular velocity of 55 000 rpm. Note that the carbon fibre material is assumed to behave isotropically.

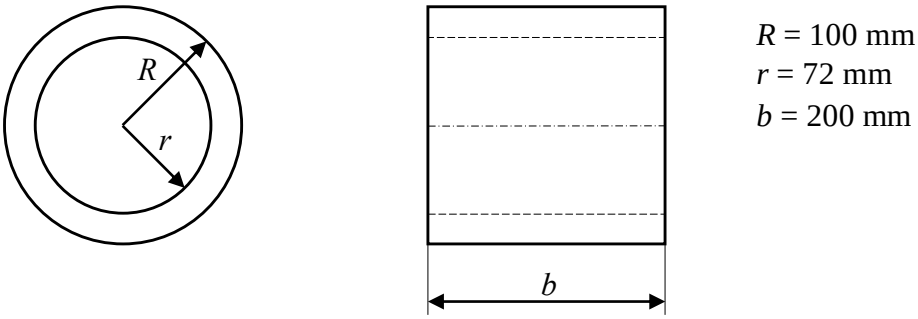

Figure 32: Flywheel design, without inner hub.

The concept with FEM is to divide the design into tiny, finite, elements and then approximately calculate the targeted quantities for each element. In this chapter a triangular mesh is used, where the elements are tetrahedron shaped and divided over the mesh for a solid design. Two types of triangular mesh, linear or parabolic are used and compared. The main difference between linear and parabolic is that linear has a linear shape between the nodes and the parabolic has a parabolic shape between the nodes, thus making the parabolic much more resource intensive to calculate. The whole idea of FEM is to find a good enough representation of the studied case to be able to draw some conclusions from the results. Thus it is important to try different constraints while modelling to ensure that the results are as reliable as possible.

Another important thing to note when it comes to the FEM software built into CATIA is that the mesh for each part is calculated automatically. The size of the elements and the sag[12] between them can thereafter be set to fine tune the results. Later in this chapter tables will be presented where size and sag are important. This because it is necessary when doing a FEM analysis to find a good size of sag and elements to ensure a good result while not having to utilize too much computer power.

The analytical results to which the FEM computations will be compared to are presented in table 11.

Max Radial stress	18 MPa
Max Tangential stress	500 MPa
Max v.M stress	500 MPa
Max Displacement	250 μm

Table 11: Calculated results from part B

[12] Sag is a program specific option that is available in CATIA. It basically decides some dimension specifics about the tetrahedron.

CAD modelling

The parts used in this FEM chapter are modelled using a CAD software called CATIA V5. This program enables the user to both design and to some extent test parts virtually.

There are two parts modelled in this chapter and both are modelled as solids. The first is the flywheel, which is the outer ring of the design, see figure 33 (left). The other part is the hub, which is the part of the design that is shrink fitted into the flywheel, see figure 33 (right). The dimensions of the flywheel are taken directly from the previous dimension calculations in section 5.4, where both width *b* and inner radius *r* were calculated. The dimensions and design of the hub are partly based on the dimensions of the flywheel, such as the radius of the hub, and partly based on estimations from observing the lower powered Volvo-Torotrak system mentioned in an earlier chapter. It is not deemed necessary to make calculations verifying the optimal dimension ratios of the hub at this time since the hub is only incorporated into the FEM computations to test the hypothesis that a shrink fitted part inside of the flywheel will increase the stresses it have to sustain.

The material of the flywheel was also specified in the dimension calculations section in 5.4. It was decided to be a type of carbon fibre epoxy composite and thus the material properties of this material is incorporated into the software and applied to the part. The material applied to the hub is steel. The type of steel used is the pre-programmed steel already available in the software. The reason for doing this is that, since the dimensions are not definitely determined, it is hard to correctly decide a material. Because of this a generic type of steel will suffice. Although, it should be said that the reason for choosing steel in the first place is due to the hub of the Volvo-Torotrak system is being made of steel.

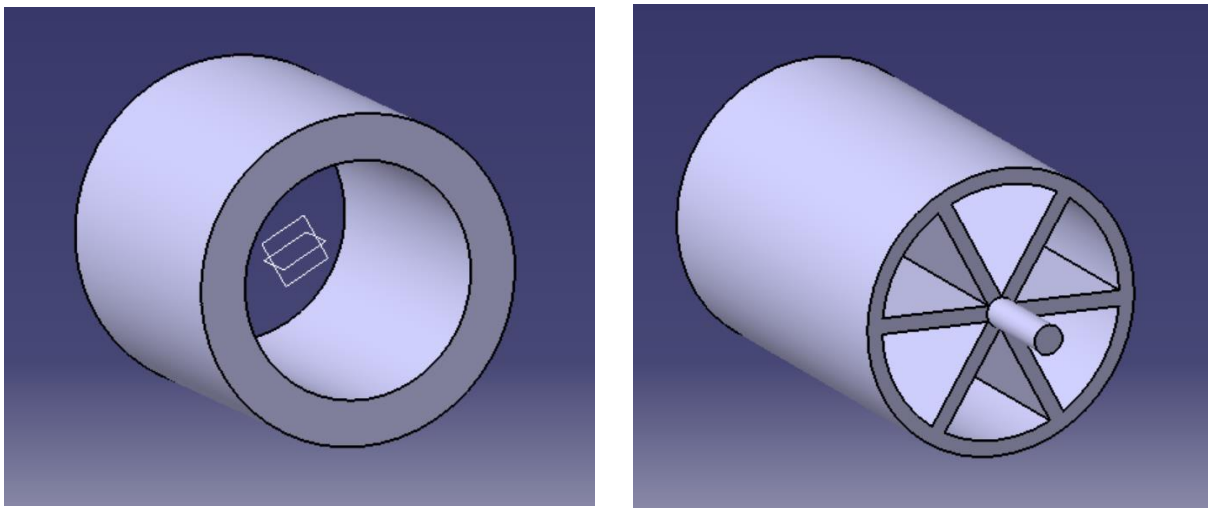

Figure 33: To the left, outer flywheel part as designed in CAD. To the right, hub part as designed in CAD.

As can be seen in figure 33, both the flywheel and the hub are symmetrical around a central axis. This is important to keep in mind later on when analyzing the results of the FEM simulations. The calculations conducted in the next section are done in two parts, one with only the flywheel and one with the hub shrink fitted into the flywheel. The constraints applied to the parts to make the shrink fitting are described there. The only constraints applied in the

CAD-model is an axial and edge coincidence constrain to join the two parts together in an assembly, see figure 34.

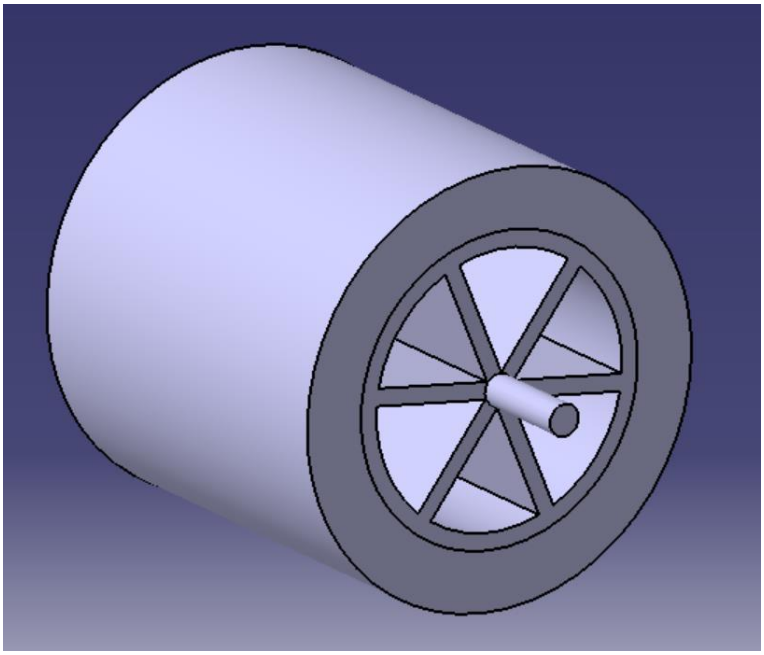

Figure 34: Assembly with both flywheel and hub.

FEM modelling

When modelling with finite elements in CATIA it is important to first define the correct constraints to make sure that the part behave in a realistic way when subjected to the intended load. The constraints applied to the parts are presented in each section. After this it is necessary to apply of load, which in the case of both only flywheel and in the flywheel-hub assembly is a rotational load called “rotation force” in CATIA, applied to the centre of the flywheel/hub. The rotational speed of this rotation force is set to be 55 000 rpm, as defined in the dimension calculations section. The FEM simulations are divided into two parts. One being only the flywheel and one being flywheel and inner hub.

Flywheel

In this section the FEM results with only the flywheel is presented.

The purpose of these simulations is to try to compare them to the calculations presented in the dimension calculations section 5.4. Because the calculations there are based on a flywheel, without hub and with no preload forces it is important to make the correct assumptions when simulating in the FEM programme.

Constraints and load on flywheel

A clamp constraint was put on something called a “smooth virtual part” on each side of the flywheel, see figure 35. This enabled the program to put the constraint in the middle of a surface with a hole in it, such as the flywheel. If some other constraint were to be put on the part, for example a “user defined restraint” or a clamp on the actual side of the flywheel, the result would be that large parts of the surface would experience stress concentrations.

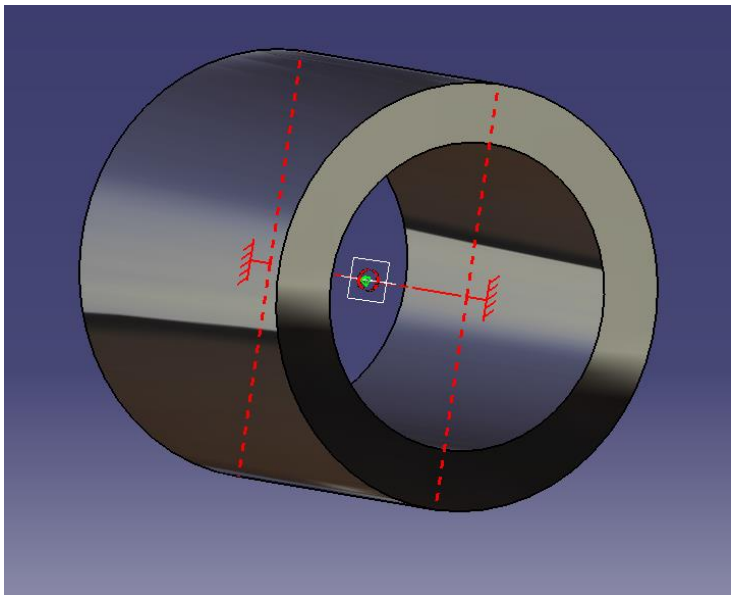

Figure 35: Constraints put on the flywheel

The load applied to the flywheel was, as mentioned in a previous section, a rotational force with a rotational speed of 55 000 rpm. This was done to match the analytical calculations as closely as possible.

Results flywheel

The results presented in table 12 are divided into two groups, namely linear and parabolic. The difference between these two is mentioned in the introduction section of this chapter. The interesting numerical results from this simulation is von Mises stress, principal stress and to some extent translational displacement for different mesh and sag sizes. This since the values are going to be compared, not only to the analytical calculations but also to the material data of the carbon fibre used in the flywheel. The numbers presented in table 12 are the maximum values for each parameter respectively. Note that all the values in table 12 appear at the inner radius of the flywheel.

LINEAR MESH			
Size	v.M	Tangential stress	Radial displacement
20x2	471 MPa	553 MPa	232 μm
10x1	472 MPa	540 MPa	240 μm
7x0.7	457 MPa	525 MPa	235 μm
5x0.5	461 MPa	520 MPa	236 μm
3x0.3	459 MPa	512 MPa	236 μm
PARABOLIC MESH			
Size	v.M	Tangential stress	Radial displacement
20x2	463 MPa	521 MPa	238 μm
10x1	460 MPa	518 MPa	240 μm
7x0.7	456 MPa	518 MPa	243 μm

Table 12: Data collected for the flywheel only. Note that size is "mesh size" x "absolute sag".

Table 12 shows that the difference between linear and parabolic mesh structure in this case is pretty small. Although not as many low mesh size computations were conducted with the parabolic structure as with the linear due to the parabolic being more computationally intensive. The maximum stress, both in the tangential direction and the v.M stress were achieved at the inner radius of the flywheel. The v.M stress was in the range of 450-470 MPa, regardless of if the mesh grid was computed in a parabolic or linear manner. The tangential stress was calculated to be around 520-550 MPa. This is to be expected since the constraints and the load case is very simple and thus coincides nicely with the analytical calculations, which had a maximum tangential stress and v.M-stress of about 500 MPa. When it comes to displacement, the highest displacement occurred in the radial direction at the inner radius of the flywheel, also as can be expected considering that this area experiences the highest stress levels. The value was calculated to be around 240 μm. This can be compared to the analytical maximum displacement which was calculated to be around 250 μm.

Von Mises stress flywheel

As can be seen in figure 36 the highest v.M stress occurred at the inner radius of the flywheel. Although in this particular figure, a large mesh size with a linear structure was used. This highlights that, during computations performed on a linear mesh the maximum stress occurs symmetrical, but in stripes. These "stripes" does however increase in number and becomes thinner the smaller mesh size is applied.

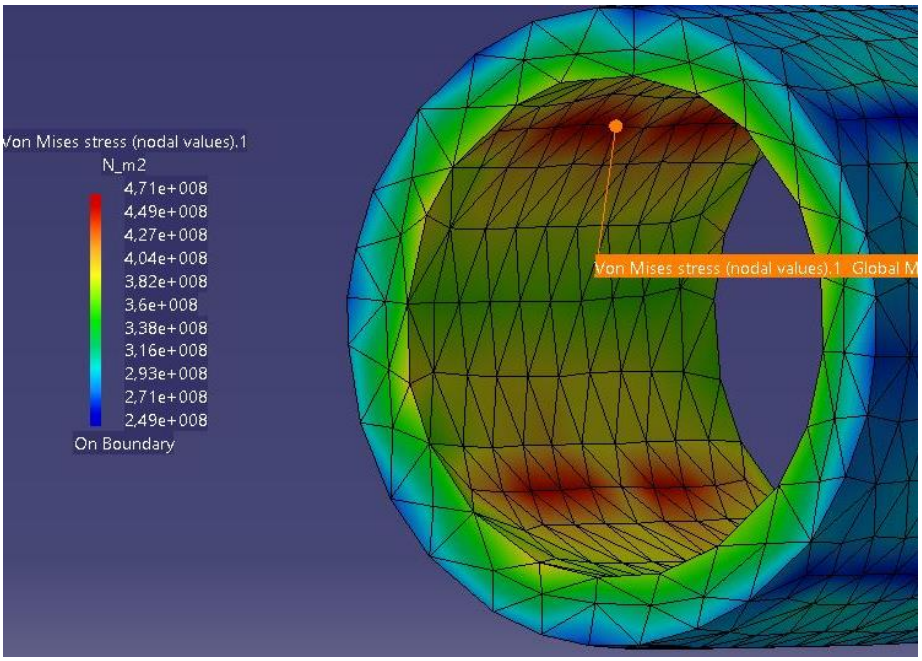

Figure 36: von Mises stress on flywheel with a linear 20x2 mesh size.

In figure 37 it can be seen that a parabolic mesh structure makes the stress spread out more evenly at the inner radius of the flywheel. The figure also highlights some stress concentration areas. These occur due to there being a 90-degree edge between the sides and the inner and outer surface of the flywheel. Thus it can be concluded that these are stress concentrations produced in the calculations, since there are no perfect edges.

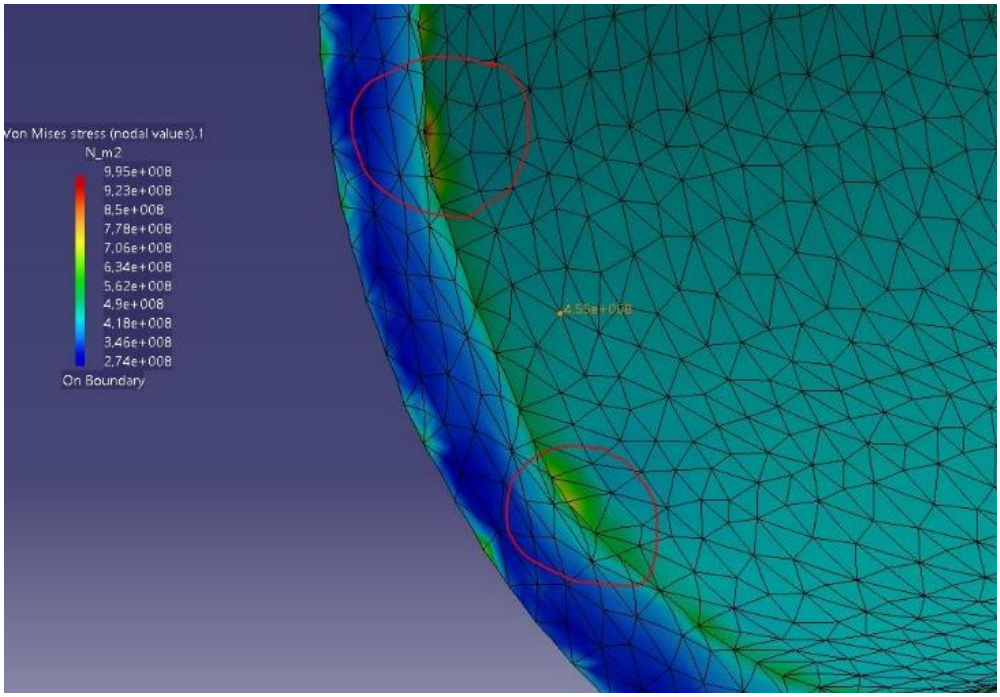

Figure 37: von Mises stress on flywheel with a parabolic 7x0.7 mesh size.

Tangential stress flywheel

As stated previously in this section, the highest amount of stress measured on the flywheel was at the inner radius in the tangential direction, in the form of tensile stress. This can be seen in figure 38. Also note that the tangential stress decreases when the radius increases. Again there are some stress concentrations shown closer to the edge of the flywheel. These are however not relevant as stated previously.

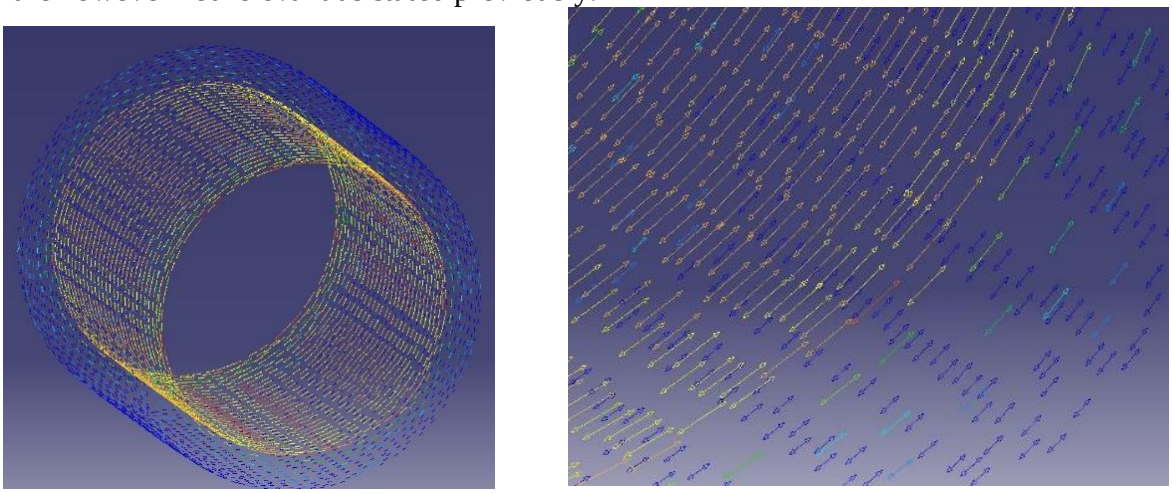

Figure 38: Tangential stress on flywheel with a linear 7x0.7 mesh size.

Radial stress flywheel

The radial stress was considerably lower than the tangential stresses, exactly as the analytical calculations predicted, note though that the FEM stress levels was higher than the analytical results. The maximum value attained was around 31 MPa tensile stress, which is low enough compared to the tangential stress that it can be neglected in this particular case. In figure 39, it can be seen that the entire cross section, apart from some parts in the middle of the flywheel experienced a tensile stress.

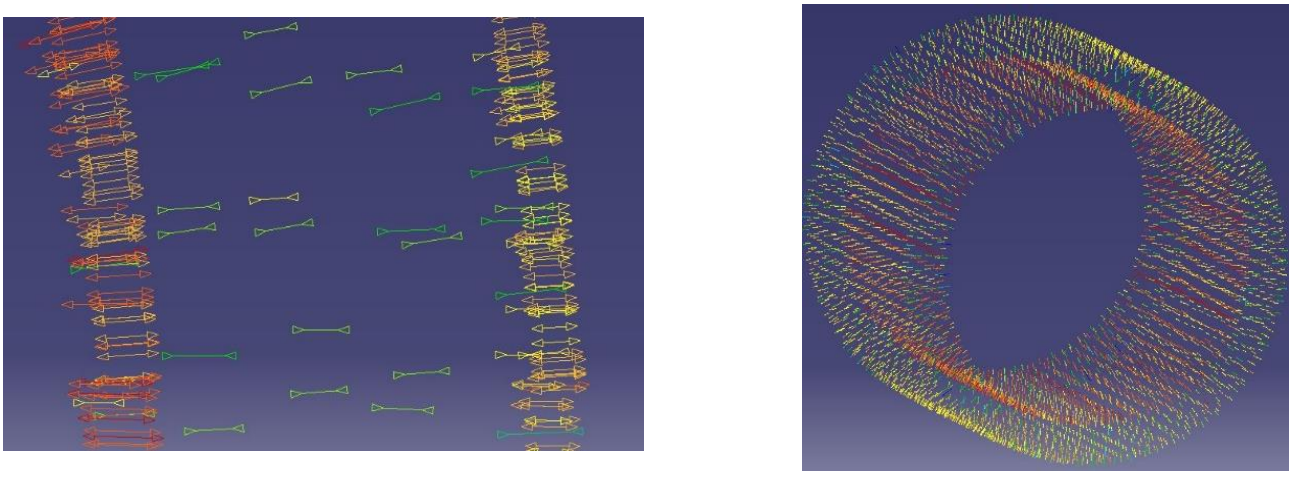

Figure 39: Principal stress in radial direction on flywheel with a linear 7x0.7 mesh size.

Flywheel and Hub

In this section a flywheel-hub designed as a shrink/pressure fitting connection is analysed in a general way. This means the complete flywheel design which contains a flywheel and an inner hub. The purpose with this section is to illustrate that the tensions increase in a flywheel concept when including a shrink/pressure fitting connection. In other words, it is not of interest how the stress changes throughout the hub. The aim is to illustrate where the highest stress can be found for the flywheel itself when designed with an inner hub.

Constraints and load on flywheel-hub

In order to gain a shrink/pressure fitting connection between the hub and the flywheel a "General Analysis Connection" was applied to the outer radius of the hub and the inner radius of the flywheel. The general analysis connection was then given a "Pressure Fitting Connection Property" with a diametrical interference of $\Delta = 2u = 500$ µm. The interference is in this particular case an estimation based upon the radial displacement u of the inner surface for a carbon fibre flywheel while rotating at 55 000 rpm. This displacement is roughly $u =$ 250 µm at the inner radius through part B, section 5.4.3.

Since the rotational force is transformed through the hub out to the flywheel via the interference fitting, no further constraints where set to the flywheel. The hub on the other hand was fitted with a clamp constraint applied via the shaft using smooth virtual parts at the end surfaces, see orange in figure 40. A rotational force of 55 000 rpm was also applied to the shaft.

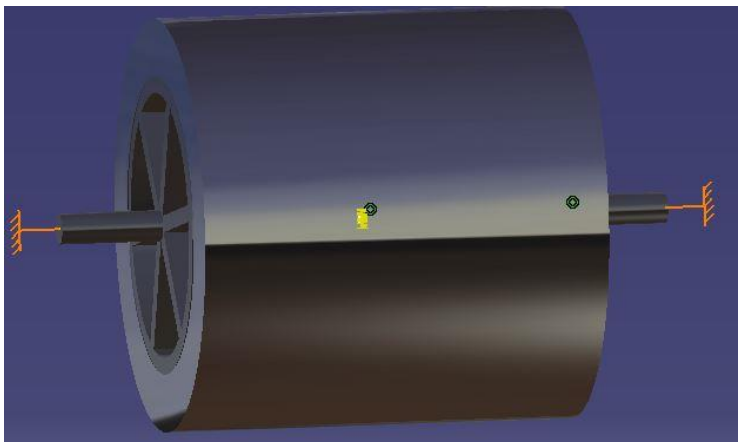

Figure 40: Constraints of the flywheel-hub

Results flywheel-hub

The main purpose of these results is to support the hypotheses that if a hub were to be fitted inside of the flywheel all stress levels would increase. The exact values are thus not of great importance. This since the hub is only designed conceptually with little calculation and thought being put into the exact dimensions. The interesting factor in this chapter is to visualize how the stress changes in the flywheel when using a shrinking/pressure connection between the hub and the flywheel. The results gathered are max v.M-, max radial- and max tangential stress at the inner radius of the flywheel while changing the mesh size and type from linear to parabolic. Table 13 shows the calculated stresses with different mesh types and sizes. Note in the table that different mesh sizes are evaluated with linear and parabolic mesh. This is due to the previously stated problem with parabolic requiring a lot more computer

power and, since the stresses almost converge it was not necessary to run 7x0.7 with parabolic mesh.

LINEAR MESH			
Size	v.M stress	Tangential stress	Radial stress
20x2 mm	830 MPa	830 MPa, tensile	100 MPa, compressive
10x1 mm	910 MPa	800 MPa, tensile	250 MPa, compressive
7x0.7 mm	900 MPa	790 MPa, tensile	240 MPa, compressive
PARABOLIC MESH			
Size	v.M stress	Tangential stress	Radial stress
20x2 mm	990 MPa	860 MPa, tensile	370 MPa, compressive
15x1.5 mm	990 MPa	820 MPa, tensile	370 MPa, compressive
10x1 mm	980 MPa	850 MPa, tensile	400 MPa, compressive

Table 13: Data collected for the flywheel and hub solution. Note that the values are gathered at the inner radius of the flywheel, not maximum values. Size is "mesh size" x "absolute sag".

From table 13 it can be concluded that the tangential stress calculated with linear mesh is almost in the same range as the results from the parabolic mesh calculation. However, when comparing the radial stress in table 13 it is clear that the linear mesh type underestimates the stress levels in comparison to the parabolic mesh type. The same could be concluded with the von Misses stress. The linear mesh type is about 80 MPa lower in v.M stress then with a parabolic mesh type, where it converged on around 980 - 990 MPa. The radial stress for the linear mesh reaches approximately about 240 MPa verses 400 MPa for the parabolic mesh. The parabolic results are in this instance to be considered as the more reliable data.

Von Misses stress in flywheel-hub

Figure 41 illustrates how the v.M stress is divided over the flywheel-hub solution. It is only of interest how the stress is distributed across the flywheel itself. From figure 41 it can be concluded that the highest v.M stress is found at the inner radius of the flywheel. High risk areas are illustrated with white arrows in the figure. Worth mentioning though is that the hub also attain the highest stress levels in the same regions as the flywheel.

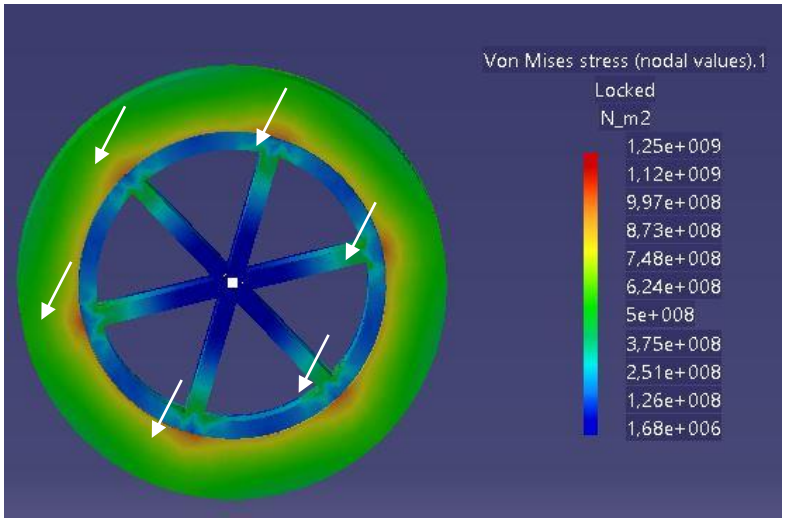

Figure 41: Front view of v.M stress for the flywheel-hub solution, using parabolic 10x1 mesh

Tangential stress in flywheel-hub

Figure 42 (left) illustrates how the tangential stress varies across the flywheel-hub. It is clear that the highest tangential stress is found at the inner radius of the flywheel. The stress levels are quite evenly distributed along the inner radius of the flywheel. Figure 42 (right) shows that the flywheel is exposed to tensile stress and not compressive stress. By observing figure 42 (left) it can also be noted that the hub is exposed to compressive rather than tensile tangential stress.

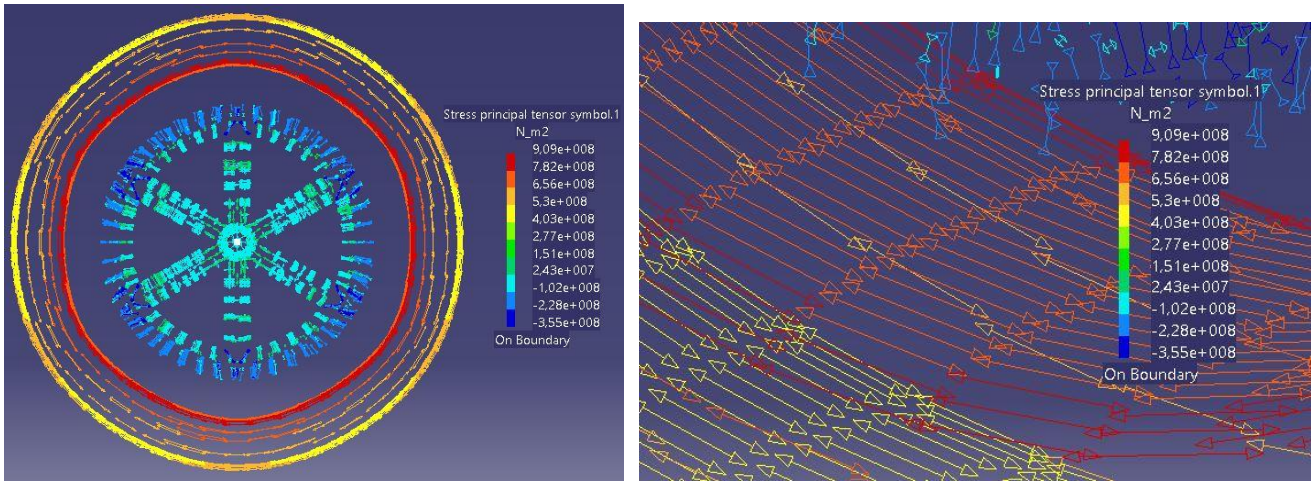

Figure 42: (left) Front view of tangential stress for flywheel-hub, using parabolic mesh 10x1 mm
(right) Illustrating tensile tangential stress near the inner radius of the flywheel, using parabolic mesh 20x2 mm

Radial stress in flywheel-hub

From figure 43 it can be concluded that the inner radius of the flywheel is submitted to compressive radial stress and the outer surface to tensile radial stress. The highest levels of radial stress are found on the inner surface and high risk areas are the same as the ones examined earlier in v.M stress and illustrated with white arrows in figure 43 (left). If the hub were to be designed as in this chapter it is important to note, from figure 43 (left) that it would be subject to high levels of compressive stress on the connecting areas (outer surface of the hub).

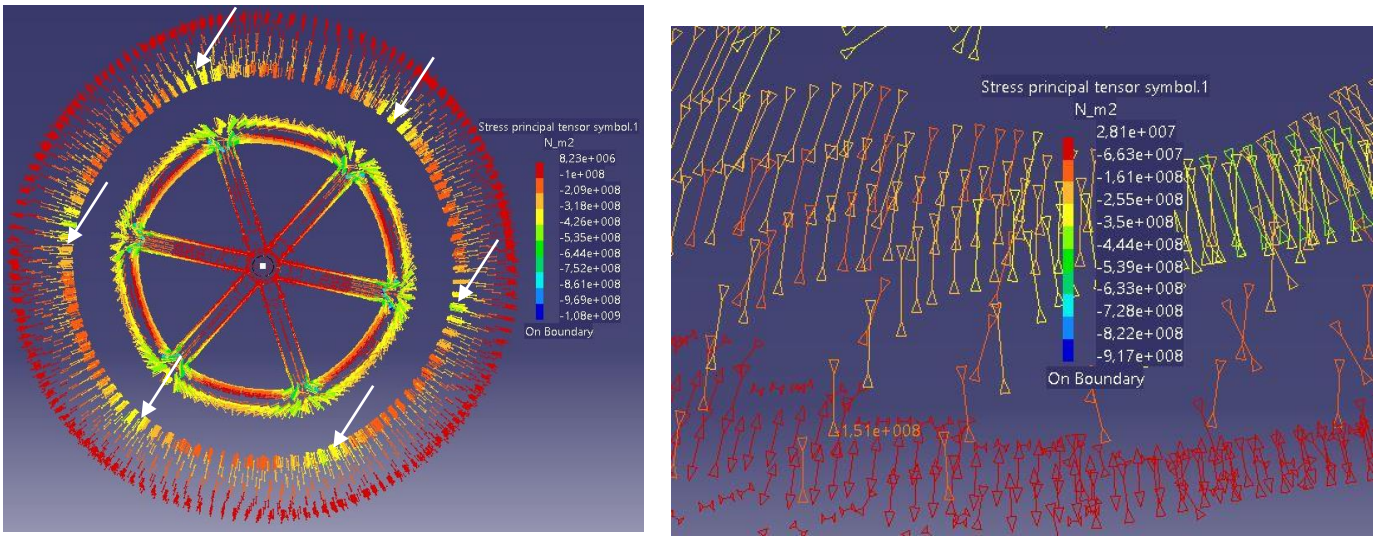

Figure 43: (left) Front view of radial stress for flywheel-hub, using parabolic mesh 10x1 mm
(right) Illustrating compressive radial stress nearby the inner radius of the flywheel, using parabolic mesh 20x2 mm

FEM summary and evaluation

When considering only the flywheel presented in the beginning of this chapter it can be concluded that the results of the FEM analysis conducted in CATIA coincided very well with the analytical calculations. It should be said though, that the radial stress was estimated to be a little bit higher in CATIA. This is probably due to some of the assumptions made in the analytical calculations such as plane stress.

The reason why the results from CATIA were so similar to the previous calculations could in part be attributed to the simple load case and the symmetrical design of the flywheel. In other words, it may not be necessary to conduct a FEM analysis on such a simple design, since the analytical theory is quite comprehensive for this scenario. For further investigation it might be preferable to chamfer some of the edges to minimize stress concentrations and make the scenario more realistic from a design stand point.

When it comes to the hub and flywheel assembly it can be concluded that the stress levels in the flywheel are increased in all directions when applying a shrink/pressure fitting connection. This coincides with the hypothesis stated in the beginning of the flywheel-hub section. Although the results are, as previously stated, not conclusive since the calculations and geometry of the hub are not definitive. Here it is again important to note that the carbon fibre is assumed to be isotropic, which is not the case for all composites. Because of this, the values of the stress levels are only indications of how the stress is increased in the case of a flywheel with a hub, rather than just a flywheel. If further investigation were to be conducted

on the design, it would be preferable to look more closely into the geometry of the hub, the size of the shaft and a calculate a more accurate interference fitting connection.